TEMPLATE-DIRECTED PHOTOCHEMICAL CYCLOADDITION REACTIONS OF DIENOIC ACIDS AND STUDIES TOWARD FLUORANTHENE SYNTHESIS

THESIS SUBMITTED TO

THE GRADUATE SCHOOL OF ENGINEERING AND SCIENCE

OF BILKENT UNIVERSITY

IN PARTIAL FULFILLMENT OF THE REQUIREMENTS FOR

THE DEGREE OF

MASTER OF SCIENCE

IN CHEMISTRY

By

Badar Munir

December 2023

TEMPLATE-DIRECTED PHOTOCHEMICAL CYCLOADDITION REACTIONS OF DIENOIC ACIDS AND STUDIES TOWARD FLUORANTHENE SYNTHESIS

By Badar Munir

December 2023

We certify that we have read this thesis and that, in our opinion, it is fully adequate, in scope and in quality, as a thesis for the degree of Master of Science.

Yunus Emre TÜRKMEN (Advisor)

Engin Umut AKKAYA

Bilge BAYTEKİN

Akın AKDAĞ

Çağatay DENGİZ

Approved for the Graduate School of Engineering and Science:

Orhan ARIKAN

Director of the Graduate School

ABSTRACT

TEMPLATE-DIRECTED PHOTOCHEMICAL CYCLOADDITION REACTIONS OF DIENOIC ACIDS AND STUDIES TOWARD FLUORANTHENE SYNTHESIS

Badar Munir

M.Sc. in Chemistry

Advisor: Dr. Yunus Emre Türkmen

December 2023

Carbocyclic compounds are an essential class of organic compounds as they occur broadly in natural products and constitute the heart of pharmaceutically relevant compounds. Photochemical dimerization reactions exhibit great potential for the rapid synthesis of carbocyclic compounds. To circumvent the regio- and diastereoselectivity challenges associated with the photochemical dimerization reactions, template-directed solid-state (topochemical) reactions furnish an efficient solution. We utilized inexpensive and commercially available 1,8-dihydroxynaphthalene (1,8-DHN) as a covalent-bonding template for photochemical dimerization reactions of dienes. 1,8-DHN align the alkenes, fulfilling Schmidt's criteria for topochemical reactions, and irradiation of template-bound diene gave products displaying high regio- and diastereoselectivity. Reaction conditions were optimized, which taught us that the powder, ground powder and ground crystals gave almost similar results. Furthermore, irradiation of template-bound diene in the solution resulted in a high yield and good diastereoselectivity. It should be noted that our work represents the first example of selective homodimerization and heterodimerization reactions of 5-arylpentadienoic acids. After irradiation, facile removal of the template was achieved by hydrolysis

and transesterification reactions. Experiments to convert the divinylcyclobutane product to cyclooctadiene were not successful due to troubles with the Cope rearrangement reaction.

In the second part, we aimed to synthesize the substituted fluoranthenes starting from 1,8-diiodonaphthalene. Functionalization of 1,8-diiodonaphthalene with Suzuki-Miyaura borylation to connect pyridazine ring as a dienophile for inverse electron-demand Diels-Alder reaction was tried under different conditions. Unfortunately, the reaction did not yield the desired conversion. To examine the possibility of the Ullmann coupling reaction, we performed studies with 1,8-diiodonaphthalene and iodobenzene under Ullmann coupling conditions, which resulted in complex mixtures.

Keywords: Photochemical Dimerizations, Schmidt's Topochemical Principles, Cope Rearrangement, Fluoranthenes, Inverse Electron-Demand Diels-Alder Reaction

ÖZET

DİENOİK ASİTLERİN ŞABLON KULLANILARAK FOTOKİMYASAL SİKLOKATILMA REAKSİYONLARI VE FLORANTEN SENTEZİNE YÖNELİK ÇALIŞMALAR

Badar Munir

Kimya, Yüksek Lisans

Tez Danışmanı: Dr. Yunus Emre Türkmen

Aralık 2023

Karbosiklik bileşikler, doğal ürünlerin yapısında bulundukları ve farmasötik bileşenlerin yapıtaşını oluşturdukları için önemli bir organik bileşik sınıfıdır. Fotokimyasal dimerizasyon rekasiyon, karbosiklik bileşiklerin hızlı sentezinde önemli bir rol oynamaktadır. Bu reaksiyonlarda bölgesel seçicilik ve diyastereoseçicilik ile ilgili zorlukları çözmek için şablon kullanılarak gerçekleştirilen katı hal (topokimyasal) reaksiyonları etkili bir yöntemdir. Biz de bu amaçla dienlerin fotokimyasal dimerizasyonu için kovalent bağlanma şablonu olan aynı zamanda ucuz ve hazır olarak temin edilebilen 1,8-dihidroksinaftalini (1,8-DHN) kullandık. 1,8-DHN, bileşenlerin Schmidt'in topokimyasal reaksiyonlar kriterine göre hizalanmasını sağladı ve sonrasında şablona bağlı dienin ışınlanmasıyla bölgesel seçicilik ve diastereoseçicilik sergileyen bir ürün ana ürün olarak elde edildi. Reaksiyon koşulları optimize edildi ve bu süreçte elde edilen sonuçlar, bize başlangıç maddesinin toz halinin, öğütülmüş toz halinin ve öğütülmüş kristallerin benzer performansta çalıştığını gösterdi. Şablona bağlı dienin ışınlanması, çözelti fazında gerçekleştirildiğinde de reaksiyon, yüksek verimle ve diastereoseçicilik ile sonuçlandı. Işınlanma reaksiyonundan sonra, hidroliz ve transesterifikasyon reaksiyonu ile şablonun kolayca üründen ayrılması sağlandı.

Divinilsiklobütanı siklooktadiene dönüştürmek için yapılan deneyler, Cope yeniden düzenleme reaksiyonundaki sorunlar nedeniyle başarılı olmadı.

İkinci kısımda 1,8-diiyodonaftalinden başlayarak florantenler sentezlemeyi amaçladık. İnvers Diels-alder reaksiyonunun dienofili olan maddenin sentezi için, 1,8-diiyodonaftaline Suzuki-Miyaura borilasyonu ile piridazin halkasının bağlanması farklı koşullarda denendi, fakat istenilen dönüşüm gerçekleşmedi. Daha sonra Ullmann kenetlenme reaksiyonunun başarılı olma olasılığını incelemek için, 1,8-diiyodonaftalin ve iyodobenzen ile Ullmann kenetlenme reaksyionu koşulları kullanılarak deneyler yapıldı; fakat bu deneyler karmaşık karışımların elde edilmesi ile sonuçlandı.

Anahtar Kelimeler: Fotokimyasal Dimerizasyon, Schmidt'in Topokimyasal Kriterleri, Cope Yeniden Düzenleme Reaksiyonu, Floranten, İnvers Diels-Alder Reaksiyonu.

ACKNOWLEDGMENTS

I would like to express my heartfelt gratitude to my advisor Dr. Yunus Emre Türkmen for his unwavering support, guidance and expertise that proved invaluable throughout the research journey. Along with his exceptional knowledge, his encouraging attitude during tough times and his patient approach towards my mistakes contributed significantly to my learning. I feel honored to have worked under his supervision.

I am thankful to my thesis committee members Prof. Dr. Engin Umut Akkaya, Dr. Bilge Baytekin, Prof. Dr. Akın Akdağ and Dr. Çağatay Dengiz for their valuable feedback.

Special thanks go to my lab fellows Eylül Çalıkyılmaz, Merve Temel, Suay Bilgin, Umut Mert, Gizem Yildiz, Palvan Jumayev and Kaan Berkey for their assistance and enjoyable lab atmosphere. I am also grateful to our former group member, Bilge Banu Yağci. She was an expert, and I learned a lot from her. I would also like to mention Merve Temel, as she always extended support when I needed help.

My appreciation extends to my friend Najeeb Ullah for his amazing companionship and for standing with me during challenging times. I also thank Rashid Mahmood, Zain Siddiqui, and Sobia Farooq for their support and encouragement.

I owe a debt of gratitude to my family, who supported me in every situation. The efforts and sacrifices of my parents are the driving force for all of my accomplishments and empower me to face life’s challenges. The beauty in my life is a direct result of your presence.

I am also thankful to Dr. Yunus Zorlu at Gebze Technical University for SC-XRD measurements. Finally, TÜBİTAK (The Scientific and Technological Research Council of Türkiye) is gratefully

acknowledged for the financial support regarding the second part of the thesis entitled “Studies Toward Fluoranthene Synthesis” (Project No: 119Z534).

To my lovely family!

LIST OF ABBREVIATIONS

APCI	Atmospheric-pressure chemical ionization
DCM	Dichloromethane
DCC	N,N`-Dicyclohexylcarbodiimide
DMAP	4-Dimethylaminopyridine
DME	1,2-Dimethoxyethane
dr	Diastereomeric ratio
EtOAc	Ethyl acetate
FTIR	Fourier-Transform Infrared
HRMS	High Resolution Mass Spectrometry
MeOH	Methanol
NMR	Nuclear Magnetic Resonance
R_f	Retention Factor
THF	Tetrahydrofuran
TLC	Thin-Layer Chromatography
TMS	Tetramethylsilane
UV	Ultraviolet

TABLE OF CONTENTS

LIST OF SCHEMES

LIST OF FIGURES

LIST OF TABLES

CHAPTER 1: TEMPLATE-DIRECTED PHOTOCHEMICAL CYCLOADDITION REACTIONS OF 5-ARYLPENTA-2,4-DIENOIC ACIDS

1.1 INTRODUCTION

1.1.1 Cycloaddition Reactions

Carbocyclic compounds are an essential class of organic compounds. They are structural motifs of various biologically active natural products and medicinally important compounds.[1,2] Due to their prevalence in organic compounds, organic chemists focused their attention on the synthesis of carbocyclic compounds. Cycloaddition reactions provide a direct way to access carbocyclic compounds. Cycloaddition reactions are a class of pericyclic reactions in which bond-breaking and bond-forming occur simultaneously, and a cyclic transition state is involved.[3] Cycloaddition reactions are further classified depending on the number of π electrons of both reactants involved in these reactions. The most common types of cycloadditions are [4+2] cycloaddition reactions, [2+2] cycloaddition reactions, and [4+4] cycloaddition reactions. Examples of these reactions are shown in Scheme 1.[4,5,6,7]

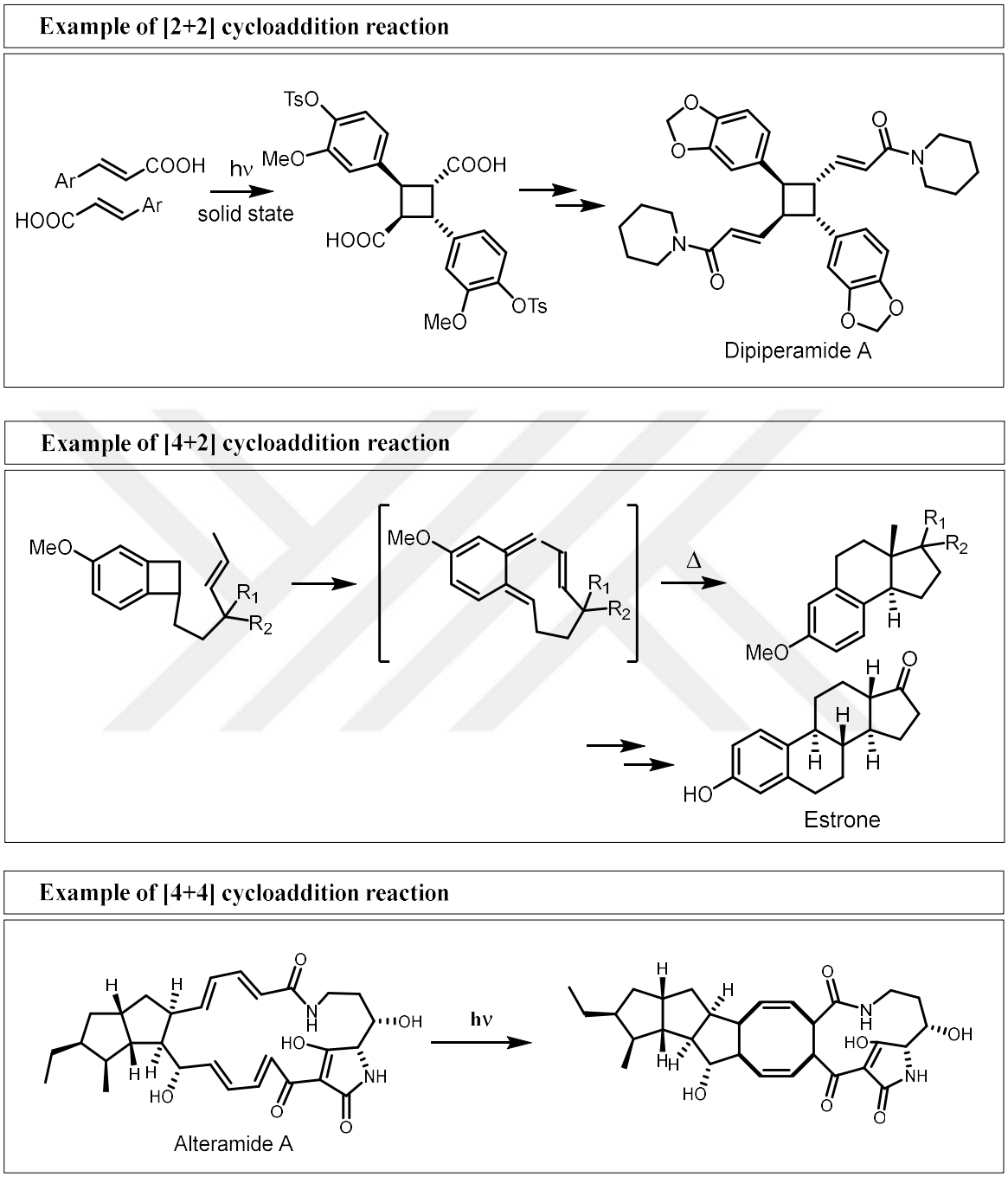

Scheme 1. Examples of cycloaddition reactions.

The activation and stereochemical outcome of these reactions can be rationalized by the Woodward-Hoffmann rules - a set of rules devised by Robert Burns Woodward and Roald Hoffmann.[8] These rules are based on the conservation of the orbital symmetry and imply that

cycloaddition reactions involving 4n+2 π electrons are symmetry allowed under thermal conditions only, while the cycloaddition reactions involving 4n π electrons are symmetry allowed under photochemical conditions. It should be noted that these are valid for suprafacial reactions on both components. Pericyclic cycloaddition reactions involving antarafacial attack follow an opposite trend in terms of the reaction conditions, but they are rare.

1.1.2 Cycloaddition Reactions in the Solid State

Intermolecular photochemical [2+2] cycloaddition reactions of olefins, particularly cinnamic acids, in solution phase mostly lead to the E-Z isomerization and thus result in the mixture of isomers.[9] So, controlling the outcome of such photochemical reactions in solution is quite challenging. Detailed investigation of these reactions by Schmidt and co-workers demonstrated that solid-state reactions have the potential to overcome the aforementioned problem.[10] Solid-state photochemistry of cinnamic acid was the first example and provides useful insight into this area. Cinnamic acid crystallizes in three polymorphic forms. The irradiation of the α-polymorph structure of trans-cinnamic acid results in the formation of α-truxillic acid, while the irradiation of the β-polymorph structure of trans-cinnamic acid results in the formation of β-truxinic acid. Moreover, the γ-polymorph structure of trans-cinnamic acid does not show any reaction upon irradiation (Figure 1).[11,12]

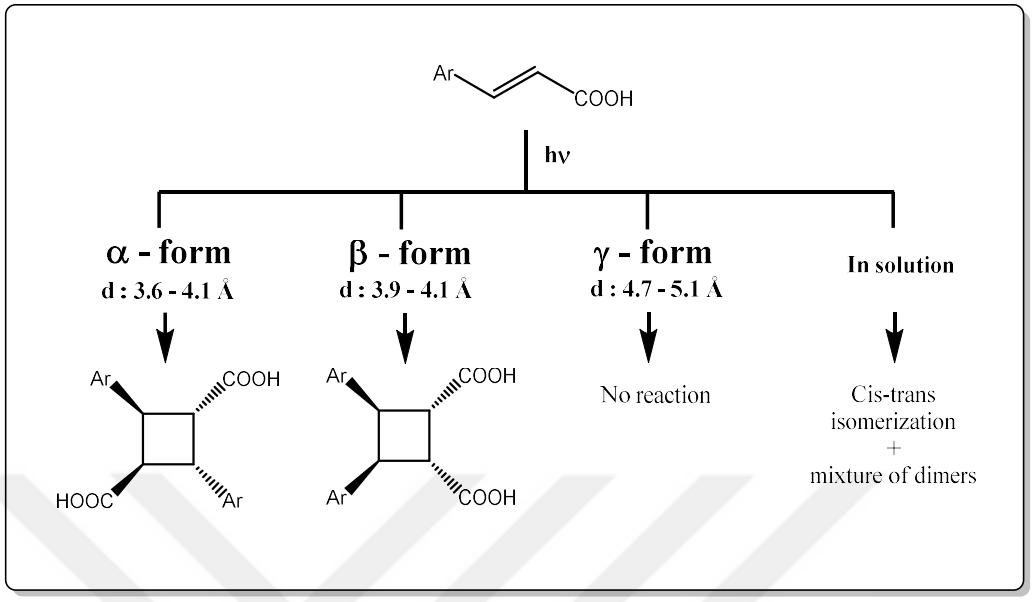

Figure 1. Irradiation products of cinnamic acids

Based on these studies, followed by a comprehensive investigation of the relationship between the crystal structure and photoreactivity, Schmidt devised a set of rules for successful photochemical reactions, which are known as Schmidt's topochemical principles. These rules are based on the main idea that for solid-state reactions, minimal atomic or molecular movement occurs. According to these principles, for photochemical cycloaddition reactions in the solid state, the following criteria must be fulfilled:

1. The two reacting alkenes must be on top of each other.
2. The two reacting alkenes must be aligned parallel to each other.
3. The distance between the olefin centers must be greater than 3.5 Å and less than 4.2 Å.

Since least movements are involved in solid-state reactions, this also limits cis-trans isomerization because for such a process to occur, large movements must occur. Additionally, these reactions are solvent-free, so they also contribute to the mission of Green Chemistry.[13]

1.1.3 Use of Templates

After these findings by Schmidt, chemists started investigating the photochemical cycloaddition reactions in the solid state. A major concern was the proper arrangement of reacting molecules so that they follow Schmidt's criteria, and not every molecule can crystallize the way as required. In order to address this challenge, the idea of using templates was introduced. The template can attach to the molecules and arrange them for a photochemical cycloaddition reaction. After the cycloaddition reaction, the template can be removed to afford the desired cycloaddition product (Figure 2).

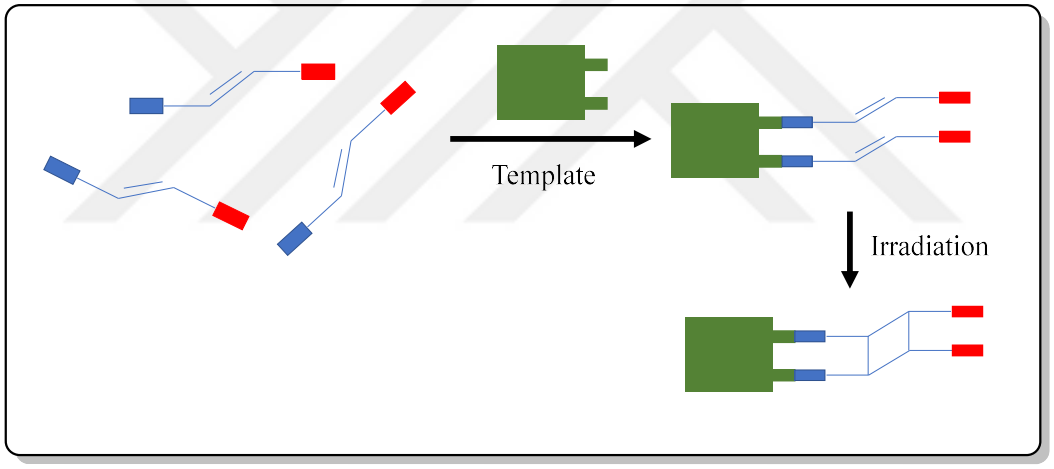

Figure 2. Representation of the use of templates

1.1.4 Template-directed Photochemical Dimerizations of Alkenes

In 2000, MacGillivray and co-workers used resorcinol as a template for [2+2] photochemical cycloaddition reaction. By employing hydrogen bonding interactions between resorcinol and the substrate molecules, they were able to orient the double bonds properly. Irradiation resulted in the formation of desired cyclobutane in high yield (Scheme 2).[14]

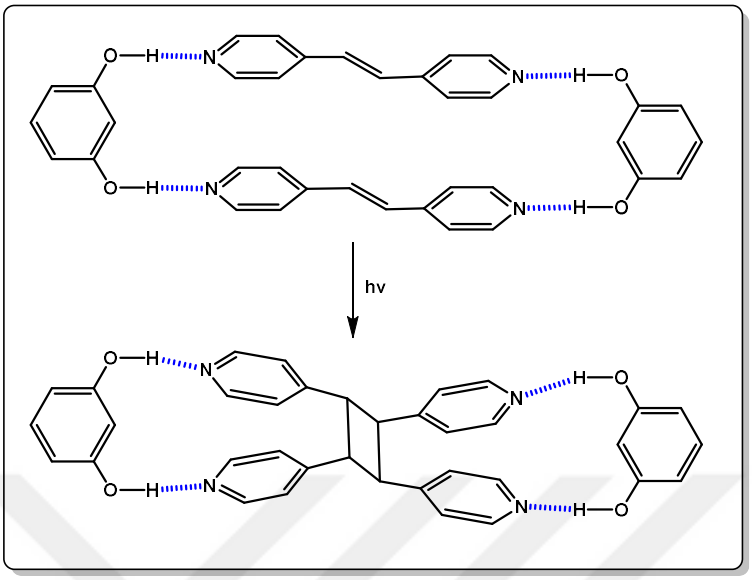

Scheme 2. Hydrogen bonding template for [2+2] cycloaddition

Hopf and co-workers used 4,15-diamino[2.2]*para*-cyclophane to align the alkenes so that alkenes fulfill Schmidt's criteria. After attachment of the substrates covalently to the cyclophane template, they were successful in synthesizing the cyclobutane product **1** selectively in the solution phase (Scheme 3).[15]

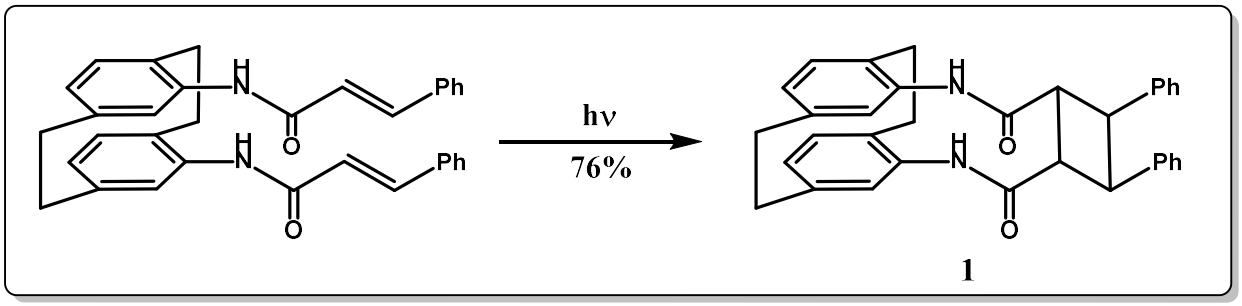

Scheme 3. Covalent template for [2+2] cycloaddition

Metrangolo and Resnati used halogen bonding interactions for meeting the Schmidt's requirements for [2+2] cycloaddition reactions. They employed iodoperfluoroarenes as halogen bond-donors and co-crystallized them with *trans*-1,2-bis(4-pyridyl)ethylene which aligned the alkenes perfectly

for the photoreaction. Irradiation of the resulting cocrystal for three hours resulted in 100% conversion into the cyclobutane product without the formation of any side product (Scheme 4).[16]

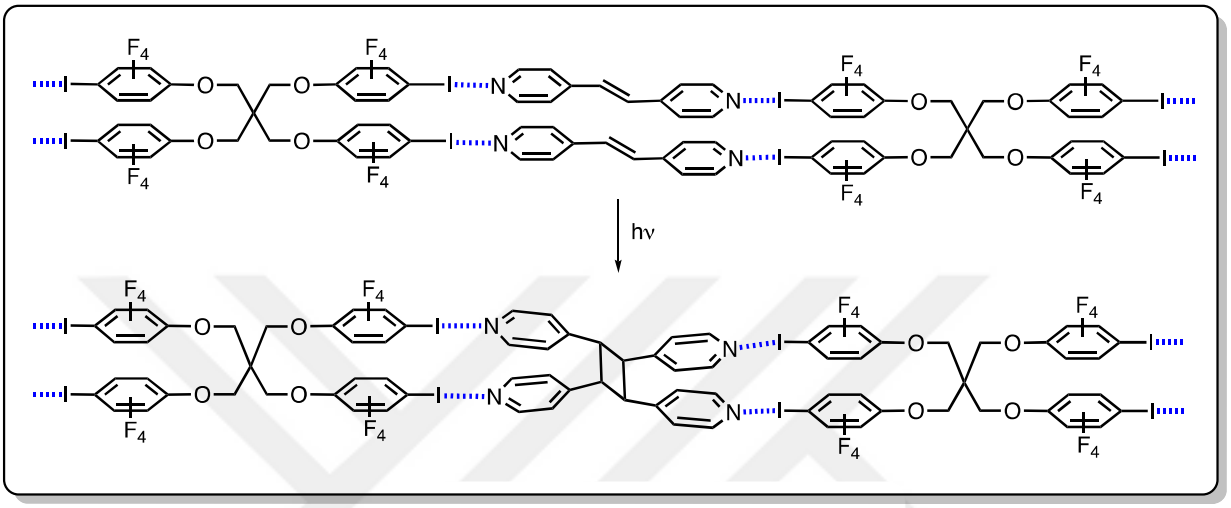

Scheme 4. Halogen bonding template for [2+2] cycloaddition reaction.

A major shortcoming with all these strategies is that they only allow homodimerization reactions, i.e., cycloaddition reactions between two same olefins. Co-crystallization of the substrate with the template molecules in case of non-covalent interactions and substrate attachment in case of the covalent template is also challenging. This imposes a severe limitation on the synthetic utility of these templates.

1.1.5 Photochemical Dimerization Reactions of Dienes

Photochemical dimerization reactions of dienes are also of interest to synthetic organic chemists as they can lead to several cyclic molecules exhibiting biological activities. A few of these examples include variecolin,[17] kalmanol,[18] taxol,[19] and pentacycloanammoxic acid[20] (Figure 3). The pentacycloanammoxic acid methyl ester is an interesting molecule and is isolated from the membrane of Candidatus Brocadia anammoxidans. Because of the rigidity in the structure, these membranes possess high density and impermeability.

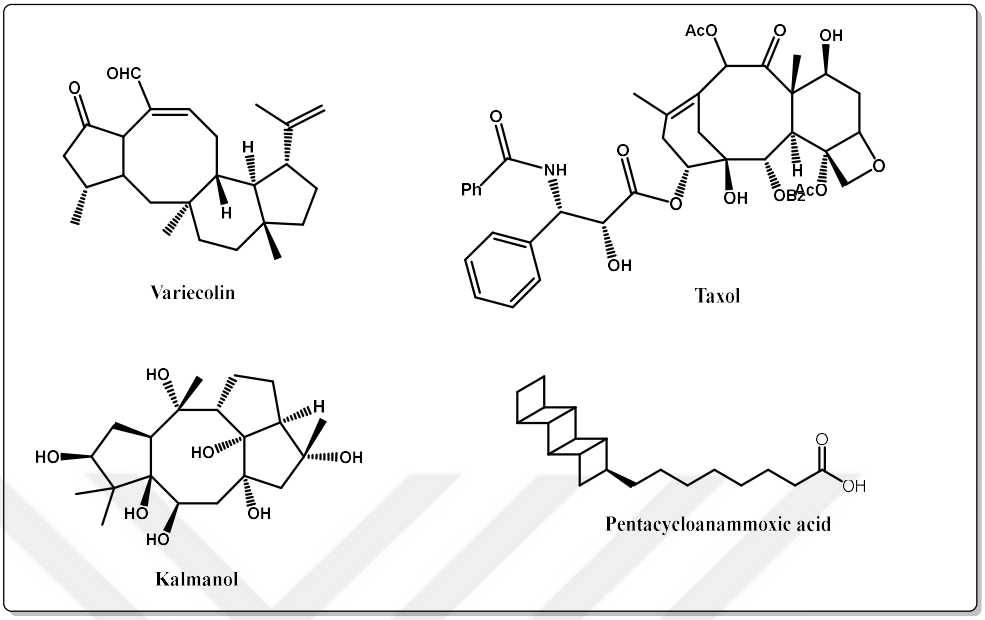

Figure 3. Examples of natural products involving eight-membered carbocycle and ladderanes.

But at the same time, they also pose a lot more challenges as compared to the dimerization reactions of mono-alkenes. The possible outcomes of the dimerization reaction of unsymmetrical dienes are shown below in Figure 4.

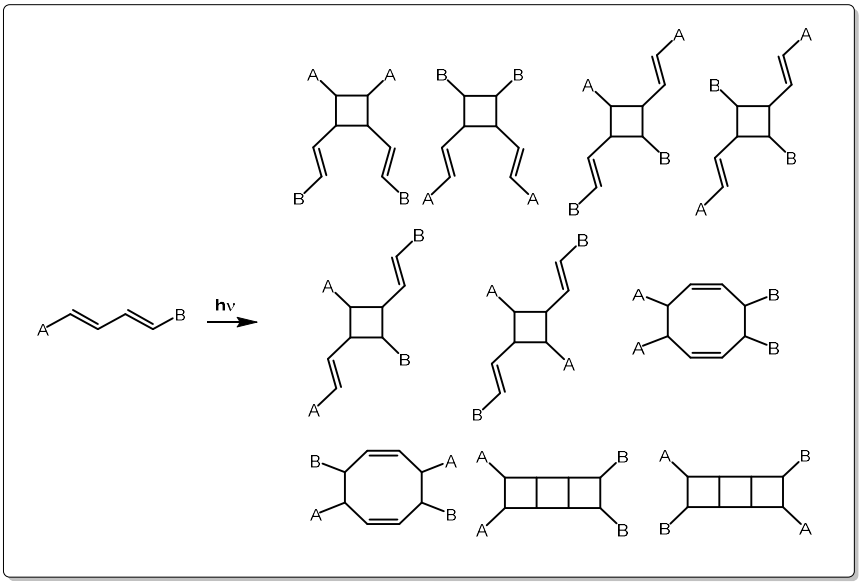

Figure 4. Possible products from dimerization reaction of dienes

First, there are different possibilities for the formation of cyclobutanes by [2+2] cycloaddition reactions which can be head-to-head and head-to-tail. Then, there are possibilities for the formation of cyclooctadienes by head-to-head and head-to-tail [4+4] cycloaddition reactions. These may also lead to ladderanes if both double bonds undergo [2+2] cycloadditions. It should be noted that stereoisomers are not considered in this analysis, and all products can have syn and anti-stereoisomers. These can get even more complicated if we are interested in the heterodimerizations of dienes.

Schmidt, in 1971, reported the dimerization reaction of 5-phenylpentadieneoic acids in the solid state.[21] As expected, irradiation of 5-phenylpentadieneoic acid **(2)** resulted in a complex mixture of products. A few of the products which can be identified are shown in Scheme 5. It should be noted that the cyclooctadiene product was not initially formed by a [4+4] cycloaddition reaction; rather, it was rendered by the Cope rearrangement of the divinyl cyclobutane product.

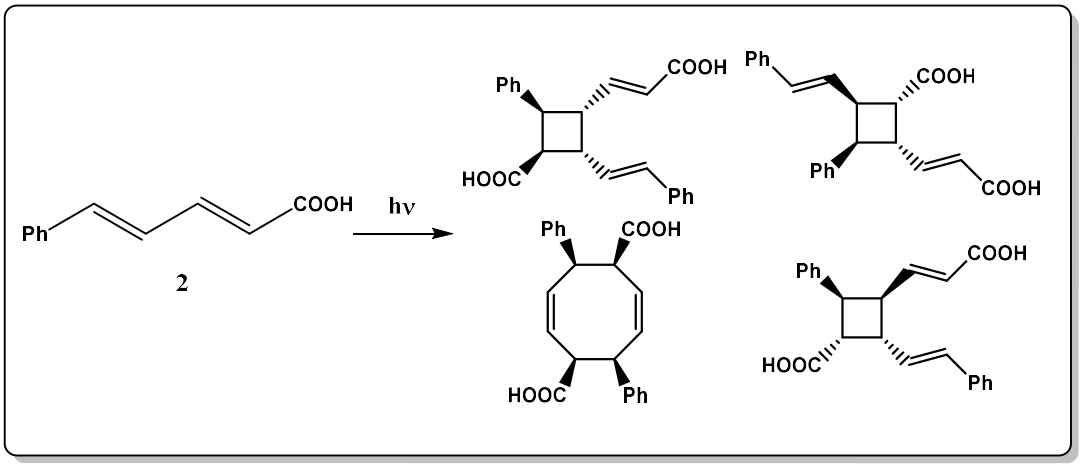

Scheme 5. Irradiation of 5-phenylpentadienoic acid (**2)**

1.1.6 Template-directed Photochemical Dimerization Reactions of Dienes

In order to achieve selectivity for these transformations, the orientation of the substrate prior to irradiation can be done. For this purpose, the use of templates was introduced. These templates align the substrates in such a way that only one or two products can be obtained.

For the dimerization reaction of dienes, MacGillivray and co-workers used 3-methoxy resorcinol as a hydrogen bonding template. With this template, they were able to align the alkenes in such a way that both double bonds followed Schmidt's criteria. Irradiation then led to the formation of ladderanes (Scheme 6).[22]

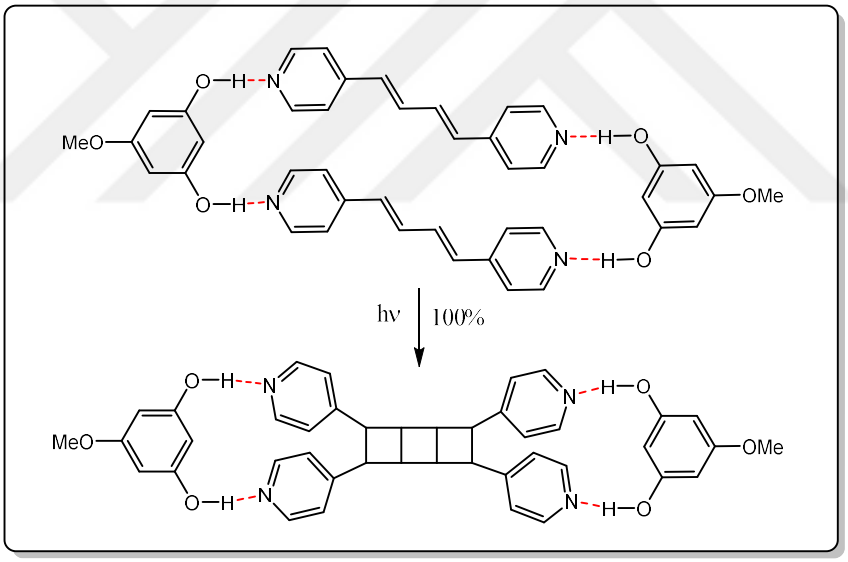

Scheme 6. Hydrogen bonding template for dimerization reaction of diene

Another interesting example is the synthesis of ladderanes by Hopf and co-workers. By using cinnamophane vinylogs, they were successful in synthesizing ladderanes, and this was the first example of access to ladderanes using photochemistry. Something interesting happened when they tried irradiation with sunlight. In this case, they observed the formation of cyclooctadiene by an initial [2+2] cycloaddition reaction followed by a Cope rearrangement reaction. The lower light

flux can explain this difference in the case of sunlight, which makes it difficult for a second [2+2] cycloaddition (Scheme 7).[23]

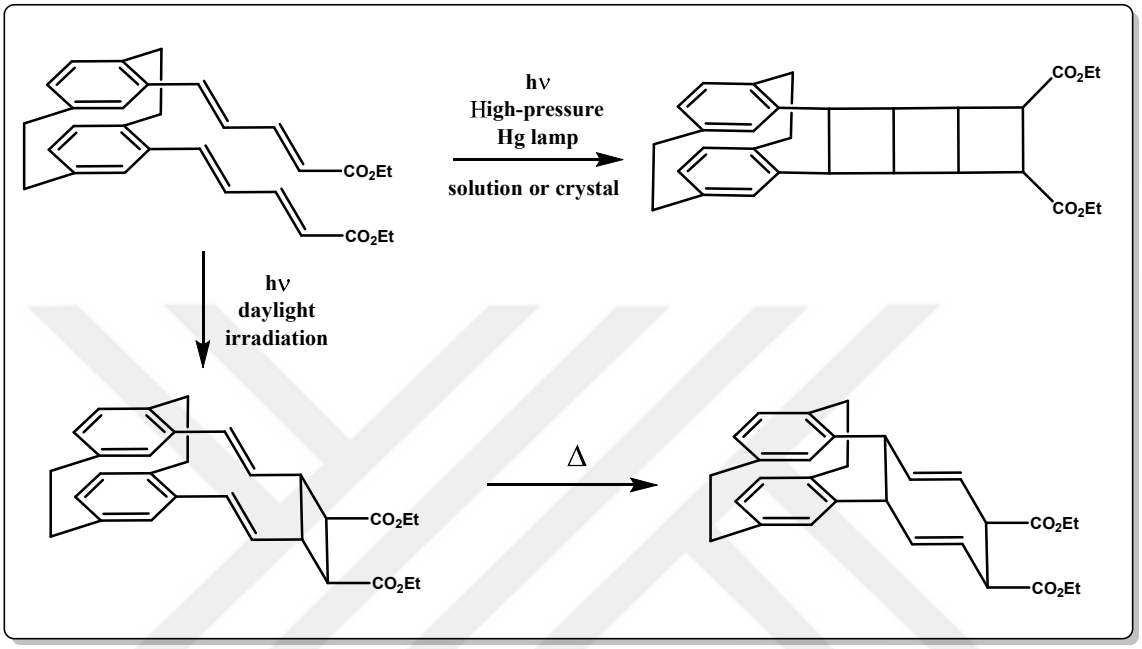

Scheme 7. Covalent template for dimerization of dienes

Another approach by Yamada involves utilizing π-cation interactions between 1-aryl-4-pyridylbutadiene in the presence of 1 equiv. of HCl. Upon irradiation, they obtained cyclobutane products from *syn*-head-to-tail and *anti*-head-to-tail [2+2] cycloaddition reactions. *Syn*-head-to-tail product was then converted to cyclooctadiene through Cope rearrangement by heating it to 60 ˚C in $CDCl_3$.[24] (Scheme 8)

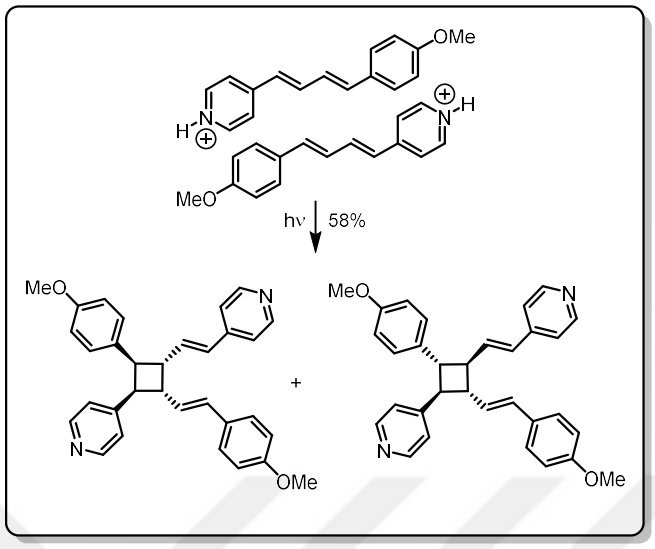

Scheme 8. Cation-π interactions for dimerization reaction of dienes

J. Vittal and co-workers in 2011, synthesized Au(I) macrocycles with trans, trans muconic acids and were able to align the two conjugated trans double bonds of muconic acids at a distance of 3.958 Å and parallel to each other. Hence, the compound is expected to be photoreactive. Irradiation with UV A light using a Xenon lamp for 2 h resulted in the formation of cyclooctadiene dimer as a result of [4+4] cycloaddition reaction (Scheme 9).[25]

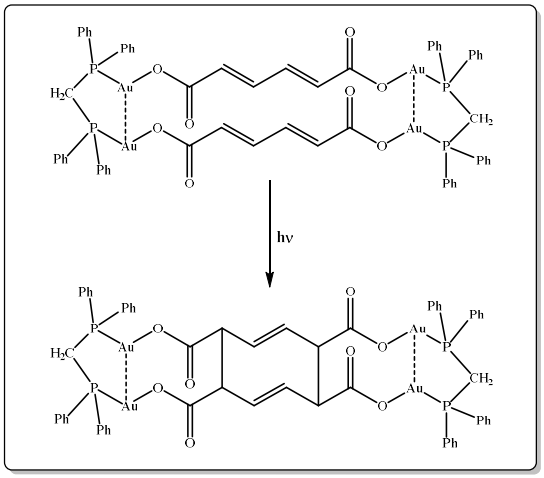

Scheme 9. Dimerization reaction of muconic acid by Au(I) macrocycle

These dimerization reaction strategies for dienes suffer from the same limitations as that of mono-alkenes. They involve laborious co-crystallizations and are limited to homo-dimerization reactions.

1.1.7 1,8-Dihydroxynaphthalene as a Template for Photochemical Dimerization Reactions

In 2018, an investigation by the Türkmen group into the hydrogen bonding ability of 1,8-dihydroxynaphthalene (1,8-DHN) **3** revealed the presence of an intramolecular hydrogen bond in 1,8-DHN.[26] Because of this intramolecular hydrogen bonding, the first pK_a value for 1,8-DHN is 6.7, while the second pK_a value is greater than 13.[27] This significant difference in the reactivity can be utilized for sequential and selective functionalization of 1,8-DHN. Also, the distance between the two -OH groups is 2.58 Å which can align the alkenes in accordance with Schmidt's criteria. These features of 1,8-DHN make it an excellent covalent template for topochemical cycloaddition reactions. Furthermore, 1,8-DHN is commercially available, not expensive, and can provide facile attachment and detachment of the substrate.

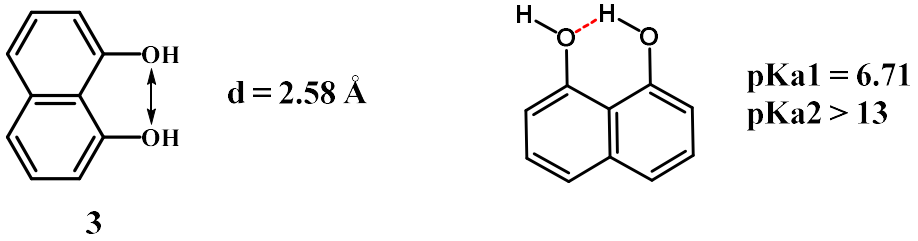

3

Figure 5. Important features of 1,8-DHN **(3)**

Inspired by these, our group in 2021 successfully employed 1,8-DHN as a template for solid-state [2+2] cycloaddition dimerization reactions of cinnamic acids. Use of 1,8-DHN allowed the homo- and heterodimerization reactions of cinnamic acids to yield symmetrical and unsymmetrical β-truxinic acids in excellent regio- and diastereoselectivity and with efficient yields (Scheme 10).[28,29]

It should be noted that this work provided for the first time a general solution for the selective heterodimerization reactions of cinnamic acids.

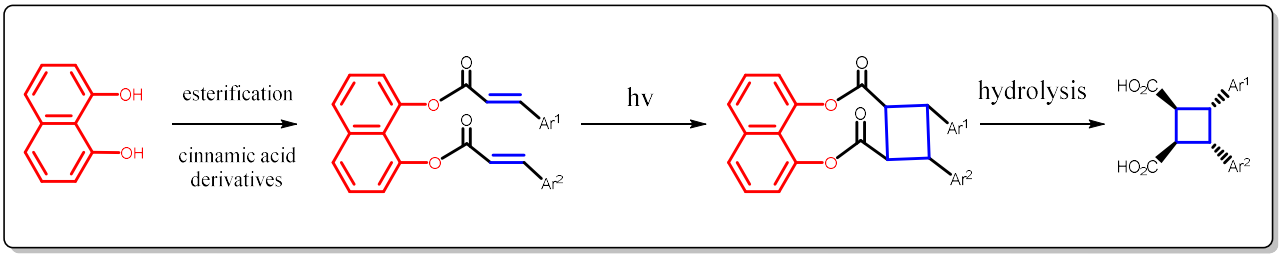

Scheme 10. Use of 1,8-DHN **(3)** in dimerization reactions of cinnamic acids

1.1.8 Aim of this project

With all the difficulties associated with the photochemical dimerization of dienes via cycloaddition reactions in view, we embarked on solving this problem. We decided to explore the potential of 1,8-dihydroxynaphthalene (1,8-DHN) as a template for dimerization reactions of 5-arylpenta-2,4-dienoic acids. The template will not only provide the proper arrangement of olefinic bonds for selective cycloaddition reactions, but the structural features of the template will also lead us to heterodimerizations along with homodimerizations. Our synthetic plan involves the following steps:

1. In the first step, we will attach our substrates (5-arylpentadienoic acids) to the template. This can be achieved using esterification reactions.

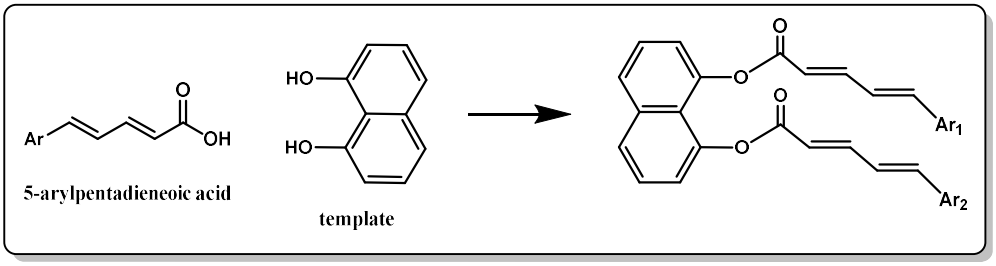

Scheme 11. Proposed synthesis plan for attachment of template

2. Then, with the template-bound substrate in hand, we will irradiate these compounds with a light source to affect the photochemical cycloaddition reaction. There are various possibilities for this step. The first possibility is the [4+4] cycloaddition reaction between the two dienes to form cyclooctadienes. The second possibility is the [2+2] cycloaddition reaction for only one pair of alkenes. This will result in the formation of divinylcyclobutanes which can be subsequently converted into cyclooctadienes by the well-known thermal Cope rearrangement. Yet another possibility is individual [2+2] cycloaddition reactions for both double bonds, leading to ladderanes.

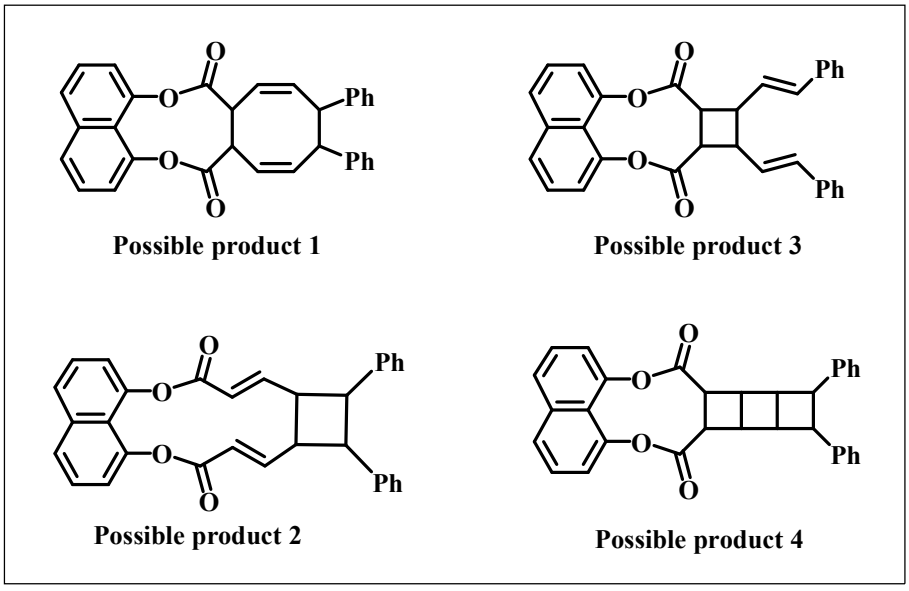

Figure 6. Possible products from the template-bound substrate

3. After the formation of cycloadducts by irradiation experiments, we will detach the product from the template. This will give us our final dimerization products and the template will also be recovered. The detachment of the template can be done using a hydrolysis reaction.

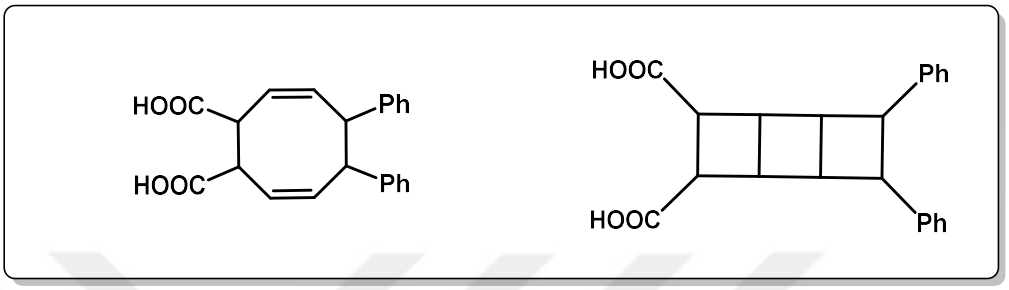

Figure 7. Possible products after template detachment

1.2 RESULTS AND DISCUSSIONS

1.2.1 Synthesis of 5-arylpenta-2,4-dieneoic acids

We started with the synthesis of 5-arylpenta-2,4-dieneoic acids. For this purpose, we first tried the Knoevenagel-Doebner-Stobbe condensation reaction of *trans*-cinnamaldehyde (**4**) with malonic acid (**5**). Heating the cinnamaldehyde with malonic acid to reflux in the presence of piperidine as a base and pyridine as a solvent resulted in the formation of a mixture of (2E,4E)-5-phenylpenta-2,4-dienoic acid (**2**) and (2Z,4E)-5-phenylpenta-2,4-dienoic acid (**6**) with a total yield of 53%.

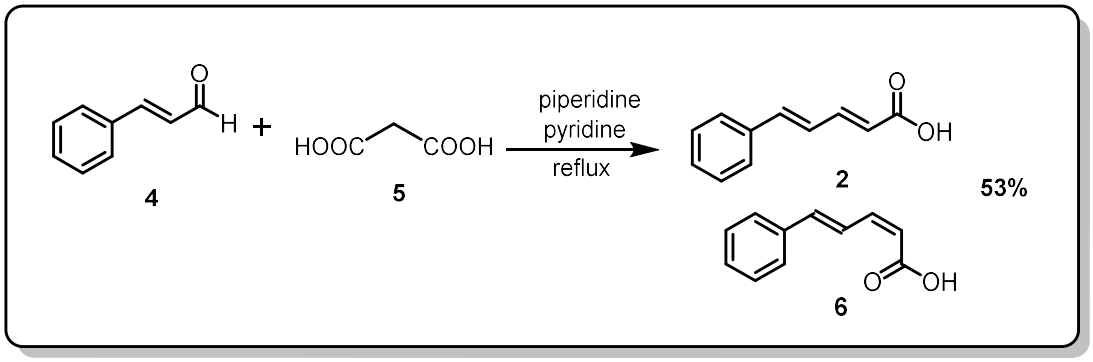

Scheme 12. Synthesis of 5-phenylpentadieneoic acid using condensation reaction

The isolation of these products by column chromatography proved to be challenging. So, we started to look for a way to achieve the conversion of cis-alkenes into trans-alkenes. A highly efficient method for the conversion of cis-cinnamic acid **6** to trans-cinnamic acid **7** using iodine is reported by Ding and co-workers.[30]

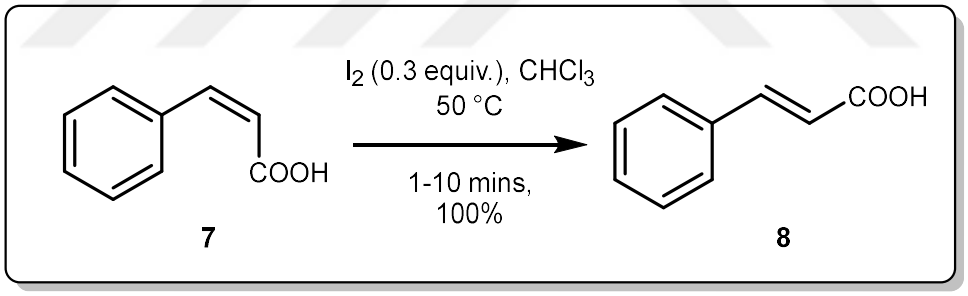

Scheme 13. Conversion of cis-cinnamic acid **7** to trans-cinnamic acid **8**

We also tried to use the same reaction conditions on our substrates. We tried several different sets of conditions by varying the solvents and the temperature shown in the table below, but we were unsuccessful to achieve our desired conversion.

Table 1. Reaction conditions for conversion of compound **6** to compound **2**

Entry	Solvent	Temp (°C)	Result
1	$CHCl_3$	40	No conversion
2	$CHCl_3$	50	No conversion
3	$CHCl_3$	60	No conversion
4	MeOH	60	No conversion
5	pyridine	60	No conversion
6	acetonitrile	60	No conversion

Being unable to synthesize (2E,4E)-5-arylpenta-2,4-dienoic acids using Knoevenagel-Doebner-Stobbe condensation reaction, we then moved on to different route to synthesize it. By employing Horner-Wadsworth-Emmons (HWE) reaction conditions, triethylphosphonoacetate **9** was deprotonated using NaH and was then reacted with the trans-cinnamaldehyde. After purification by column chromatography, the product ethyl (2E,4E)-5-phenylpenta-2,4-dienoate **10** was obtained whose structure was confirmed using ^{1}H-NMR and ^{13}C-NMR spectroscopy.

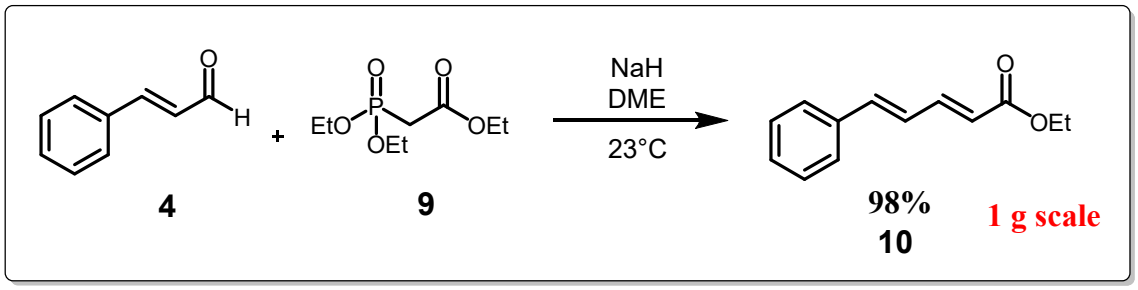

Scheme 14. Synthesis of ethyl (2E,4E)-5-phenylpenta-2,4-dienoate **(10)**

Basic hydrolysis of ethyl (2E,4E)-5-phenylpenta-2,4-dienoate **10** using 5 N KOH aqueous solution in a 2:1 mixture of THF and MeOH yielded the desired (2E,4E)-5-phenylpenta-2,4-dienoic acid **2** in 92% yield. The structures were confirmed by ^{1}H-NMR and ^{13}C-NMR spectroscopy and were found to match the literature data.

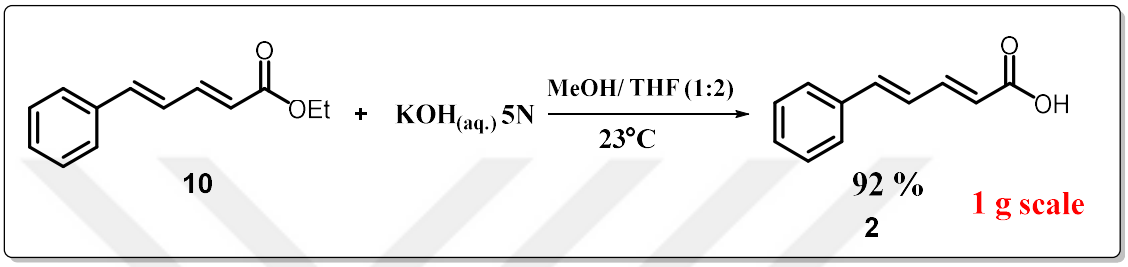

Scheme 15. Synthesis of (2E,4E)-5-phenylpenta-2,4-dienoic acids **(2)**

In order to further validate the structure of (2E,4E)-5-phenylpenta-2,4-dienoic acid **2**, single crystal X-ray crystallography analysis was done. This analysis was done by Prof. Yunus Zorlu from the Chemistry Department of Gebze Technical University. The solid-state structure of compound **2** shows the presence of trans configuration of both double bonds. The typical dimeric structure for carboxylic acids can also be observed.

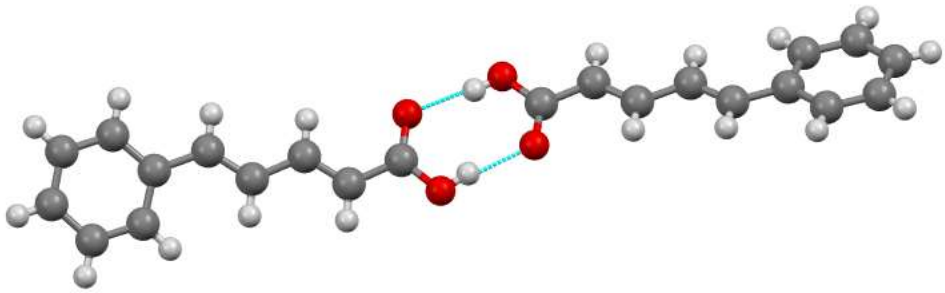

Figure 8. Single crystal XRD structure of (2E,4E)-5-phenylpenta-2,4-dienoic acid **(2)**

Using the same sequence of reactions starting from cinnamaldehydes, different substituted 5-arylpentadienoic acids were prepared. The HWE reaction yielded the esters **11**, **12**, and **13** in 83%,

88%, and 78% yields respectively (Scheme 16). The NMR data of these compounds matched the literature data.

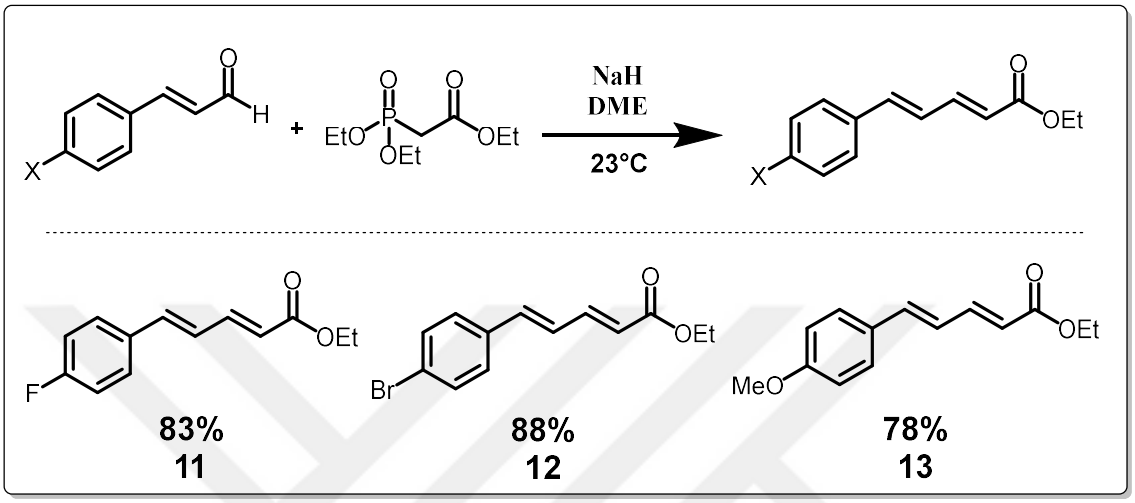

Scheme 16. Synthesis of ethyl (2E,4E)-5-arylpenta-2,4-dienoates

Subsequently, basic hydrolysis of the esters **11**, **12**, and **13** resulted in the desired substituted 5-arylpentadienoic acids **14**, **15**, and **16** in excellent yields (Scheme 17). The NMR data for these compounds were found to be in agreement with the reported data.

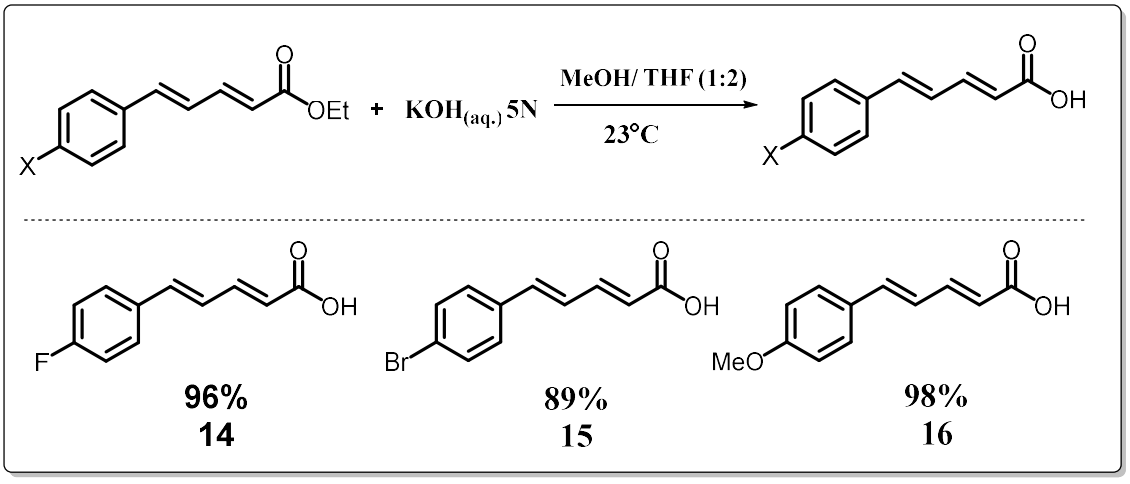

Scheme 17. Synthesis of (2E,4E)-5-arylpenta-2,4-dienoic acids

1.2.2 Irradiation Experiments of (2E,4E)-5-phenylpenta-2,4-dienoic acid (2)

We then checked the reactivity of substrate **2** by irradiating it. First, upon irradiation of the powder with medium pressure Hg lamp for 4h, the substrate was found to be decomposing (Scheme 18).

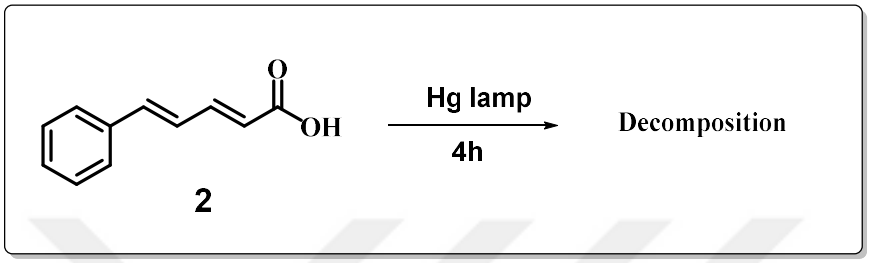

Scheme 18. Irradiation of (2E,4E)-5-phenylpenta-2,4-dienoic acid **(2)** in Hg lamp

After seeing the decomposition of our material by Hg lamp, we then switched our irradiation source and used a commercially available and inexpensive nail gel dryer. A complex mixture of products was obtained as a result of irradiation of the powder sample. These results are in accordance with the results of Schmidt's work.[18]

Irradiation of a solution of (2E,4E)-5-phenylpenta-2,4-dienoic acid **2** in $CDCl_3$ leads to E-Z isomerization of the double bonds observed by the appearance of doublet at 5.75 ppm with a coupling constant of 11.0 Hz in the crude ^{1}H-NMR (Scheme 19). Moreover, in the crude ^{1}H-NMR analysis, there were no signals in the aliphatic region thus ruling out any possibility of cycloaddition reaction.

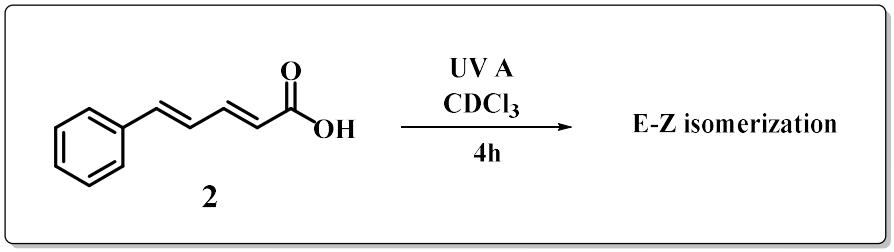

Scheme 19. Irradiation of (2E,4E)-5-phenylpenta-2,4-dienoic acid **(2)** in solution

We also checked the photochemical behavior of a single crystal of (2E,4E)-5-phenylpenta-2,4-dienoic acid **2**. We did not observe any reactivity and the single crystal stayed intact. Analysis of the crystal packing of the substrate revealed that there are no two double bonds which are exactly obeying Schmidt's criterion of a successful cycloaddition reaction.

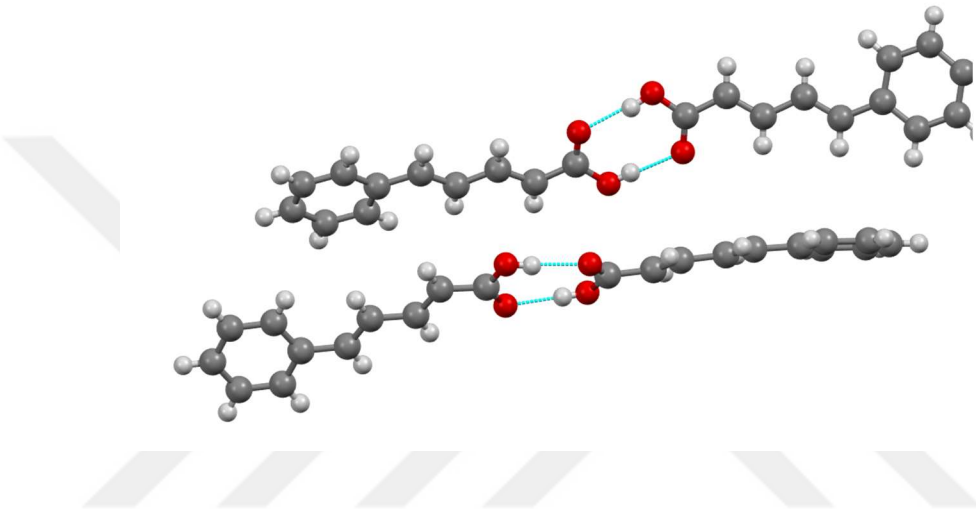

Figure 9. Crystal packing of (2E,4E)-5-phenylpenta-2,4-dienoic acid **(2)**

These experiments proved that the attempts towards the dimerization reaction of dienes by directly irradiating them poses a lot of problems and thus is not a practical strategy.

1.2.3 Attachment to the Template

Substrate can easily be attached to the template using an esterification reaction. We used Steglich esterification reaction conditions for this purpose. 3 equivalents of (2E,4E)-5-arylpenta-2,4-dienoic acids **2**, **14**, and **15** were reacted with 1,8-dihydroxynaphthalene (**3**) in the presence of dicyclohexylcarbodiimide (DCC) and *N*,*N*-dimethylaminopyridine (DMAP) (Scheme 20). After purification by column chromatography, the formation of the desired symmetrical diester products **17**, **18**, and **19** was confirmed using ^{1}H-NMR, ^{13}C-NMR, and ^{19}F-NMR spectroscopy as well as by ATR-IR spectroscopy and high-resolution mass spectrometry (HRMS).

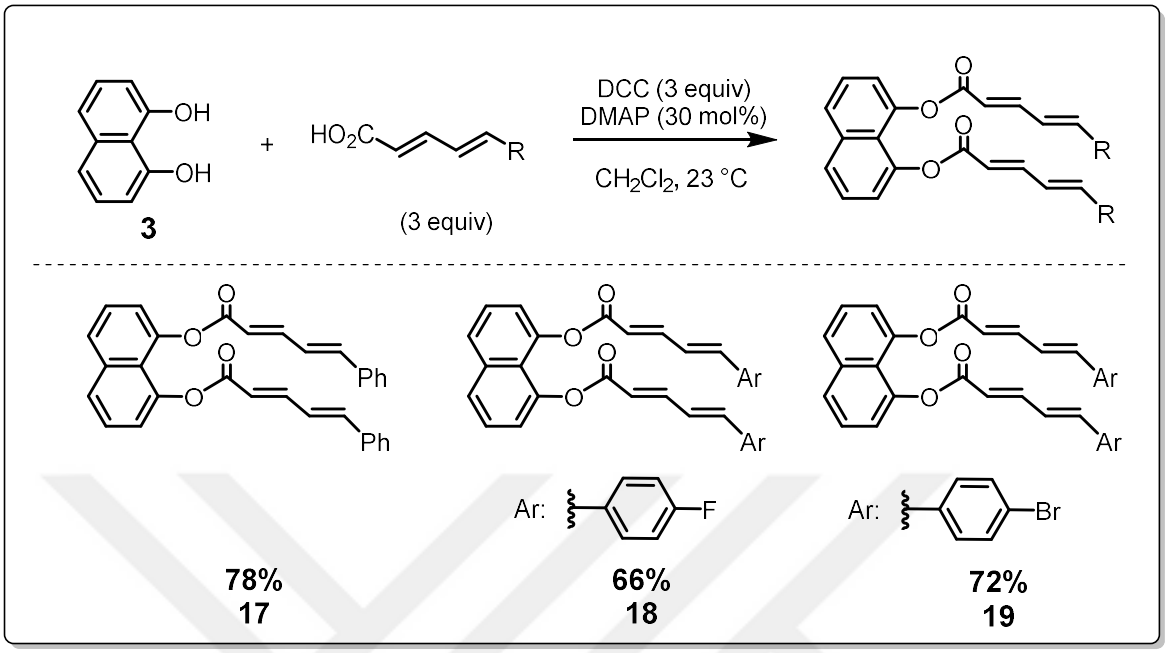

Scheme 20. Attachment of (2E,4E)-5-arylpenta-2,4-dienoic acids to template **3**

This esterification reaction between 1,8-dihydroxynaphthalene and dienoic acid **2** proceeded with a yield of 78% and is found to be easily scalable as well. Similarly, the attachment reaction for compounds **14** and **15** also proceeded with good yields. Esterification reaction for (2E,4E)-5-(4-methoxyphenyl)penta-2,4-dienoic acid (**16**) and 1,8-DHN (**3**) was also tried, but unfortunately we were not able to obtain the purified product.

After successful synthesis of symmetrical diester products by attachment of two same dienoic acids with 1,8-DHN, we then used a different reaction sequence for synthesis of unsymmetrical diester products by attachment of two different dienoic acids. For this purpose, first the carboxylic acid group of compound **2** was transformed into acyl group **20** by reacting it with oxalyl chloride. Then, this acyl chloride **20** (1 equiv.) was reacted with 1,8-DHN (**3**) in THF to yield monoester **21** in 71% yield. Finally, a Steglich esterification reaction was employed between the monoester **21** and compound **16** for the synthesis of unsymmetrical diester compound **22** (Scheme 21). Both the

monoester **21** and unsymmetrical diester compound **22** were characterized by ^{1}H-NMR, ^{13}C-NMR, and ATR-IR spectroscopies, and HRMS.

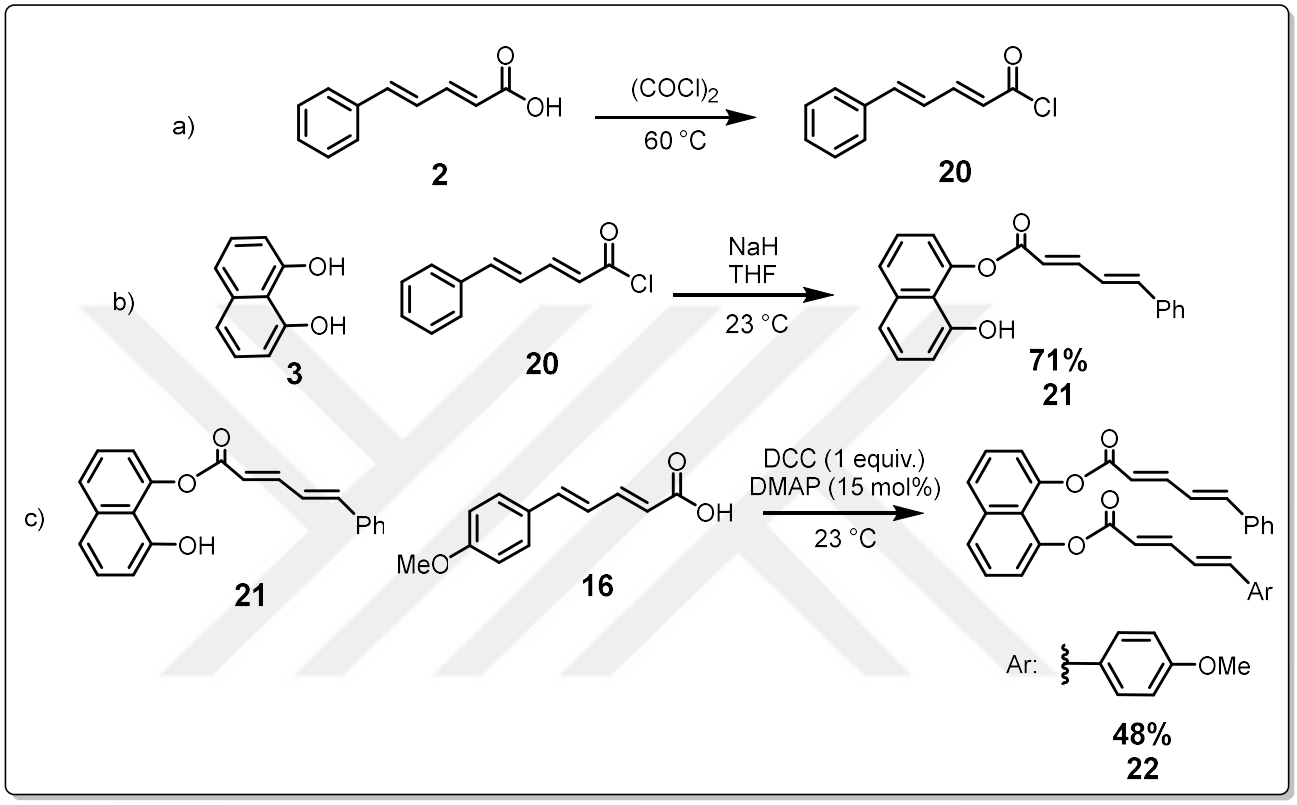

Scheme 21. Synthesis of unsymmetrical 1,8-diester compound **22**

Since we were interested in the solid-state photochemical dimerization reactions and Schmidt's criteria need to be fulfilled for these reactions as mentioned already, we decided to investigate the single crystal X-ray structure of **17**. By using the vapor-diffusion method, crystals of the diester **17** were grown. Analysis of these crystals revealed that the difference between the two pairs of double bonds is 4.001 Å and 5.056 Å. These measurements show that only one pair of the double bonds is in accordance with Schmidt's principles while the other pair of double bonds does not follow it. Based on it, only one pair of the double bonds is expected to undergo [2+2] cycloaddition reaction, and the irradiation product will be divinylcyclobutane.

Another interesting piece of information from the single crystal X-ray analysis of compound **17** is that both pairs of the double bonds are criss-crossed to each other because of the opposite orientations of the carbonyl groups. This criss-cross orientation of the double bonds is not in accordance with Schmidt's rules and thus reaction is expected to be photochemically unfavorable.

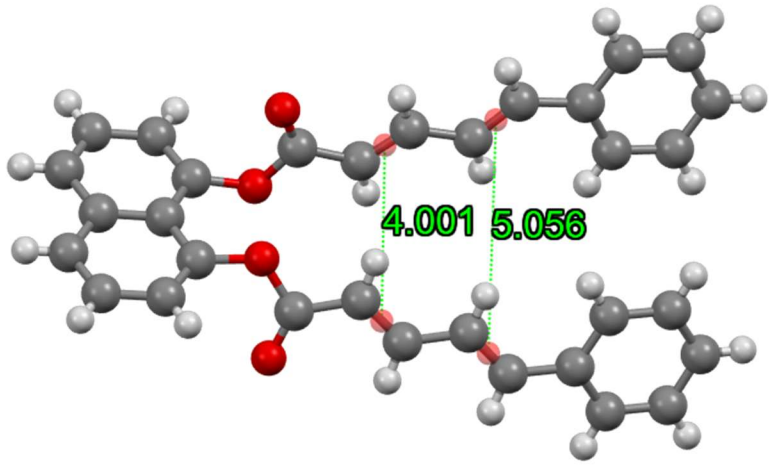

Figure 10. Single crystal XRD structure of the diester **17**

1.2.4 Pedal Motion

As discussed earlier, the crystal structure of the diester **17** indicates the opposite orientation of two carbonyl groups and as a result, the double bonds are criss-crossed. This criss-cross alignment of alkenes contradicts Schmidt's criteria, and the molecule is expected to be unreactive. But irradiation of the diester **17** with UV light results in the dimerization leading to divinylcyclobutane product. This type of behavior can be attributed to the pedal motion prior to photocycloaddition reactions and has also been proposed by others.[31,32] Pedal motion is a type of molecular motion usually observed in the organic molecules whose crystal structures are similar to pedals of the

bicycle and crank arms like azobenzenes and stilbenes. This pedal motion for the diester **17** has been shown in Figure 11.

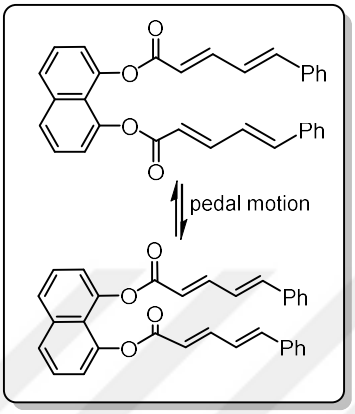

Figure 11. Pedal motion in the diester **17**

Although direct proof for the pedal motion is very scarce in the literature, high temperature XRD measurements can shed light on this by showing crystal defects.[33] Unfortunately, we were unable to make these measurements.

1.2.5 Investigation of the Irradiation Experiments

After successfully synthesizing the template-bound substrate **17** and its analysis by single crystal structure, we then investigated the effect of irradiating it by different light sources. We started our studies by using a 400 W broadband medium-pressure mercury lamp (Scheme 22). The material was placed between two microscopic slides and was subjected to UV light for 6 hours. Irradiation was stopped after every 2 hours, and the reaction mixture was mixed with a clean spatula to ensure homogenous exposure to light. After 6 hours, 50% conversion was observed along with the decomposition of the material. The product was isolated by column chromatography and was characterized as [2+2] cycloaddition reaction product of the expected alkenes while the other

double bonds remained intact. The structure of the cycloadduct **23** was confirmed by ^{1}H-NMR and ^{13}C-NMR spectroscopy.

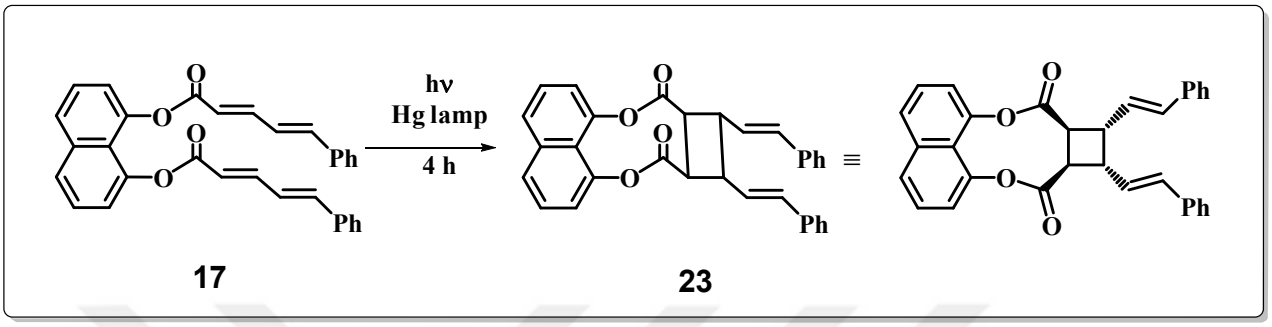

Scheme 22. Irradiation of diester **17** in Hg lamp

We also did the single crystal structure analysis of **23** to validate the stereochemistry around the cyclobutane ring. Crystals of **23** were grown by the vapor-diffusion method using dichloromethane and pentane as solvents. The single-crystal structure of **23** shows its stereochemistry and confirms the stereoselective nature of the photochemical cycloaddition. Another important piece of information obtained from the single-crystal structure of **23** is that the distance between the double bonds in **23** is 3.954 Å. Moreover, the double bonds are not top of each other and are oriented in opposite reactions which rule out the possibility of further cycloaddition reaction (Figure 12).

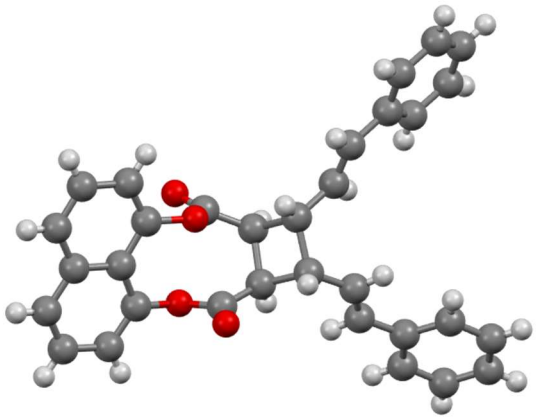

Figure 12. Single crystal XRD structure of template-bound cycloadduct **23**

In order to avoid the decomposition of the substrate, we placed the microscopic slides at a distance of 1.7 cm from the Hg lamp and placed a fan in the reaction chamber. Irradiation was done for 8 hours, and the reaction mixture was mixed after every 2 hours. After 8 hours, 16% conversion was observed for the reaction.

In order to optimize the reaction conditions, we then tried different light sources, reaction types and sample types. These reaction optimizations are summarized in the table below.

Table 2. Optimization of photochemical reaction conditions of diester **17.**

Entry	UV source	Sample	Time (h)	*Conversion (%)	Yield (%)
1	Hg lamp (broadband)	Powder	6	50 SM decomposition	ND
2	UV A	Powder	8	16	ND
3	UV A	Powder	16	40	30
4	UV A	Powder	24	50	35
5	UV A	Powder	48	65	52
6	UV B	Powder	16	25	ND
7	Daylight	Powder	216	9	ND
8	UV A	Ground powder	16	66 SM decomposition	32
9	UV A	Ground powder	48	80	53
10	UV A	Crystals	16	25 Clean reaction	ND
11	UV A	Crystals	48	37 Clean reaction	ND
12	UV A	Crushed crystals	48	50 Clean reaction	ND
13	UV A	Ground crystals	16	66	50
14	UV A	Ground crystals	24	66	56
15	UV A	Ground crystals	48	66	58
15	UV A	Solution**	4	Almost completion	88

17	Daylight	Solution In $CDCl_3$	168	57% (some cis-trans isomerization)	ND
18	UV B	Solution**	2	Almost completion	58%

Medium pressure Hg lamp, UV A : 365 nm, UV B : 310 nm

***** Conversion is the ratio of the product to the starting material plus the product. Therefore, it is not very accurate when there are side reactions.

** Solution in $CHCl_3$

After observing decomposition of starting material **17** under Hg lamp, we then used nail dryer as our UV source. Irradiation of the powder sample for 8 hours with mixing after every 2 hours in the nail dryer resulted in 16% conversion. More importantly, we did not observe any decomposition of the starting material. We then increased the reaction times to 16 hours and 24 hours which resulted in the increase of conversion to 40% (isolated yield: 30%) and 50% (isolated yield: 35%) respectively. Upon further increasing the reaction time to 48 hours, conversion increased up to 65% (isolated yield: 52%). So, there was not a significant increase in the conversion and also starting material started decomposing. On changing the light source to UV B and irradiating the powder sample for 16 hours, we got a 25% conversion which was less than the UV A light source with the same irradiation time. This shows that the UV B light source is less effective than the UV A light source for this conversion. We also studied the effect of daylight on the reaction. The diester **17** compound was placed between two microscopic slides and was placed close to the window for 7 days (average sunny days of May). The reaction mixture was mixed once a day. After 7 days, we were able to see conversion, although, in much smaller amounts, that is 7%.

Grinding has been found to accelerate the pedal-like motion.[34] Moreover, it has been found that grinding and milling affect solid-state reactions by causing molecular motions.[35] So, we also decided to grind our diester powder and then irradiate it. For this purpose, we ground the diester

powder in mortar and pestle for 5 minutes. Irradiation of the ground powder for 16 h resulted in the conversion of 66% but decomposition was also observed. Because of the decomposition isolated yield was 32% - a slight improvement. On increasing the reaction time to 48 h for ground powder, more decomposition was observed but yield rose up to 53% - again marginal improvement.

We then decided to check the photoreactivity of the diester in a crystal state. Upon irradiation of the crystal directly for 16 hours, a 25% conversion was observed. Importantly, this reaction was very clean, and no signs of decomposition were observed. Conversion increased up to 37% on increasing the irradiation time to 48 hours. To increase the interaction of the light with the material while keeping the reaction clean, we simply crushed the crystals with the help of a spatula. When we irradiated these crushed crystals for 48 hours, we observed a conversion of 50% and the reaction was clean. Based on these results, we took the diester crystals and finely ground them in mortar and pestle for 5 mins. Irradiation of these ground crystals for 16 hours led to a yield of 50% approx. When the irradiation of these ground crystals was done for 24 and 48 hours, we were able to see 56% and 58% yields, respectively and with high diastereoselectivities (ca. 25:1).

Finally, we also observed the effect of irradiating the diester in solution. For this purpose, the diester **17** was dissolved in $CHCl_3$ and placed under UV lamps in a nail dryer. TLC indicated full consumption of the starting material after 4 hours of irradiation which the crude ^{1}H-NMR of the reaction mixture also confirmed. Crude ^{1}H-NMR also indicated cis-trans isomerization to a small extent. Purification of the reaction mixture by column chromatography resulted in a yield of 88% with a dr of 8:1. Irradiation of the solution of diester in $CHCl_3$ with UV B light gave 58% yield and the dr was 8:1. In order to study the effect of daylight on the photoreactivity of the diester in solution, the diester was dissolved in $CDCl_3$ and placed in daylight (average sunny days of May).

After 7 days, ^{1}H-NMR analysis indicated 57% conversion. Again, to a little extent, cis-trans isomerization was observed along with the formation of dimerization cyclobutane product.

The UV-vis absorption spectrum of the diester **17** in DCM and the UV-vis diffused reflectance spectrum for the solid sample of **17** is shown in Figure **13**.

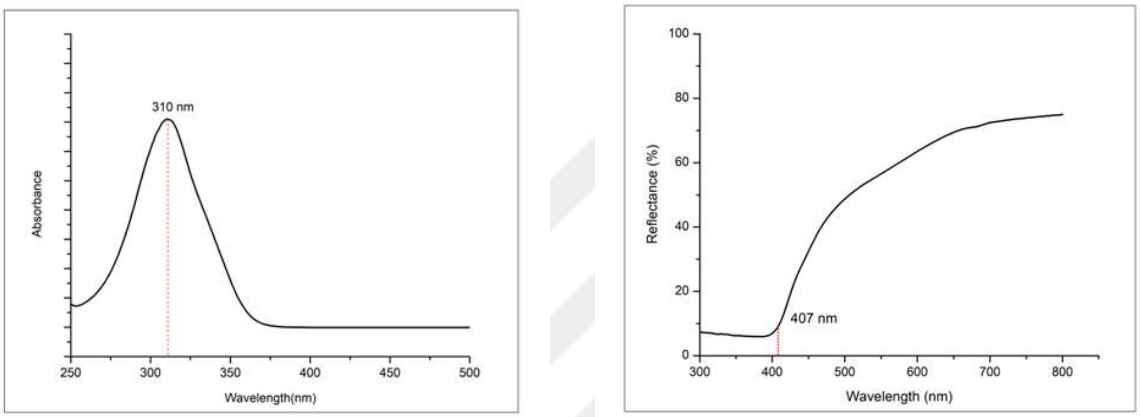

A B

Figure 13. A) UV-vis spectrum of compound **17** in DCM. B) UV-vis diffused reflectance spectrum of compound **17**

In solution phase, diester **17** has a maximum absorption at 310 nm whereas in the solid state the absorption goes up to 407 nm after which it starts reflecting the light.

In order to confirm whether the structure of different forms of diester **17** have the same crystal structure as that of single crystal XRD structure, we did the powder XRD measurements for the samples and compared them with the simulated powder XRD pattern from single crystal XRD obtained using Mercury software. These powder XRD patterns for diester **17** are shown in Figure 14.

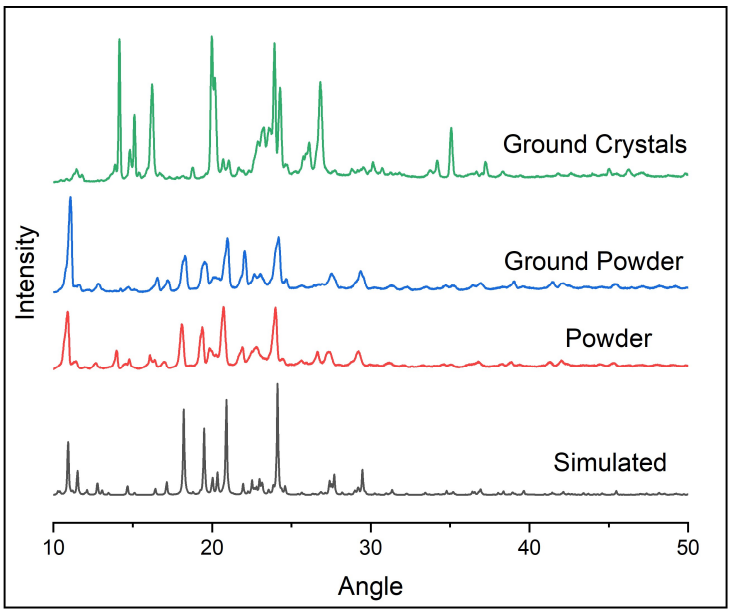

Figure 14. Powder XRD patterns of diester samples

It can be seen from Figure 14 that the powder XRD patterns of the powder and the ground powder match with the simulated XRD pattern although the diffraction intensities are weaker while the powder XRD pattern for ground crystal is different than the simulated XRD pattern. This difference in powder XRD patterns can have following two implications:

(i) The double bonds in the ground crystals may be parallel to each other and hence are suitable for photochemical dimerization.

(ii) The weaker diffraction intensities may imply that the crystals are loose, thus facilitating the pedal motion.[36]

After these detailed studies for photochemical reactivity of compound **17**, we decided to check the photoreactivity of other diester substrates **18**, **19**, and **22**. We opted irradiation of the powder in solid state for 24 h as well as irradiation in solution in $CHCl_3$. These results are summarized in Scheme 23.

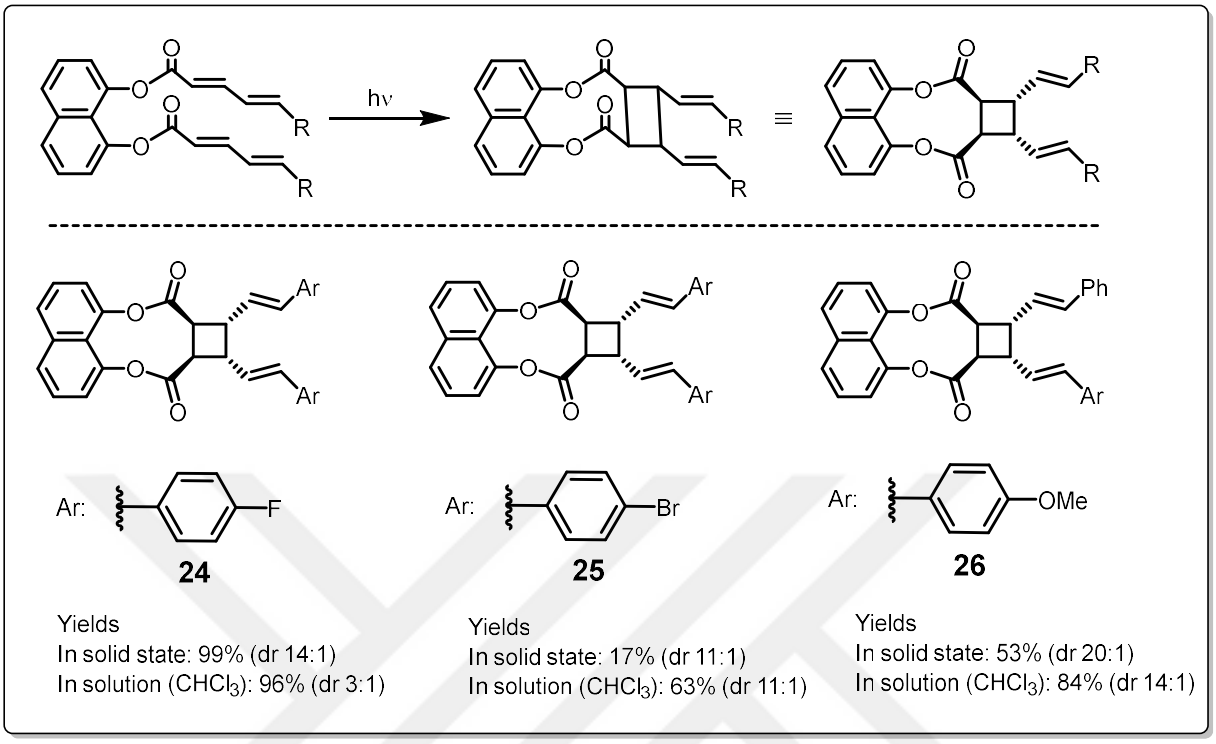

Scheme 23. Irradiation of the diester compounds **18**, **19**, and **22**

The symmetrical diester compound **18** underwent [2+2] cycloaddition in excellent yields both in solid-state and in solution in $CHCl_3$. The dr for the reactions in the solid-state and in solution were found to be 14:1 and 3:1 respectively. The diester compound **19** did not work well in the solid state but gave good results for the photochemical cycloaddition reaction in the solution in $CHCl_3$. The dr for both the reaction in solid-state and solution was 11:1. Finally, we tried the photochemical cycloaddition reaction with the unsymmetrical diester **22**. To our delight, this reaction also proceeded with good yields of 53% and 84% for solid-state and solution in $CHCl_3$ conditions, respectively. The diastereomeric ratios were also quite good for these cases. It is important to highlight that this is the first example of dimerization of two different dieneoic acids by photochemical cycloaddition reactions.

1.2.6 Investigation of the Cope Rearrangement Reaction

With the divinyl cyclobutane products obtained after irradiation, we then started investigating the thermal Cope rearrangement reaction. Our results for efforts to affect Cope rearrangement reaction of **23** are summarized below in Table 3.

Table 3. Reaction conditions for Cope rearrangement reaction of **23**

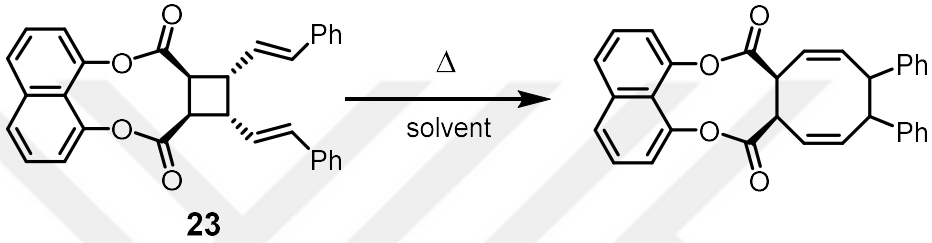

23

Entry	Temperature (°C)	Solvent	Time (h)	Result
1	60	$CDCl_3$	4	No conversion
2	100	Toluene	4	No conversion
3	130	Chlorobenzene	4	No conversion
4	130 (sealed tube)	Benzene	4	No conversion
5	160 (sealed tube)	Chlorobenzene	8	Decomposition
6	160 (sealed tube)	Chlorobenzene	4	Cyclobutane ring opening

We started our studies by heating the divinylcyclobutane **23** at 60 °C in $CDCl_3$ for 4 hours. At the end of the reaction, crude ^{1}H-NMR indicated that no reaction occurred. We then decided to increase

the reaction temperature. Heating the divinyl cyclobutane to 100 °C in toluene and 130 °C in chlorobenzene also did not affect the reaction. Literature procedures for Cope rearrangement reactions mostly involve the use of benzene as a solvent.[37,38] In our case, heating to 130 °C with benzene in a sealed tube also did not work. Heating of the reaction material at 160 °C with chlorobenzene in a sealed tube for 8 hours resulted in the decomposition of the material. But when we decreased the reaction time to 4 hours, we observed our starting diester compound by the cyclobutane ring opening. The reason might be the radical ring-opening reactions at higher temperatures.

1.2.7 Template detachment followed by Cope Rearrangement: Alternative Strategy

After our unsuccessful attempts toward the Cope rearrangement reaction, we thought that the reason for the reaction might be associated with the steric constraints implicated by the template moiety. So, we adopted an alternative strategy and decided to detach the template first, and then try the Cope rearrangement reaction.

We used a hydrolysis reaction under basic conditions to detach the template for compound **23**. Treating the template-bound cycloadduct **23** with KOH followed by acidic workup resulted in liberating the product **27** and the template **3**. Product **27** was obtained using column chromatography and characterized by ^{1}H-NMR and ^{13}C-NMR spectroscopy.

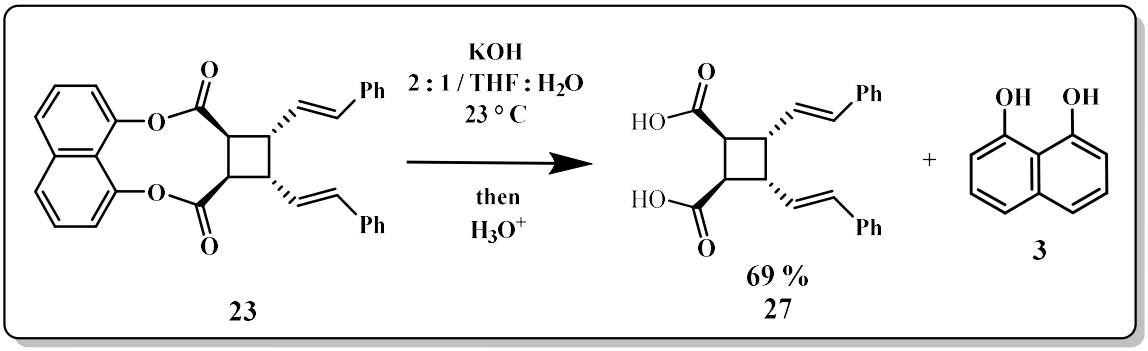

Scheme 24. Detachment of template from **23** using basic hydrolysis reaction

The reaction works well in good yields. Furthermore, we can also recover our template which can be used again making the process economical as well in accordance with the principles of green chemistry.

Although the hydrolysis reaction can be effectively used to detach the template, the resulting dicarboxylic acid product **27** might be difficult to handle for the next step. So, we also tried template detachment through a transesterification reaction. The product of this will be another diester compound which will be much easier to deal with as compared to the dicarboxylic acid product of the basic hydrolysis reaction. For this purpose, template-bound cycloadduct **23** was treated with sodium methoxide in methanol and tetrahydrofuran at room temperature (Scheme 25). The reaction progress was monitored by thin-layer chromatography. After the complete conversion of the starting material, the products of the reaction were isolated by column chromatography. Analysis of the product was done by ^{1}H-NMR and ^{13}C-NMR spectroscopy which indicated the successful synthesis of the methoxy ester cycloadduct product **28** and 1,8-dihydroxynaphthalene **3**. Similarly, other cycloadducts **24**, **25** and **26** were also subjected to the similar reaction conditions resulting in the easy detachment of the template and afforded our desired dimerization products **29**, **30**, and **31** in good yields and with a dr of 10:1, 16:1, and 14:1 respectively.

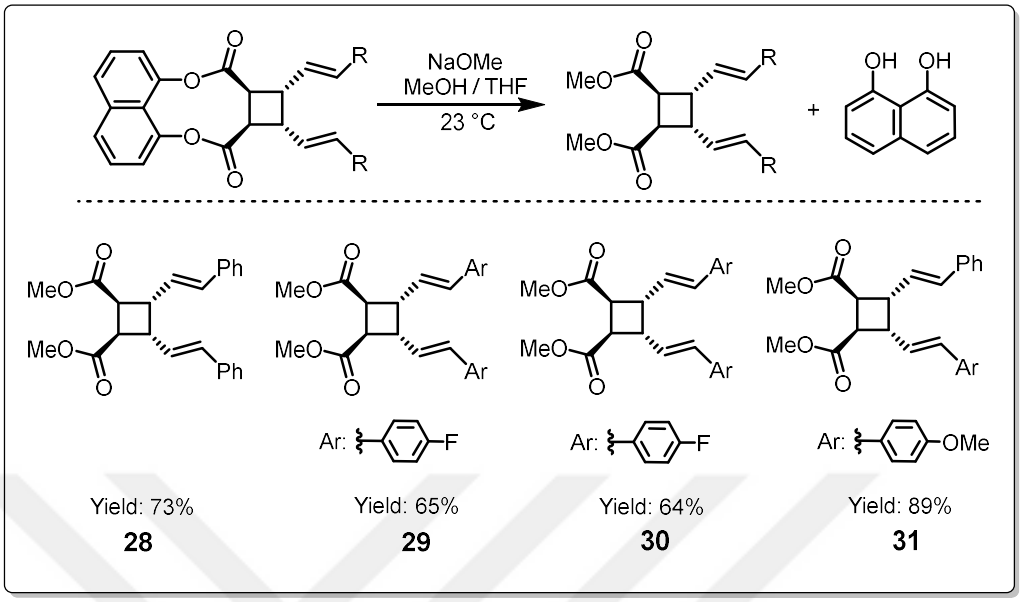

Scheme 25. Detachment of template using transesterification reaction

We also investigated the template removal using reduction reaction. By reacting the cycloadduct **23** with $LiAlH_4$, we were able to achieve template removal along with the formation of corresponding diol **32** (Scheme 26). The reaction proceeded with a yield of 65% and the obtained product **32** was characterized by ^{1}H-NMR, ^{13}C-NMR spectroscopy, ATR-IR spectroscopy and HRMS.

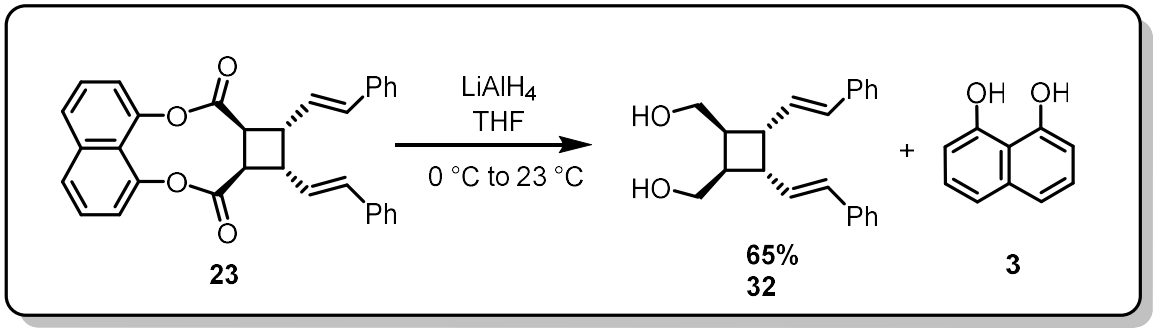

Scheme 26. Template removal of compound **23** using reduction reaction.

After the successful removal of the template molecule, we again focused our efforts on the Cope rearrangement reaction of **28**. Heating this methyl ester cyclobutane **28** in benzene at 130˚C in a sealed tube for 4 h resulted in no reaction.

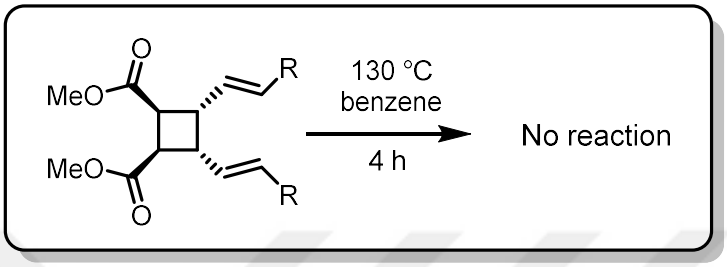

Scheme 27. Investigation of Cope rearrangement reaction of **28** at 130˚C

We then increased the reaction temperature and heated it to 160˚C in chlorobenzene for 4 h in a sealed tube. After 4 h the analysis of the reaction indicated the cyclobutane ring opening. The ^{1}H-NMR of methyl (2E,4E)-5-phenylpenta-2,4-dieneoate **33** exactly matches the reported spectrum in the literature.[39]

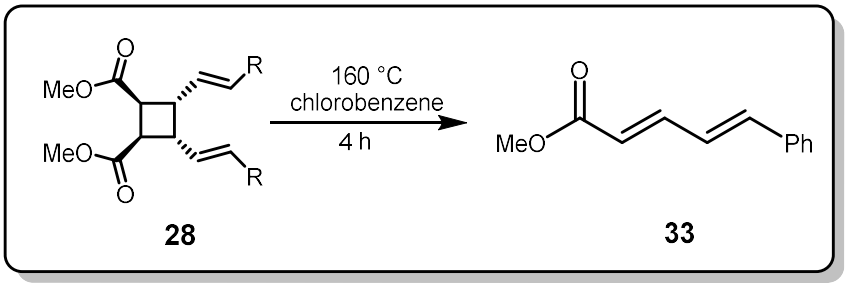

Scheme 28. Investigation of Cope rearrangement reaction of **28** at 160˚C

One of the reasons for the failure of the desired Cope rearrangement may be the difficulty in achieving the boat-like transition state. It has been observed that the presence of even a methyl group at terminal carbon of vinyl groups in divinyl cyclobutanes causes a decline in the rate of boat-like rearrangements because of steric reasons.[40,41] In our case, we have two phenyl groups at two terminal carbons of vinyl groups which may be causing severe steric repulsions in transition

state and thus hindering the Cope rearrangement. Moreover, the ring opening reaction of divinyl cyclobutanes under heating conditions has also been observed by Schmidt.[18] So, future work will be directed towards solving the Cope rearrangement reaction.

1.3 CONCLUSIONS

Photochemical dimerization reactions of dienes provide exciting opportunities as they can facilitate the rapid access to various carbocyclic compounds. Irradiation of the dienes usually gives a complex mixture of regio- and diastereomers. The use of 1,8-DHN (**3**) as a covalent template provided a solution to this problem as it aligned the alkenes according to Schmidt's criteria (observed by single crystal XRD studies) and irradiation of the template-bound diene gave selectively only the single product. Irradiation of the template-bound substrates worked almost equally well with the powder as well as ground powder and ground crystals. Furthermore, irradiation of the template-bound diene in the solution gave the cyclobutane product in high yield and with good diastereoselectivity. An important point to be stressed is that we reported the first successful unsymmetrical dimerization reaction of 5-arylpenta-2,4-dienoic acids. After dimerization, the template was removed easily either by basic hydrolysis or by transesterification reactions. Studies on the Cope rearrangement reaction of the divinyl cyclobutane product revealed the difficulties associated with the Cope rearrangement reaction. In the future, further investigations on the Cope rearrangement reaction may lead to eight-membered carbocyclic compounds.

CHAPTER 2: STUDIES TOWARD FLUORANTHENE SYNTHESIS

2.1 INTRODUCTION

2.1.1 Fluoranthenes

Fluoranthenes are a class of polycyclic aromatic hydrocarbons (PAH) having a fused cyclopentane core. The fluoranthene skeleton is shown in Figure 15.

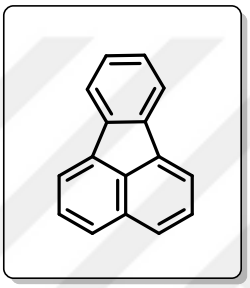

Figure 15. Fluoranthene skeleton

Fluoranthenes derive their name because of their fluorescence properties in UV light due to their rigid planar and highly conjugated structure. Frequently, fluoranthene skeleton is part of biologically active natural products which can be transformed into scaffolds for drugs. A few of the examples include Hortein which is obtained from secondary metabolites of sponge *Aplysina aerophoba,*[42] bulgarein which is present in fungus *Bulgaria inquinans* as a secondary metabolite[43] and xylarenol obtained from the extracts of xylariaeceous fungus PSU-A80.[44] Furthermore, owing to their fluorescent properties, fluoranthenes get wide utility in materials science as fluorescent materials,[45] fluorescent probes,[46] organic semi-conductors,[47] and organic light-emitting diodes (OLEDs) (Figure 16).[48]

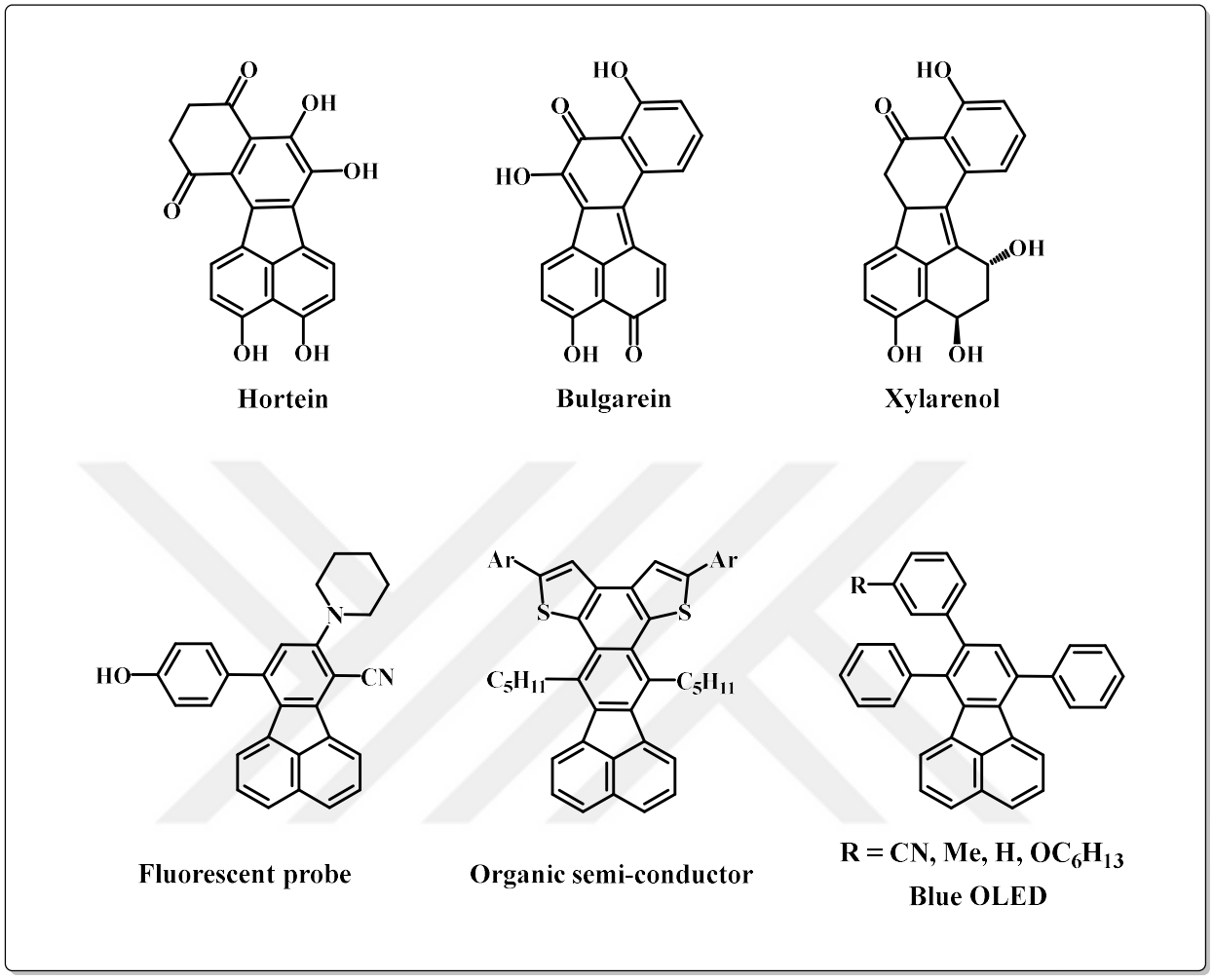

Figure 16. Applications of fluoranthene derivatives

Another interesting example of the applications of fluoranthenes is the use of fluoranthene derivative as a chemosensor for the detection of explosives. 7,10-bis(4-bromophenyl)-8-phenylfluoranthene was used successfully by Patil and co-workers for the selective detection of picric acid and trinitrotoluene (TNT) at ppb levels (Figure 17).[49]

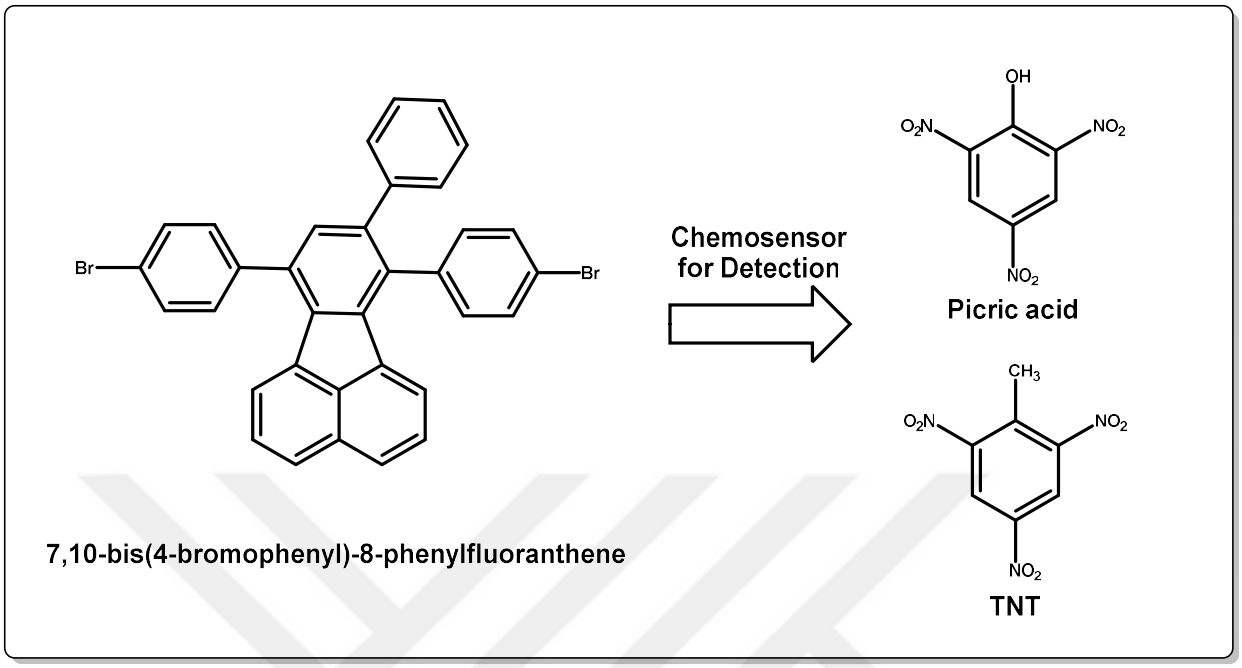

Figure 17. Fluoranthene derivative as a chemosensor for the detection of explosives

2.1.2 Syntheses of Fluoranthene Derivatives

Considering the extensive applications of fluoranthene derivatives, their synthesis is a critical subject in organic chemistry research. Therefore, several synthetic strategies for fluoranthene derivatives are devised by organic chemists, and a few of these strategies are described here.

The first strategy for the synthesis of fluoranthene derivatives was reported by Allen and co-workers in 1952. The starting material acenapthenequinone was condensed with alkyl ketones to form cyclopentadienones. Reactions of suitable unsaturated compounds with cyclopentadienones yielded fluoranthene derivatives (Scheme 29).[50]

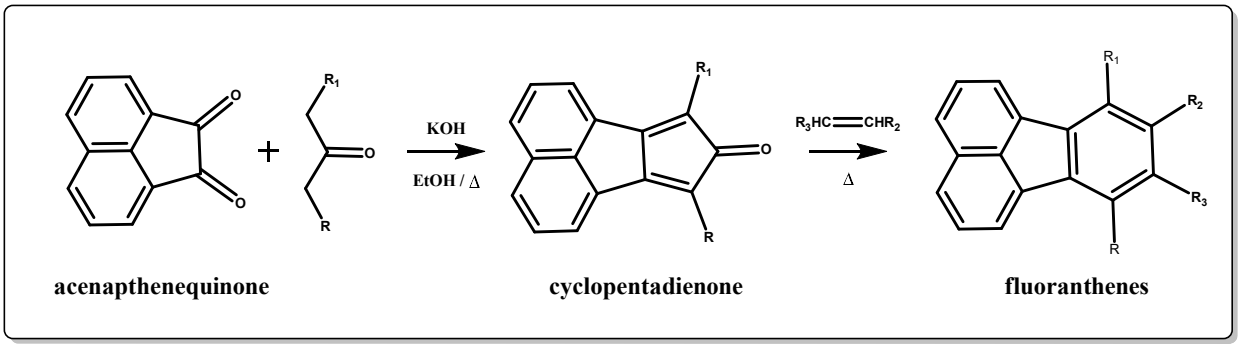

Scheme 29. Fluoranthene synthesis by Allen and co-workers

In 2011, a strategy to access 3-arylfluoranthenes **34** by hydroarylation reaction using a Gallium (III) catalyst was reported by Echavarren et al. It was also found that highly electrophilic gold(I) catalyst also works equally well and can provide the added benefit in case of aryl bromides as it does not undergo oxidative addition easily (Scheme 30).[51]

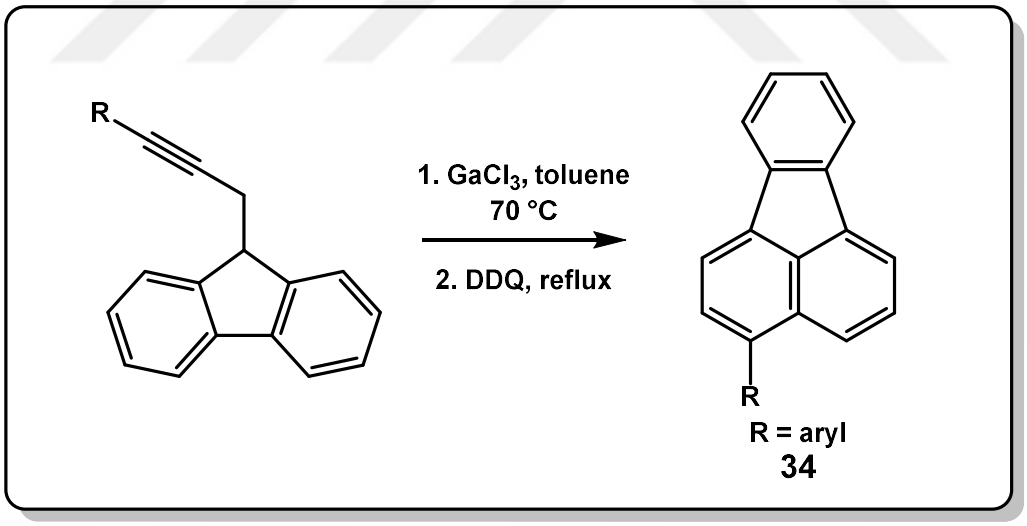

Scheme 30. Synthesis of 3-arylfluoranthenes by hydroarylation reaction

Meijere and co-workers developed a strategy for the synthesis of fluoranthene skeleton by employing a Suzuki-Heck type coupling cascade reaction. It involves the coupling of 1,2-dibromobenzene **35** with 1-napthaleneboronic acid **36** using a palladium catalyst (Scheme 31).[52]

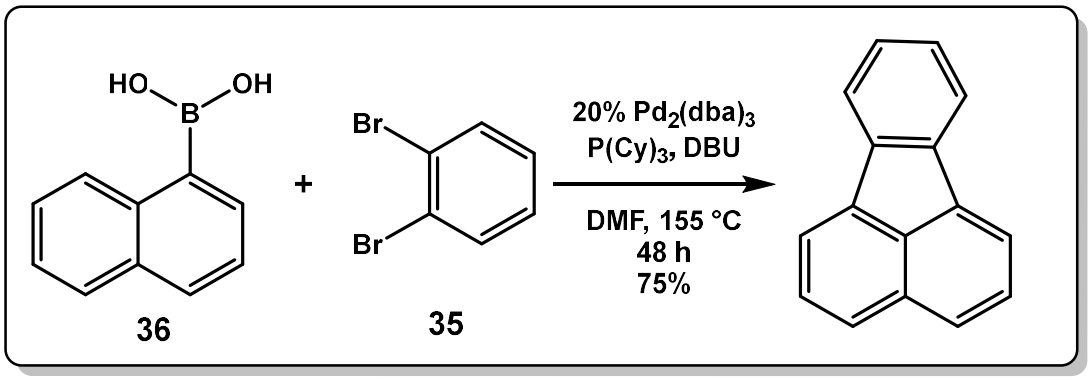

Scheme 31. Suzuki-Heck type coupling cascade reaction for fluoranthene skeleton

Another synthetic strategy involves Ruthenium-catalyzed [4+2] cycloaddition of acenaphthalene diol **37** and dienes **38** to affect the benzannulation leading to fluoranthene derivatives (Scheme 32).[53]

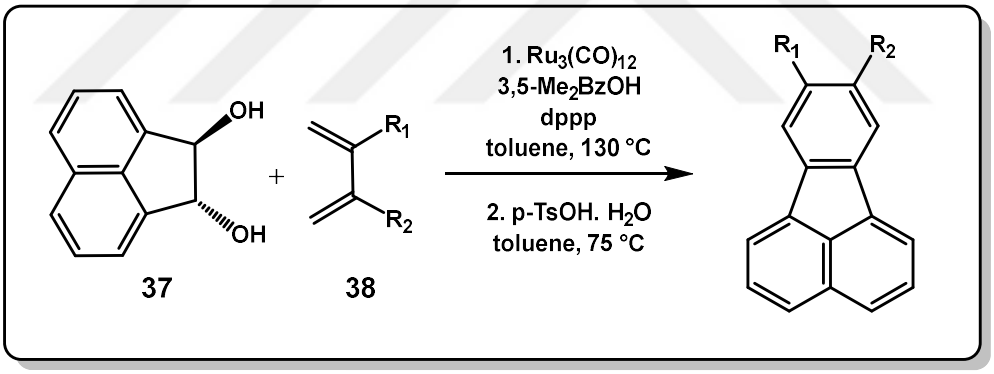

Scheme 32. Ruthenium-catalyzed [4+2] cycloaddition reaction for fluoranthenes synthesis

Tanaka and co-workers successfully attained the synthesis of fluoranthene core by rhodium-catalyzed [2+2+2] cycloaddition reaction. Reactions of 1,8-alkynylnapthalenes **39** with various alkynes **40** in the presence of cationic Rh(I) catalyst at room temperature gave substituted fluoranthenes in up to 99% yield (Scheme 33).[54]

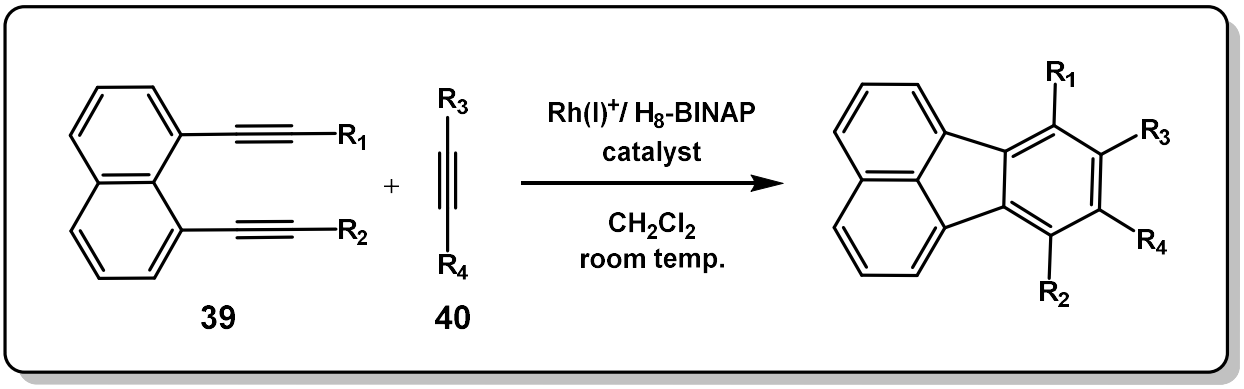

Scheme 33. Substituted fluoranthenes via Rh catalyzed [2+2+2] cycloaddition reactions.

Our group has been interested in the chemistry of fluoranthenes in the past few years. In 2017, our group reported the synthesis of fluoranthene derivatives via tandem Suzuki-Miyaura and intramolecular C-H arylation reactions. Reactions of 1,8-diiodonapthalene **41** with arylboronic acids **42** in the presence of $Pd(dppf)Cl_2$ as a homogenous catalyst or reduced graphene oxide-CuPd nanocatalyst as a heterogeneous catalyst yielded fluoranthene derivatives in good to high yields (Scheme 34).[55]

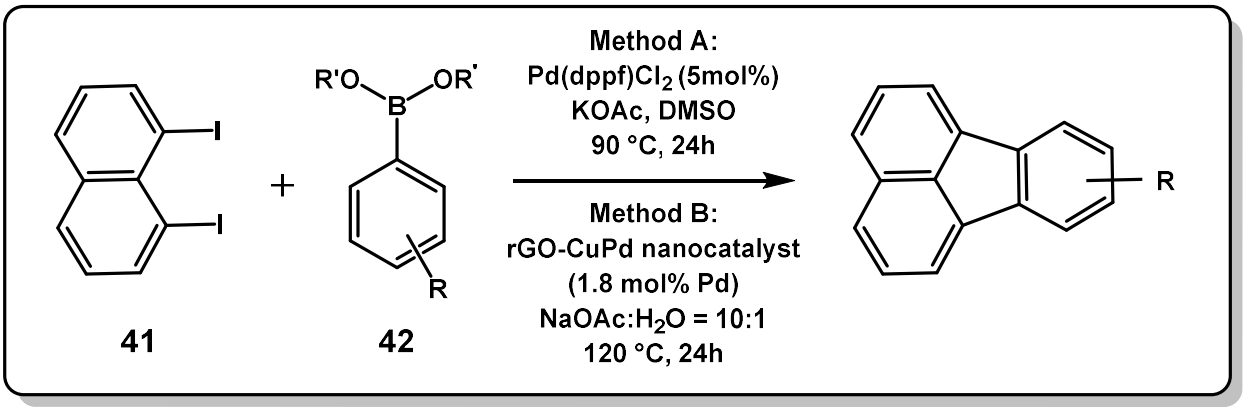

Scheme 34. Fluoranthenes from tandem Suzuki-Miyaura and intramolecular C-H arylation reactions

Having the functionalization sites on the fluoranthene skeleton can provide amazing opportunities for further expanding the substrate scope. For this purpose, hydroxyfluoranthenes can prove useful. Our group in 2021 came up with an efficient synthesis of hydroxyfluoranthenes involving domino

sequence of Suzuki-Miyaura, intramolecular Diels-Alder reaction, and ring-opening reactions. 1,8-diiodonapthalene **41** was subjected to a Sonogashira coupling reaction to get 1-iodo-8-alkynlnapthalene **43** selectively. Reactions of 1-iodo-8-alkynlnapthalene with 2-furylboronic acid initiate a domino sequence resulting in the direct synthesis of hydroxyfluoranthenes (Scheme 35).[56]

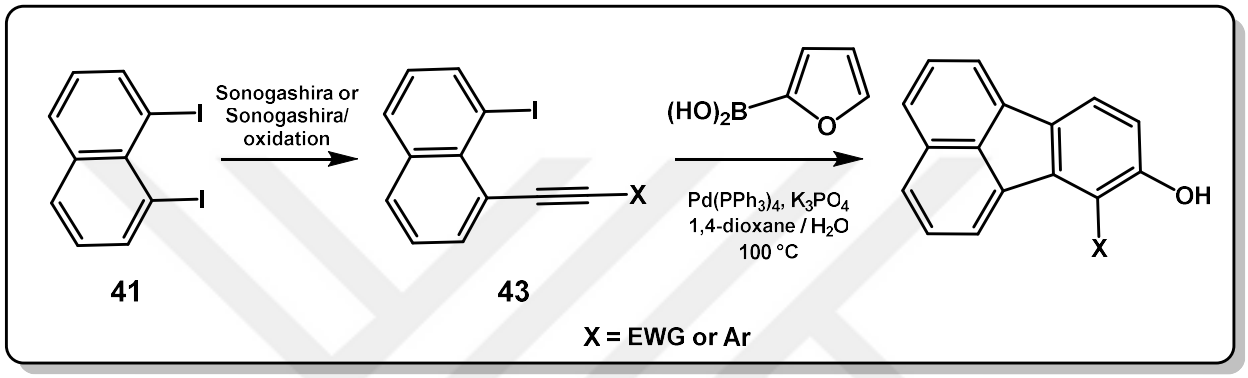

Scheme 35. Domino reaction sequence for hydroxyfluoranthenes synthesis

2.1.3 Aim of the work

Although a number of synthetic pathways to access substituted fluoranthenes have been devised by organic chemists in the past few decades, the problem is that most of these pathways suffer from harsh reaction conditions. Moreover, they also have a limited substrate scope. Synthesis of hydroxyfluoranthenes by domino sequence (Scheme 35), provided an excellent solution to these problems. This sequence involves a Diels-Alder reaction between a furan-an electron-rich diene and electron-poor alkynes as a dienophile. The aim of this work is to utilize an inverse electron demand Diels-Alder (IEDDA) reaction between a pyridazine- an electron-poor diene and electron-rich alkynes as dienophiles to synthesize fluoranthene derivatives. For this purpose, again 1,8-positions of naphthalene can be employed to bring the dienes and dienophiles closer for a successful IEDDA reaction. The use of both different substituted pyridazines and various alkynes will lead to diverse fluoranthenes. The proposed synthesis plan is shown in Scheme 36.

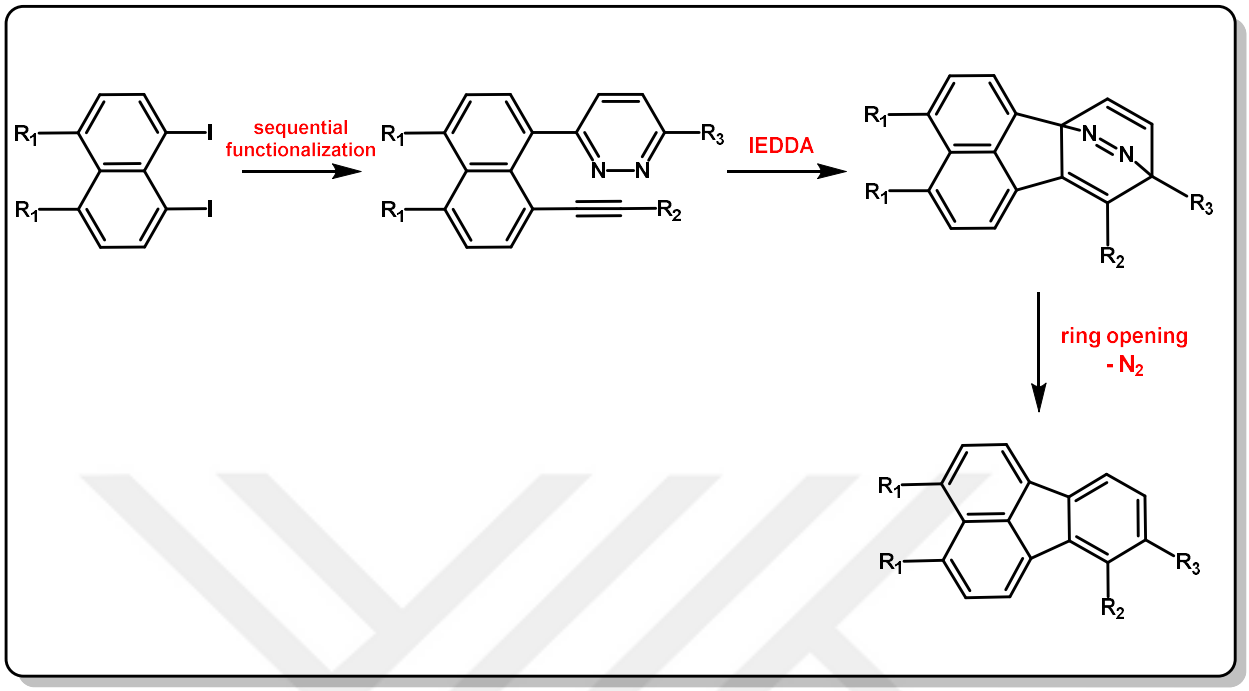

Scheme 36. Aim of the work

2.2 RESULTS AND DISCUSSIONS

The first steps in the synthetic sequence involve the functionalization of 1,8-diiodonapthalene to introduce suitable diene and dienophile analogs for an inverse electron-demand Diels-alder reaction. We first focused on the attachment of the pyridazine ring to the naphthalene core which will function as electron-poor diene. For this purpose, we first converted commercially available 3,6-dibromopyridazine (**44**) to 3-bromo-6-methoxypyridazine (**45**). This was achieved by a nucleophilic aromatic substitution reaction with sodium methoxide in methanol/THF at 55˚C and is shown in Scheme 37.

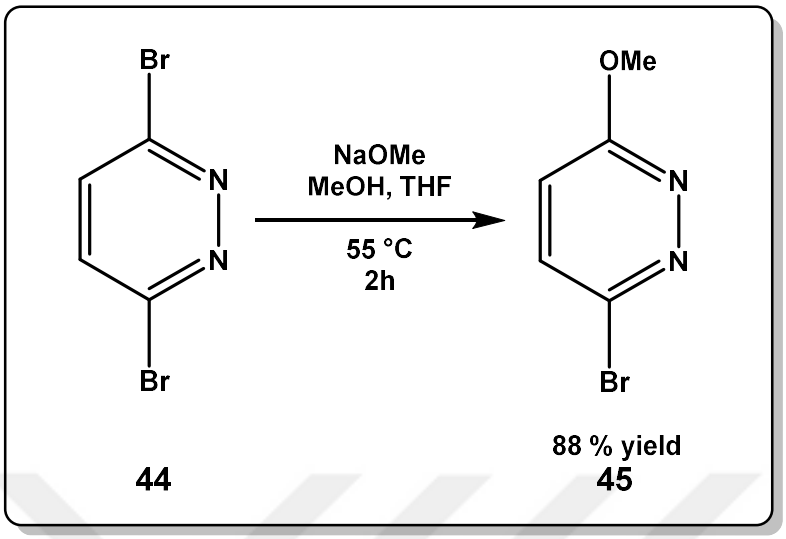

Scheme 37. Synthesis of 3-bromo-6-methoxypyridazine **45**

After synthesizing 3-bromo-6-methoxypyridazine, we tried borylation reactions with **45** to get corresponding boronic esters. Treatment of compound **45** with B_2pin_2 and HBpin as borylation agents was found to lead to the dimerization product and protodeboronation product respectively by our former group members. So, we tested *i*-PrOBpin as a borylation agent, but unfortunately, these conditions could not afford desired boronic esters (Scheme 38).

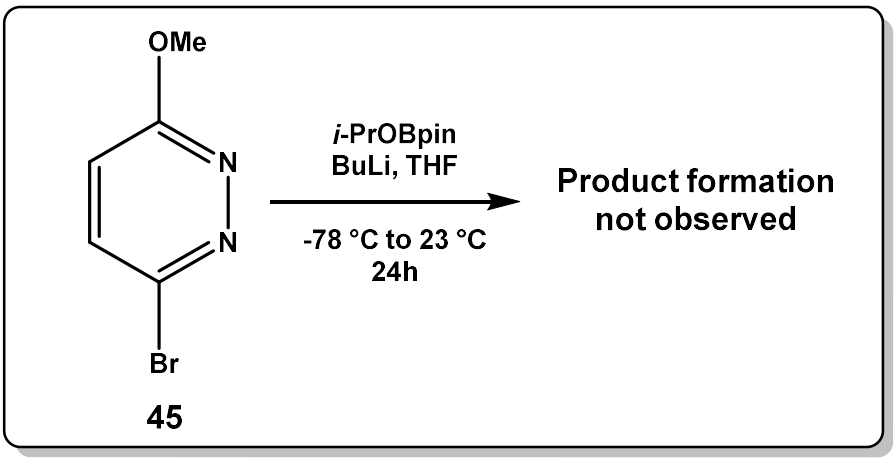

Scheme 38. Borylation of **45** using *i*-PrOBpin reagent

One of the reasons for getting the dimerization product in the case of Suzuki-Miyaura borylation conditions can be the presence of an electron-donating methoxy group at the pyridazine ring. To solve this problem, we decided to introduce a group that is not electron-donating. 2,2,2-trifluoroethoxy group has been used for medicinal compounds, and it also provides an added benefit of facile removal. So, it can provide a solution to our problem. Treatment of 3,6-dibromopyridazine (**44**) with trifluoroethanol and potassium tert-butoxide as a base in THF resulted in our desired 3-bromo-6-(2,2,2-trifluoroethoxy)pyridazine (**46**) in 58% yield (Scheme 39).

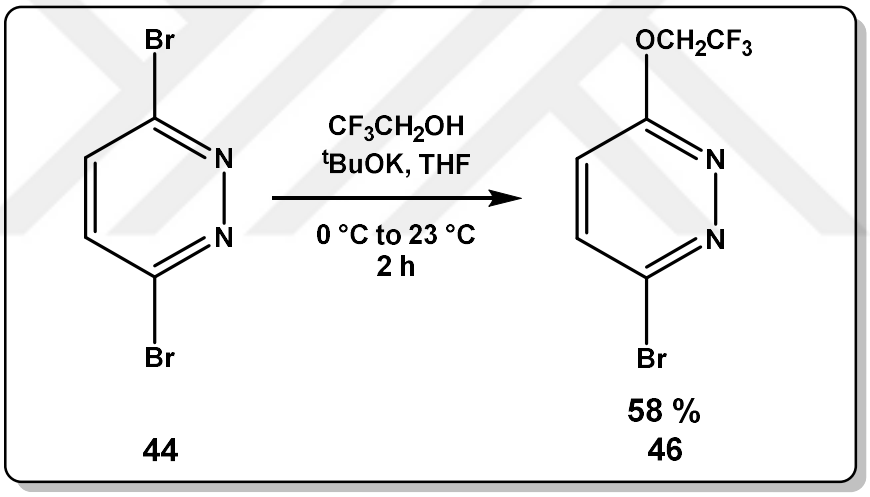

Scheme 39. Synthesis of 3-bromo-6-(2,2,2-trifluoroethoxy)pyridazine (**46**).

Suzuki-Miyaura borylation reaction of 3-bromo-6-(2,2,2-trifluoroethoxy)pyridazine (**46**) once again resulted in the formation of the dimerization product **47** which was characterized by ^{1}H-NMR, ^{13}C-NMR, and ^{19}F-NMR spectroscopy (Scheme 40).

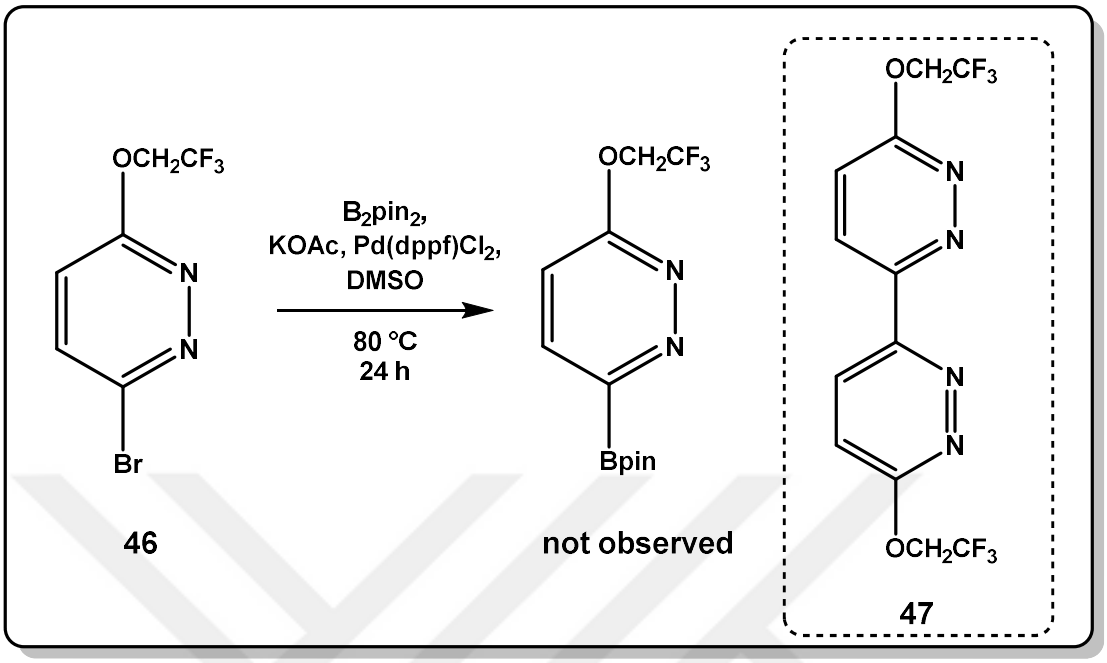

Scheme 40. Suzuki-Miyaura borylation of 3-bromo-6-(2,2,2-trifluoroethoxy)pyridazine (**46**).

After being unable to achieve the essential borylation reaction, we steered towards a different C(aryl)-C(aryl) bond formation reaction. Ullmann coupling reaction has been demonstrated as a useful reaction for connecting two aryl groups for almost a century. In order to establish the optimized reaction conditions for the Ullmann coupling reaction, we experimented with iodobenzene (**48**) and 3-bromo-6-methoxypyridazine (**45)** as coupling partners. Different reaction conditions are shown in Table 4.

Table 4. Reaction conditions for Ullmann coupling reaction between **45** and **48**

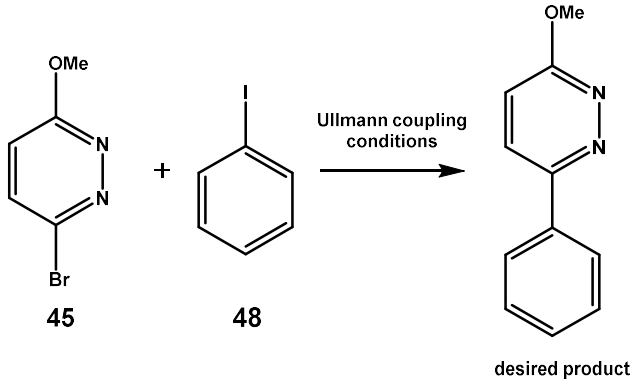

Sr. No.	Cu Source (equiv.)	Solvent	Temperature (°C)	Time (h)	Result
1	Sigma-Aldrich (3)	DMF	140	4	Product not obtained
2	Acros (3)	DMF	140	4	Product not obtained
3	Cu-bronze (3)	DMF	140	4	Product not obtained
4	Acros (3)	DMF	140	7	Product not obtained
5	Acros (4)	DMF	140	18	Product not obtained
6	Acros (7)	DMF	140	3	Product not obtained
7	Acros (3)	DMSO	160	5	Complex mixture observed
8	Acros (3)	DMSO	160	20	Complex mixture observed

Ullmann coupling reaction did not yield the desired product. Then, we opted to introduce the boronic ester group at 1-iodo-8-alkynylnapthalene **49**. We tried borylation reactions under two

different reaction conditions; both of these resulted in complex mixtures rendering this strategy ineffective (Scheme 41).

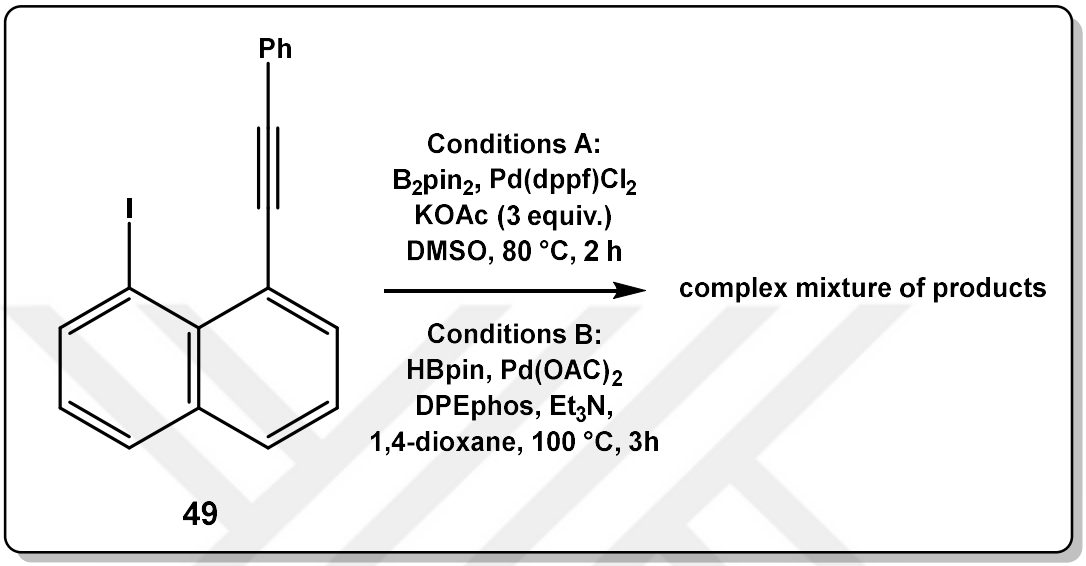

Scheme 41. Borylation reactions for 1-iodo-8-alkynlnapthalene **49**

After futile attempts to affect borylation reaction of 1-iodo-8-alkynlnapthalene **(49)**, the Ullmann coupling reaction was tested with 1-iodo-8-alkynlnapthalene **(49)** and 3-bromo-6-methoxypyridazine (**45**). This effort also could not find success as our desired compound was not obtained (Scheme 42).

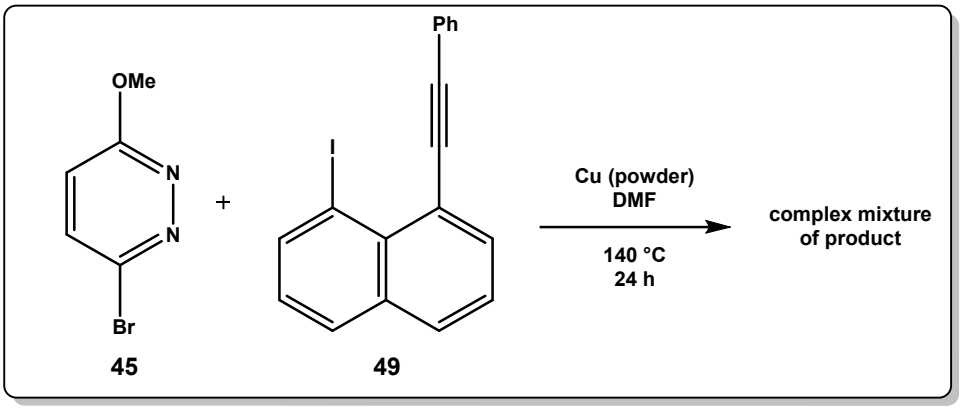

Scheme 42. Ullmann coupling reaction between **44** and **49.**

2.3 CONCLUSIONS

We investigated the synthesis of precursors for an inverse electron demand Diels-Alder reaction starting from 1,8-diiodonapthalene (**40**) having the potential to undergo domino reaction sequence ultimately yielding fluoranthenes. For this purpose, we tried several borylation reactions of the pyridazine ring, which can be used as an intermediate for aryl-aryl bond formation. After being unable to achieve the desired boronic ester of pyridazine, we tried the Ullmann coupling reaction. Different reaction conditions were screened for Ullmann coupling between 3-bromo-6-methoxypyridazine (**44**) and iodobenzene (**47**) (as a model substrate), all of which gave complex mixtures of products. Lastly, our attempts at the Suzuki-Miyaura borylation reaction and the Ullmann coupling reaction with 1-iodo-8-alkynlnapthalenes **48** were also unsuccessful.

Please note that although a lot of research has been done on the development of aryl-aryl bond formation reactions, to the best of our knowledge, there is no aryl-aryl bond formation for pyridazines at position 3. The development of such a reaction can be advantageous for the success of our strategy to access fluoranthenes.

CHAPTER 3: EXPERIMENTAL SECTION

3.1 Materials and Methods

All the solution-phase chemical reactions were carried out in oven-dried or flame-dried glassware and under an inert atmosphere (nitrogen). Photochemical experiments were performed using either a reactor consisting of a 400-W medium-pressure mercury lamp purchased from Photochemical Reactors Ltd. (inside a safety cabinet) or using a commercial UV gel nail dryer (Beurer) consisting of four 9-W UV lamps. Thin layer chromatography (TLC) using aluminum-backed plates with precoated silica gel (Merck, Silica Gel 60 F_{254}) was used to monitor the progress of the reactions. UV light (254 nm) and $KMnO_4$ solutions were used for the TLC visualization. Silicycle 40-63 μm (230-400 mesh) flash silica gel was used for the purification by flash column chromatography. NMR spectra were obtained using a Bruker NMR spectrometer at 400 MHz for ^{1}H-NMR spectra, 100 MHz for ^{13}C-NMR spectra, and 376 MHz for ^{19}F-NMR. Calibrations were done from internal standard TMS (0 ppm) or residual solvent signals (chloroform at 7.26 ppm and methanol at 3.31 ppm) for ^{1}H-NMR spectra, chloroform at 77.16 ppm, and methanol at 49.00 ppm for ^{13}C-NMR spectra and trifluoroacetic acid at -76.55 ppm for ^{19}F-NMR spectra. ^{1}H-NMR data is reported as follows: chemical shift (parts per million, ppm), multiplicity (s = singlet, d = doublet, t = triplet, q = quartet, dd = double of doublet, m = multiplet, app = apparent), coupling constant (Hz) and integration. Powder XRD patterns were recorded on a Rigaku Miniflex diffractometer equipped with a Cu K_α (λ = 1.5405 Å) X-ray source. Infrared (FTIR) spectra were recorded on a Bruker Alpha-Platinum-ATR spectrometer, and only selected peaks are reported. Single crystal XRD measurements were performed at Gebze Technical University. Mass Spectral Analyses were performed using Q-TOF/LCMS at National Nanotechnology Research Center and Institute of Materials Science and Nanotechnology, Bilkent University.

All of the chemicals used were purchased from Merck, Acros Organics, Sigma-Aldrich, TCI, and Alfa Aeser and were used without further purification.

3.2 Reaction Procedures for Chapter 1

3.2.1 Compound 10

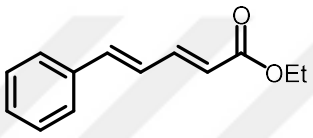

Triethylphosphonoacetate **9** (2206 mg, 9.84 mmol) was dissolved in 13 mL of DME in an oven-dried 50 mL round-bottom flask under nitrogen at 23 ˚C. To this solution cooled in an ice bath, NaH (453 mg, 11.36 mmol, 60% dispersion in mineral oil) was added slowly. Upon the addition of NaH, gas evolution was observed. The reaction mixture was allowed to stir for 25 minutes. Then, *trans*-cinnamaldehyde **4** (1000 mg, 7.57 mmol) was added to the reaction mixture and was allowed to stir at 23 ˚C for 2h. Reaction progress was monitored using TLC (1:19 EtOAc: hexanes). The reaction was quenched with a saturated aqueous solution of NH_4Cl (15 mL). The aqueous phase was extracted thrice with DCM. The organic phases were combined, dried with Na_2SO_4, filtered, and concentrated in a vacuum. Purification was done using column chromatography (1:19 EtOAc : hexanes) to yield a pure product **10** (1499 mg, 98%) as a pale yellowish oil.

$\boldsymbol{R_f}$ = 0.42 (1:19 EtOAc : hexanes)

TLC Visualization : UV and $KMnO_4$ active

^{1}H-NMR (400 MHz, $CDCl_3$) δ : 7.44-7.36 (3H, m), 7.30-7.21 (3H, m), 6.82-6.74 (2H, m), 5.96 (1H, d, *J* = 15.3 Hz), 4.21 (2H, q, *J* = 7.1 Hz), 1.28 (3H, t, *J* = 7.1 Hz)

^{13}C-NMR (100 MHz, $CDCl_3$) δ : 167.2, 144.6, 140.5, 136.2, 129.1, 128.9, 127.3, 126.4, 121.5, 60.5, 14.5

FTIR ν_{max} (ATR, film)/cm^{-1} : 3027, 2980, 2926, 1704, 1625, 1448

NMR data for **10** match the reported data in the literature.[57]

3.2.2 Compound 11

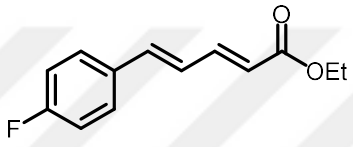

Compound **11** was prepared from (*E*)-3-(4-fluorophenyl)acrylaldehyde (500 mg, 435 µL, 3.33 mmol), triethylphosphonoacetate **9** (1119 mg, 4.995 mmol), NaH (200 mg, 4.995 mmol, 60% dispersion in mineral oil) and DME (5 mL) following the same procedure as used for compound **10**. The crude product was purified using flash column chromatography (SiO_2; EtOAc:hexanes = 1:19) to afford **11** (612 mg, 83%) as a white solid.

***R_f* =** 0.42 (1:19 EtOAc : hexanes)

TLC Visualization : UV and $KMnO_4$ active

^{1}H-NMR (400 MHz, $CDCl_3$) δ : 7.41-7.35 (3H, m), 6.99 (2H, d, *J* = 8.6 Hz), 6.81-6.69 (2H, m), 5.94 (1H, d, *J* = 15.2 Hz), 4.19 (2H, q, *J* = 7.2 Hz), 1.27 (3H, t, *J* = 7.1 Hz)

^{13}C-NMR (100 MHz, $CDCl_3$) δ : 166.9, 163.0 (d, *J* = 249.7 Hz) 144.3, 138.9, 132.3 (d, *J* =3.4 Hz), 128.9 (*J* = 8.2 Hz), 126.0 (*J* = 2.4 Hz), 121.4, 115.8 (*J* = 21.9 Hz), 60.3, 14.3

^{19}F-NMR (376 MHz, $CDCl_3$) δ : = -110.4 (s)

NMR data for **11** match the reported data in the literature.[58]

3.2.3 Compound 12

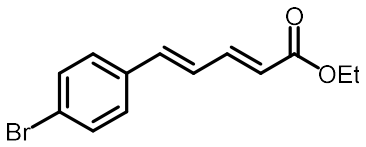

Compound **12** was prepared from (*E*)-3-(4-bromophenyl)acrylaldehyde (450 mg, 2.13 mmol), triethylphosphonoacetate **9** (621 mg, 2.77 mmol), NaH (128 mg, 3.19 mmol, 60% dispersion in mineral oil) and DME (7 mL) using the same procedure as used for compound **10**. The crude product was purified using flash column chromatography (SiO_2; EtOAc:hexanes = 1:19) to afford **12** (523 mg, 88%) as a white solid.

R_f = 0.42 (1:9 EtOAc : hexanes)

TLC Visualization : UV and $KMnO_4$ active

^{1}H-NMR (400 MHz, $CDCl_3$) δ : 7.46 (2H, d, *J* = 8.4 Hz), 7.41 (1H, ddd, *J* = 15.4, 8.7, 1.4 Hz), 7.30 (2H, d, *J* = 8.5 Hz), 6.89-6.75 (2H, m), 5.99 (1H, d, *J* = 15.3 Hz), 4.22 (2H, q, *J* = 7.1 Hz), 1.30 (2H, t, *J* = 7.1 Hz)

^{13}C-NMR (100 MHz, $CDCl_3$) δ : 167.0, 144.2, 138.9, 135.1, 132.1, 128.7, 127.1, 123.1, 122.1, 60.5, 14.4

NMR data for **12** match the reported data in the literature.[59]

3.2.4 Compound 13

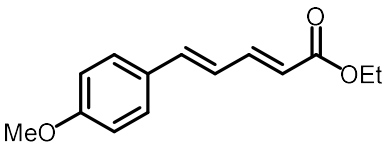

Compound **13** was prepared from (*E*)-3-(4-methoxyphenyl)acrylaldehyde (500 mg, 3.08 mmol), triethylphosphonoacetate **9** (1036 mg, 917 µL, 4.62 mmol), NaH (111 mg, 4.62 mmol, 60% dispersion in mineral oil) and DME (10 mL) using the same procedure as used for compound **10**. The crude product was purified using flash column chromatography (SiO_2; EtOAc:hexanes = 1:19) to afford **13** (557 mg, 78%) as a white solid.

R_f = 0.30 (1:19 EtOAc : hexanes)

TLC Visualization : UV and $KMnO_4$ active

^{1}H-NMR (400 MHz, $CDCl_3$) δ : 7.49-7.36 (3H, m), 6.93-6.82 (3H, m), 6.75 (1H, dd, *J* = 15.5, 10.8 Hz), 5.94 (1H, d, *J* = 15.3 Hz), 4.22 (2H, q, *J* = 7.1 Hz), 3.83 (3H, s), 1.31 (3H, t, *J* = 7.1 Hz)

^{13}C-NMR (100 MHz, $CDCl_3$) δ : 167.4, 160.6, 145.1, 140.2, 129.1, 128.8, 124.4, 120.2, 114.4, 60.4, 55.5, 14.5

NMR data for **13** match the reported data in the literature.[54]

3.2.5 Compound 2

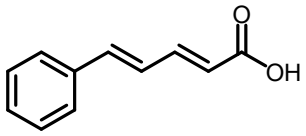

To a solution of compound **10** (1000 mg, 4.94 mmol) in 1:1 MeOH and THF (10 mL) at 23˚C in a 100 mL round-bottom flask, 5N aqueous solution of KOH (5 mL) was added, and the reaction mixture was allowed to stir. Progress of the reaction was monitored using TLC (1:1 EtOAC: hexanes). Full consumption of SM was observed after 1h. The reaction solvents were removed directly under reduced pressure, and a white slurry was obtained. This white slurry was dissolved in fresh $CHCl_3$ and conc. HCl was added dropwise to it until the pH of the solution turned 1-2. The

organic phase was washed with distilled water, and then the aqueous phase was extracted with EtOAC thrice. Organic phases were combined, dried with Na_2SO_4, filtered, and concentrated in vacuum to yield the pure product **2** (841 mg, 98%) as a shiny white solid.

R_f = 0.69 (1:1 EtOAc: hexanes)

TLC Visualization : UV and $KMnO_4$ active

^{1}H-NMR (400 MHz, $CDCl_3$) δ : 7.55 (1H, dd, *J* = 15.1, 9.7 Hz), 7.49(2H, app d, *J* = 6.9 Hz), 7.39-7.31 (m, 3H), 6.99-6.87 (m, 2H), 6.01 (d, J=15.3 Hz, 1H)

^{13}C-NMR (100 MHz, $CDCl_3$) δ : 172.5, 147.1, 141.8, 136.0, 129.5, 129.0, 127.5, 126.1, 120.5

FTIR ν_{max} (ATR, film)/cm^{-1} : 3053, 3023, 2925, 1677, 1450

NMR data for **2** match the reported data in the literature.[60]

3.2.6 Compound 14

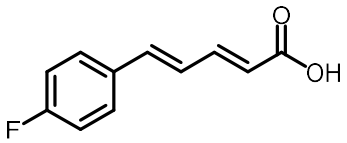

Compound **14** was prepared using **11** (620 mg, 2.82 mmol), 5N KOH aqueous sol. (10 mL), MeOH (5 mL) and THF (10 mL) using the same procedure as used for compound **2**. After workup, **14** (520 mg, 96%) was obtained as a white solid.

R_f = 0.55 (1:1 EtOAc : hexanes)

TLC Visualization : UV and $KMnO_4$ active

^{1}H-NMR (400 MHz, $CDCl_3$) δ : 7.57 (3H, m), 7.06 (2H, t, *J* = 8.2 Hz), 6.91 (1H, d, *J* = 15.7 Hz), 6.82 (1H, dd, *J* = 15.7, 10.7 Hz) 5.99 (1H, d, *J* = 15.1 Hz)

^{13}C-NMR (100 MHz, DMSO-*d6*) δ : 167.6, 162.3 (d, *J* = 247.0 Hz), 143.9, 138.3, 132.7 (d, *J* = 3.1 Hz), 129.2 (d, *J* = 8.4 Hz), 126.6 (d, *J* = 2.4 Hz), 122.6, 115.7 (d, *J* = 21.6 Hz)

^{19}F-NMR (376 MHz, $CDCl_3$) δ : -109.9 (s)

NMR data for **14** match the reported data in the literature.[55,61]

3.2.7 Compound 15

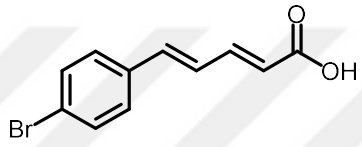

Compound **15** was prepared using **12** (520 mg, 1.86 mmol), 5N KOH aqueous sol. (6 mL), MeOH (3 mL) and THF (5 mL) using the same procedure as used for compound **2**. After workup, **15** (416 mg, 89%) was obtained as a white solid.

R_f **=** 0.38 (1:1 EtOAc : hexanes)

TLC Visualization : UV and $KMnO_4$ active

^{1}H-NMR (400 MHz, DMSO-*d6*) δ : 7.59 (2H, d, *J* = 8.5 Hz), 7.52 (2H, d, *J* = 8.5 Hz), 7.33 (1H, dd, *J* = 15.1, 10.7 Hz), 7.15 (1H, dd, *J* = 15.5, 10.7 Hz), 7.03 (1H, d, *J* = 15.6 Hz), 6.03 (1H, d, *J* = 15.1 Hz)

^{13}C-NMR (100 MHz, DMSO-*d6*) δ : 167.4, 144.0, 138.4, 135.3, 131.8, 129.0, 127.5, 122.8, 122.0

NMR data for **15** matches the reported data in the literature.[62]

3.2.8 Compound 16

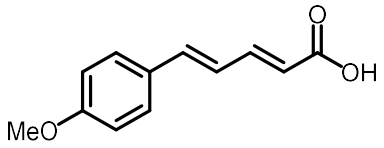

Compound **16** was prepared using **13** (495 mg, 2.13 mmol), 5N KOH aqueous sol. (20 mL), MeOH (10 mL) and THF (20 mL) using the same procedure as used for compound **2**. After workup, **16** (425 mg, 98%) was obtained as a pale yellow solid.

R_f = 0.42 (1:1 EtOAc : hexanes)

TLC Visualization : UV and $KMnO_4$ active

^{1}H-NMR (400 MHz, DMSO-*d6*) δ : 12.15 (1H, s), 7.51 (2H, d, *J* = 8.8 Hz), 7.32 (1H, ddd, *J* = 15.2, 9.0, 1.2 Hz), 7.02-6.89 (4H, m), 5.93 (1H, d, *J* = 15.2 Hz), 3.78 (3H, s)

^{13}C-NMR (100 MHz, DMSO-*d6*) δ : 167.6, 160.0, 144.8, 139.7, 128.7, 124.3, 120.8, 114.3, 56.2

NMR data for **16** match the reported data in the literature.[63]

3.2.9 Compound 17

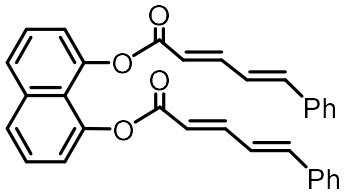

Carboxylic acid **2** (900 mg, 5.16 mmol) was dissolved in 12 mL of dry DCM in an oven-dried 100 mL round-bottom flask under nitrogen at 23 ˚C. To this solution, 1,8-DHN **3** (276 mg, 1.72 mmol), DCC (1135 mg, 5.50 mmol), and DMAP (63.5 mg, 0.52 mmol) were added sequentially. The reaction mixture was allowed to stir at 23 ˚C for 24h. The reaction mixture was filtered through celite (DCM was used to aid filtration). The organic phase was washed with distilled water, and

the aqueous phase was extracted with DCM thrice. Organic phases were combined, filtered, and concentrated in vacuum. Purification by column chromatography (SiO_2; DCM:hexanes = 1:1) gave the pure product **17** (462 mg, 57%) as a white solid.

Note: The compound is light-sensitive so it should be kept in dark.

R_f = 0.22 (1:1 DCM: hexanes)

TLC Visualization: UV and $KMnO_4$ active

^{1}H-NMR (400 MHz, $CDCl_3$) δ : 7.80 (2H, d, *J* = 8.3 Hz,), 7.62 (2H, dd, *J* = 15.3 Hz, 10.3 Hz), 7.48 (2H, t, *J* =7 .9 Hz), 7.27-7.21 (6H, m), 7.19-7.14 (6H, m), 6.92-6.80 (4H, m), 6.15 (2H, d, *J* = 15.3 Hz).

^{13}C-NMR (100 MHz, $CDCl_3$) δ: 166.0, 146.9, 145.4, 142.0, 137.0, 135.7, 129.3, 128.9, 127.4, 127.0, 126.2, 126.0, 121.6, 120.8, 120.8

FTIR ν_{max} (ATR, film)/cm^{-1} : 3055, 3024, 1728, 1621, 1448, 1345, 1312, 1225, 1167.

HRMS (ESI +) Calcd for $C_{32}H_{24}NaO_4$ $[M+Na]^+$: 495.1567, found 495.1543.

3.2.10 Compound 18

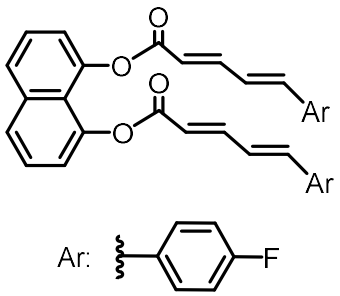

Compound **18** was prepared using **14** (179 mg, 0.93 mmol), 1,8-DHN (50 mg, 0.31 mmol), DCC (204 mg, 0.99 mmol), DMAP (11 mg, 0.09 mmol) and DCM anhydrous (10 mL) was the same

procedure as used for compound **17**. Purification by flash colomn chromatography (SiO_2; DCM:hexanes = 1:1) afforded **18** (103 mg, 66%) as a white solid.

Note: The compound is light-sensitive so it should be kept in dark.

R_f = 0.63 (1:1 DCM : hexanes)

TLC Visualization : UV and $KMnO_4$ active

^{1}H-NMR (400 MHz, $CDCl_3$) δ : 7.82 (2H, d, *J* = 8.3 Hz), 7.58 (2H, dd, *J* = 15.3, 10.7 Hz), 7.49 (2H, t, *J* = 7.9 Hz), 7.24-7.14 (6H, m), 6.90-6.79 (6H, m), 6.72 (2H, dd, *J* = 15.6, 10.7 Hz), 6.14 (2H, d, *J* = 15.3 Hz)

^{13}C-NMR (100 MHz, $CDCl_3$) δ : 165.9, 163.4 (d, *J* = 250.7 Hz), 146.6, 145.4, 140.4, 137.0, 131.9 (d, *J* = 2.9 Hz), 129.0 (d, *J* = 8.2 Hz), 127.0, 126.2, 125.8 (d, *J* = 2.4 Hz), 121.0, 120.8, 116.0 (d, *J* = 21.9 Hz)

^{19}F-NMR (376 MHz, $CDCl_3$) δ : -109.9 (s)

FTIR ν_{max} (ATR, film)/cm^{-1} : 2957, 2920, 2851, 1744, 1723, 1625, 1597, 1508, 1234, 1156.

HRMS (ESI +) Calcd for $C_{32}H_{22}NaO_4F_2$ $[M+Na]^+$: 531.1378, found 531.1380.

3.2.11 Compound 19

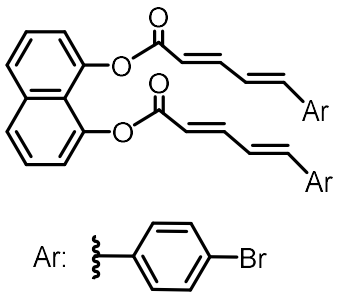

Compound **19** was prepared using **15** (50 mg, 0.21 mmol), 1,8-DHN (11.2 mg, 0.07 mmol), DCC (43.3 mg, 0.21 mmol), DMAP (2.8 mg, 0.02 mmol) and DCM anhydrous (5 mL) was the same procedure as used for compound **17**. Purification by flash colomn chromatography (SiO_2; DCM:hexanes = 1:1) afforded **19** (31.6 mg, 72%) as a white solid.

Note: The compound is light-sensitive so it should be kept in dark.

R_f = 0.45 (1:1 DCM : hexanes)

TLC Visualization : UV and $KMnO_4$ active

^{1}H-NMR (400 MHz, $CDCl_3$) δ : 7.82 (2H, d, *J* = 9.1 Hz), 7.57 (2H, ddd, *J* = 15.3, 7.1, 3.2 Hz), 7.52-7.45 (2H, m), 7.28 (4H, d, *J* = 8.5 Hz), 7.17 (2H, d, *J* = 8.3 Hz), 7.05 (4H, d, *J* = 8.5 Hz), 6.81-6.74 (4H, m), 6.15 (2H, d, *J* = 15.3 Hz)

^{13}C-NMR (100 MHz, $CDCl_3$) δ : 165.8, 146.4, 145.3, 140.3, 137.0, 134.4, 132.1, 128.6, 127.0, 126.6, 126.2, 123.7, 121.5, 120.8

FTIR ν_{max} (ATR, film)/cm^{-1} : 1726, 1620, 1599, 1581, 1484, 1313, 1264, 1122.

HRMS (APCI +) Calcd for $C_{32}H_{23}O_4Br_2$ $[M+H]^+$: 628.9958, found 628.9960.

3.2.12 Compound 21

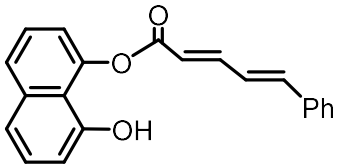

In 25 mL round bottom flask, **2** (250 mg, 1.44 mmol) was dissolved in 3 mL of oxalyl chloride at 23˚C under nitrogen atmosphere. This solution was heated in a pre-heated oil bath at 60˚C for 2 h.

After 2 h, the reaction mixture was cooled to room tempurature and all the volatiles were removed by rotary evaporator to give acyl chloride **20** (271 mg, 98%) as a yellow solid.

In another 50 mL round bottom flask, 1,8-DHN **3** (226 mg, 1.41 mmol) was dissolved in 5 mL of anhydrous THF under an inert nitrogen atmosphere. This solution was cooled to 0˚C in an ice bath and NaH (62 mg, 1.55 mmol, 60% dispersion in mineral oil) was added slowly. Reaction mixture was then allowed to stir at this tempurature for 20 mins. Acyl chloride **20** (271 mg, 1.41 mmol) which was prepared as described above, was dissolved in 5 mL of anhydrous THF and this solution was added slowly to the reaction mixture. Then the reaction mixture was allowed to stir at 23˚C for 3 h. After full consumption of 1,8-DHN **3**, the reaction was quenched with 10 mL of saturated aqueous NH_4Cl solution. Extractions were then performed with EtOAc. Combined organic phases were dried over anhydrous Na_2SO_4, filtered and concentrated in vacuum. Purification by flash colomn chromatography (SiO_2; EtOAc:hexanes = 1:5) afforded **21** (316 mg, 71%) as an orange solid.

R_f = 0.66 (1:5 EtOAc : hexanes)

TLC Visualization : UV and $KMnO_4$ active

^{1}H-NMR (400 MHz, $CDCl_3$) δ : 7.77-7.66 (2H, m), 7.53-7.46 (3H, m), 7.43-7.31 (6H, m), 7.24 (1H, d, *J* = 7.5 Hz), 7.05-6.92 (2H, m), 6.87 (1H, d, *J* = 6.9 Hz), 6.28 (1H, d, *J* = 15.2 Hz)

^{13}C-NMR (100 MHz, $CDCl_3$) δ : 164.7, 152.2, 148.1, 146.2, 142.9, 137.0, 135.8, 129.7, 129.0, 127.6, 127.3, 126.5, 125.9, 125.5, 120.3, 119.2, 118.5, 117.1, 111.5

FTIR ν_{max} (ATR, film)/cm^{-1} : 3385, 3057, 1702, 1621, 1600, 1580, 1393, 1278, 1263, 1174.

HRMS (APCI +) Calcd for $C_{21}H_{17}O_3$ $[M+H]^+$: 317.1172, found 317.1175.

3.2.13 Compound 22

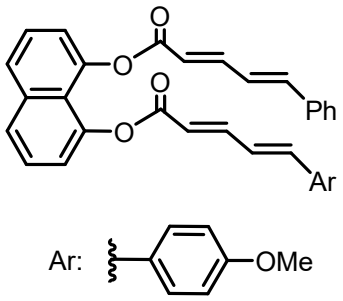

In an oven-dried 50 mL round bottom flask, **16** was dissolved in anhydrous DCM (8 mL) under an atmosphere of nitrogen at 23˚C. Monoester **21** (234 mg, 0.74 mmol), DCC (152.6 mg, 0.74 mmol), and DMAP (13.4 mg, 0.11 mmol) were added sequentially. The reaction mixture was allowed to stir at 23˚C overnight. Then, extractions were performed with DCM. The combined organic phase was dried with anhydrous Na_2SO_4, filtered and concentrated under vacuum. Purification by flash colomn chromatography (SiO_2; DCM:hexanes = 1:1) afforded **22** (178 mg, 48%) as a white solid.

Note: The compound is light-sensitive so it should be kept in the dark.

R_f = 0.39 (1:1 DCM: hexanes)

TLC Visualization : UV and $KMnO_4$ active

^{1}H-NMR (400 MHz, $CDCl_3$) δ : 7.80 (2H, d, *J* = 8.3 Hz), 7.61 (2H, ddd, *J* = 14.9, 10.6, 4.1 Hz), 7.48 (2H, t, *J* = 7.9 Hz), 7.26-7.21 (3H, m), 7.21-7.15 (6H, m), 6.92-6.78 (3H, m), 6.75-6.64 (3H, m), 6.16 (1H, d, *J* = 15.2 Hz), 6.10 (1H, d, *J* = 15.3 Hz), 3.78 (3H, s)

^{13}C-NMR (100 MHz, $CDCl_3$) δ : 166.1, 166.0, 160.7, 147.4, 146.8, 145.5, 141.8, 137.0, 135.8, 129.2, 128.9, 128.8, 128.6, 127.4, 126.9, 126.8, 126.2, 126.1, 126.1, 123.9, 121.7, 120.9, 120.8, 120.7, 119.5, 114.4, 55.4

FTIR ν_{max} (ATR, film)/cm^{-1} : 3058, 2837, 1725, 1624, 1597, 1509, 1448, 1348, 1250, 1228, 1175.

HRMS (APCI +) Calcd for $C_{33}H_{27}O_5$ $[M+H]^+$: 503.1853, found 503.1859.

3.2.14 Compound 23

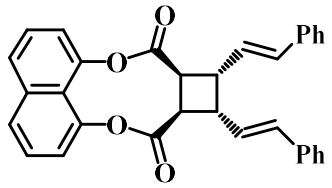

Procedure for Irradiation in Hg Lamp

Diester compound **17** (20mg, 0.04 mmol) was placed between two microscopic glass slides as a solid powder and irradiated with a medium-pressure Hg lamp for 6h. After every 2h, the irradiation was stopped, and the reaction mixture was mixed with a clean spatula. At the end of 6h, the reaction mixture was transferred into a clean vail with $CHCl_3$. Purification with column chromatography (SiO_2; DCM:hexanes = 1:1) gave the cyclobutane product **23** as an orange-yellow solid.

Procedure for Irradiation in Nail-dryer Lamp

For solid-state experiments:

Diester compound **17** (20mg, 0.04 mmol) was placed between two microscopic quartz glass slides as a solid powder (for ground samples, grinding was done in mortar and pestle for 5 mins) and irradiated with UV lamps. For the irradiation experiments for 8h, 16h, and 24h, mixing was done every 4h, but for irradiation experiments for 48h, the reaction mixture was mixed every 8h. In the end, the reaction mixture was transferred into a clean vail with $CHCl_3$. Purification with column chromatography (SiO_2; DCM:hexanes = 1:1) gave the cyclobutane product **23** as an orange-yellow solid.

For a solution with UV A:

Diester compound **17** (24.6mg, 0.05 mmol) was dissolved in 2 mL of $CHCl_3$ in a glass vial and irradiated with UV A light. Progress of the reaction was monitored using TLC (1:1 DCM: hexanes). After 4h, the irradiation stopped. Purification by column chromatography (SiO_2; DCM:hexanes = 1:1) gave an orangish-yellow solid **23** (88%, dr 8:1).

For a solution with UV B:

Diester compound **17** (24.6mg, 0.05 mmol) was dissolved in 2 mL of $CHCl_3$ in a quartz test tube and irradiated with UV B light. Progress of the reaction was monitored using TLC (1:1 DCM: hexanes). After 4h, the irradiation stopped. Purification by column chromatography (SiO_2; DCM:hexanes = 1:1) gave an orangish-yellow solid **23** (58%, dr 8:1).

R_f = 0.48 (1:1 DCM: hexanes)

TLC Visualization: UV and $KMnO_4$ active

^{1}H-NMR (400 MHz, $CDCl_3$) δ : 7.81 (2H, d, *J* = 8.4 Hz), 7.52 (2H, t, *J* = 7.9 Hz), 7.38 (4H, d, *J* = 7.4 Hz), 7.31 (6H, dd, *J* = 15.4, 7.4 Hz), 7.24 (2H, d, *J* = 7.2 Hz), 6.59 (2H, d, *J* = 15.9 Hz), 6.38 (2H, dd, *J* = 15.7, 7.4 Hz), 4.12 (2H, s), 3.87 (2H, app d, *J* = 5.1 Hz)

^{13}C-NMR (100 MHz, $CDCl_3$) δ : 170.1, 145.5, 137.1, 136.8, 132.6, 128.8, 127.9, 127.6, 127.1, 126.5, 126.5, 121.1, 119.6, 45.0, 42.1

FTIR ν_{max} (ATR, film)/cm^{-1} : 3040, 2851,1978, 1764, 1607, 1449, 1364, 1218, 1175

HRMS (APCI +) Calcd for $C_{32}H_{25}O_4$ $[M+H]^+$: 473.1747, found 473.1758.

A

B

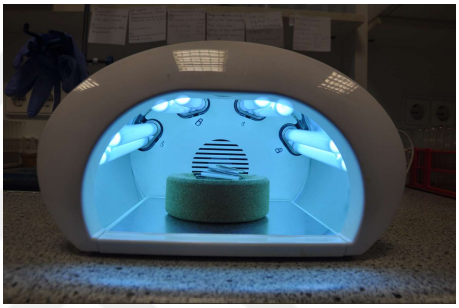

C

Figure 18. A) Reaction setup for irradiation using Hg lamp. B) Commercially available UV nail-dryer. C) Reaction setup for irradiation using UV nail-dryer

3.2.15 Compound 24

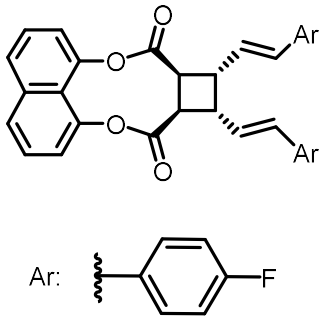

For solid-state experiment

Diester compound **18** (20.4 mg, 0.04 mmol) was placed between two microscopic quartz glass slides and irradiated with UV A lamp for 24 h. Reaction mixture was mixed with a clean spatula after every 4 h. In the end, the reaction mixture was transferred into a clean vail with $CHCl_3$. Purification with column chromatography (SiO_2; DCM:hexanes = 1:1) gave the cyclobutane product **24** (20.2 mg, 99%, dr = 14:1) as an orange-yellow solid.

For solution reaction

Diester compound **18** (20.1 mg, 0.04 mmol) was dissolved in 2 mL of $CHCl_3$ in a quartz test tube and irradiated with UV A lamp for 90 mins. In the end, the reaction mixture was transferred into a clean vail with $CHCl_3$. Purification with column chromatography (SiO_2; DCM:hexanes = 1:1) gave the cyclobutane product **24** (19.3 mg, 96%, dr = 3:1) as an orange-yellow solid.

R_f = 0.43 (1:5 EtOAc : hexanes)

TLC Visualization : UV and $KMnO_4$ active

^{1}H-NMR (400 MHz, $CDCl_3$) δ : 7.81 (2H, d, *J* = 8.3 Hz), 7.51 (2H, t, *J* = 7.9 Hz), 7.35-7.25 (6H, m), 7.00 (4H, t, *J* = 8.6 Hz), 6.54 (2H, d, *J* = 15.8 Hz), 7.27 (2H, ddd, *J* = 15.8, 5.0, 2.3 Hz), 4.10 (2H, bs), 3.91-3.80 (2H, m)

^{13}C-NMR (100 MHz, $CDCl_3$) δ : 170.0, 162.6 (d, *J* = 247.3 Hz), 145.4, 137.1, 132.9 (d, *J* = 3.4 Hz), 131.5, 128.0 (d, J = 8.0 Hz), 127.2 (d, J = 2.0 Hz), 127.1, 126.5, 121.1, 115.9, 115.6, 45.0, 42.1

^{19}F-NMR (376 MHz, $CDCl_3$) δ : -112.4 (s)

FTIR ν_{max} (ATR, film)/cm^{-1} : 3041, 2956, 2927, 1759, 1605, 1507, 1363, 1213, 1175.

HRMS (APCI +) Calcd for $C_{32}H_{23}O_4F_2$ $[M+H]^+$: 509.1559, found 509.1556.

3.2.16 Compound 25

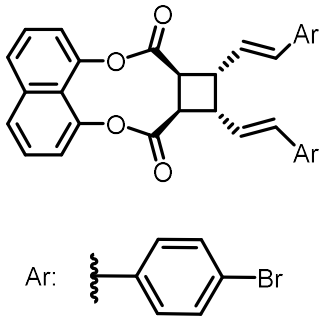

For solid-state experiment

Diester compound **19** (18.2 mg, 0.03 mmol) was placed between two microscopic quartz glass slides and irradiated with UV A lamp for 24 h. Reaction mixture was mixed with a clean spatula after every 4 h. In the end, the reaction mixture was transferred into a clean vail with $CHCl_3$. Purification with column chromatography (SiO_2; DCM:hexanes = 1:1) gave the cyclobutane product **25** (3.1 mg, 17%, dr = 11 :1) as yellow solid.

For solution reaction

Diester compound **19** (15.0 mg, 0.024 mmol) was dissolved in 1.5 mL of $CHCl_3$ in a quartz test tube and irradiated with UV A lamp for 90 mins. In the end, the reaction mixture was transferred into a clean vail with $CHCl_3$. Purification with column chromatography (SiO_2; DCM:hexanes = 1:1) gave the cyclobutane product **25** (9.4 mg, 63%, dr = 11:1) as yellow solid.

R_f = 0.56 (1:1 DCM: hexanes)

TLC Visualization : UV and $KMnO_4$ active

^{1}H-NMR (400 MHz, $CDCl_3$) δ : 7.81 (2H, d, *J* = 8.0 Hz), 7.51 (2H, d, *J* = 7.8 Hz), 7.44 (4H, d, *J* = 8.4 Hz), 7.28 (2H, d, *J* = 7.5 Hz), 7.23 (4H, d, *J* = 8.5 Hz), 6.52 (2H, d, *J* = 15.9 Hz), 6.34 (2H, ddd, *J* = 15.8, 5.2, 2.4 Hz), 4.10 (2H, bs), 3.86-3.84 (2H, m)

^{13}C-NMR (100 MHz, $CDCl_3$) δ : 169.9, 145.5, 137.1, 135.6, 132.0, 131.6, 130.6, 128.2, 128.0, 127.1, 126.5, 121.8, 121.1, 44.9, 42.0

FTIR ν_{max} (ATR, film)/cm^{-1} : 2953, 2923, 2852, 1761, 1607, 1487, 1460, 1364, 1214, 1176.

HRMS (APCI +) Calcd for $C_{32}H_{23}O_4Br_2$ $[M+H]^+$: 628.9958, found 628.9944.

3.2.17 Compound 26

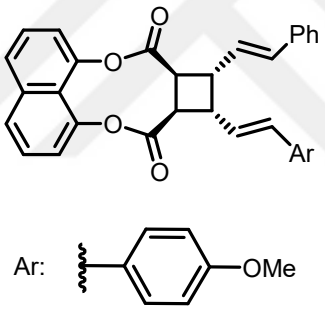

For solid-state experiment

Diester compound **22** (20.6 mg, 0.04 mmol) was placed between two microscopic quartz glass slides and irradiated with UV A lamp for 24 h. Reaction mixture was mixed with a clean spatula after every 4 h. In the end, the reaction mixture was transferred into a clean vail with $CHCl_3$. Purification with column chromatography (SiO_2; DCM:hexanes = 1:1) gave the cyclobutane product **26** (11.0 mg, 54%, dr = 20:1) as yellow solid.

For solution reaction

Diester compound **19** (20.4 mg, 0.04 mmol) was dissolved in 2 mL of $CHCl_3$ in a quartz test tube and irradiated with UV A lamp for 90 mins. In the end, the reaction mixture was transferred into a clean vail with $CHCl_3$. Purification with column chromatography (SiO_2; DCM:hexanes = 1:1) gave the cyclobutane product **26** (17.1 mg, 84%, dr = 14:1) as yellow solid.

R_f = 0.53 (1:1 DCM : hexanes)

TLC Visualization : UV and $KMnO_4$ active

^{1}H-NMR (400 MHz, $CDCl_3$) δ : 7.81 (2H, d, *J* = 8.3 Hz), 7.52 (2H, d, *J* = 7.6 Hz), 7.40-7.37 (2H, m), 7.35-7.27 (6H, m), 7.25-7.23 (1H, m), 6.86 (2H, d, *J* = 8.7 Hz), 6.58 (1H, d, *J* = 15.8 Hz), 6.53 (1H, d, *J* = 15.8 Hz), 6.42-6.35 (1H, m), 6.27-6.20 (1H, m), 4.10 (2H, bs), 3.85 (2H, d, *J* = 4.7 Hz), 3.81 (3H, s)

^{13}C-NMR (100 MHz, $CDCl_3$) δ : 170.2, 170.2, 159.5, 137.1, 136.9, 132.5, 132.0, 129.6, 128.8, 127.8, 127.7, 127.7, 127.0, 126.5, 126.5, 125.3, 121.0, 120.7, 119.6, 114.2, 55.5, 45.2, 45.0, 42.2, 42.2

FTIR ν_{max} (ATR, film)/cm^{-1} : 3058, 2954, 2851, 1761, 1606, 1577, 1510, 1364, 1216, 1174.

HRMS (APCI +) Calcd for $C_{33}H_{26}NaO_5$ $[M+Na]^+$: 525.1673, found 525.1677.

3.2.18 Compound 27

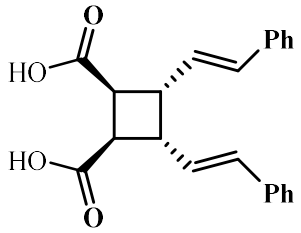

Cycloadduct **23** (8.4 mg, 0.018 mmol) was dissolved in 2 mL of THF in a 25 mL round-bottom flask at 23 ˚C. Then distilled water (1 mL) and KOH (19 mg, 0.342 mmol) were added to the reaction vessel sequentially, and the reaction mixture was allowed to stir at 23 ˚C. Reaction progress was monitored using TLC (1:1 EtOAc: hexanes). After 2 h, full consumption of SM was observed. The reaction was quenched with 1M HCl in an ice bath until the pH became 1-2. The aqueous phase was extracted with EtOAc thrice. Purification by column chromatography (SiO_2; 0.5 % (v/v) AcOH in EtOAc:hexanes = 1:1) to give the pure product **27** (4.3mg, 69%) as a yellowish solid.

R_f = 0.13 (1:1 EtOAc: hexanes + 0.5% Acetic acid)

TLC Visualization : UV and $KMnO_4$ active

^{1}H-NMR (400 MHz, CD_3OD) δ : 7.36 (4H, d, *J* = 7.5 Hz), 7.26 (4H, t, *J* = 7.5 Hz), 7.17 (2H, t, *J* = 7.2 Hz), 6.51 (2H, d, *J* = 15.9 Hz), 6.41 (2H, ddd, *J* = 7.2, 4.8, 1.9 Hz), 3.66 (2H, bs), 3.48 (2H, app d, *J* = 4.7 Hz)

Signal at 4.88 is from water and signal at 5.49 is from DCM.

^{13}C-NMR (100 MHz, CD_3OD) δ : 176.5, 138.6, 132.9, 130.0, 129.5, 128.3, 127.3, 45.3, 44.5

FTIR ν_{max} (ATR, film)/cm^{-1} : 3045, 2961, 2926, 2853, 1708, 1513, 1449, 1419, 1260

3.2.19 Compound 28

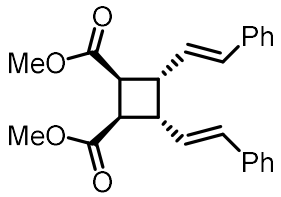

Cycloadduct **23** (11.4 mg, 0.024 mmol) was dissolved in a mixture of MeOH (4 mL) and THF (1 mL) in a vail at 23 ˚C followed by the addition of NaOMe (3.3 mg, 0.068 mmol). Upon the addition of NaOMe, the color of the solution turned from yellow to orange immediately. The reaction was allowed to stir at 23 ˚C. Reaction progress monitored by TLC (1:5 EtOAc: hexanes) indicated completion of the reaction after 8h. All the organics were directly evaporated. Purification by column chromatography (SiO_2; EtOAc:hexanes = 1:5) gave the pure product **28** (8.2 mg, 89% yield) as an orange solid.

R_f = 0.48 (1:1 DCM: hexanes)

TLC Visualization: UV and $KMnO_4$ active

^{1}H-NMR (400 MHz, $CDCl_3$) δ : 7.35-7.33 (4H, m), 7.29 (4H, t, *J* = 7.5 Hz), 7.21 (2H, t, *J* = 7.1 Hz), 6.50 (2H, d, *J* = 15.8 Hz), 6.29 (2H, dd, *J* = 15.8, 7.7 Hz), 3.70 (6H, s), 3.70 (2H, s), 3.45 (2H, app d, *J* = 5.4 Hz)

^{13}C-NMR (100 MHz, $CDCl_3$) δ : 172.9, 137.0, 132.3, 128.7, 128.1, 127.7, 126.5, 52.2, 44.0, 43.0

FTIR ν_{max} (ATR, film)/cm^{-1} : 2952, 2850, 1735, 1602, 1495, 1436, 1365, 1264, 1170

HRMS (ESI +) Calcd for $C_{24}H_{25}O_4$ $[M+H]^+$: 377.1747, found 377.1743.

3.2.20 Compound 29

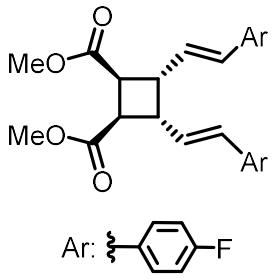

Compound **29** was prepared using **24** (20.2 mg, 0.04 mmol), NaOMe (5.4 mg, 0.1 mmol), MeOH (3 mL) and THF (3 mL) following the same procedure as used for **28**. Purification by column chromatography (SiO_2; EtOAc:hexanes = 1:5) gave the pure product **29** (10.8 mg, 65% yield, dr = 10:1) as a yellow solid.

R_f = 0.33 (1:5 EtOAc : hexanes)

TLC Visualization : UV and $KMnO_4$ active

^{1}H-NMR (400 MHz, $CDCl_3$) δ : 7.32-7.27 (4H, m), 7.00-6.95 (4H, m), 6.45 (2H, d, *J* = 15.8 Hz), 6.18 (2H, ddd, *J* = 15.8, 5.4, 2.5 Hz), 3.73 (6H, s), 3.71 (2H, app d, *J* = 3.2 Hz), 3.42-3.41 (2H, m)

^{13}C-NMR (100 MHz, $CDCl_3$) δ : 172.9, 162.5 (d, *J* = 246.9 Hz), 131.2, 127.9 (d, *J* = 8.0 Hz), 127.8 (d, *J* = 2.0 Hz), 125.2, 115.6 (d, *J* = 21.6 Hz), 52.2, 44.0, 43.0

^{19}F-NMR (376 MHz, $CDCl_3$) δ : -113.4 (s)

FTIR ν_{max} (ATR, film)/cm^{-1} : 3054, 2953, 1736, 1601, 1508, 1264, 1226, 1158.

HRMS (ESI +) Calcd for $C_{24}H_{23}O_4F_2$ $[M+H]^+$: 413.1559, found 413.1546.

3.2.21 Compound 30

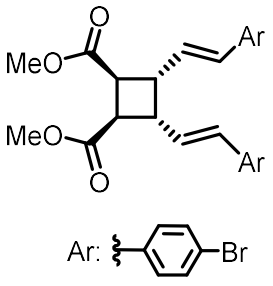

Compound **30** was prepared using **25** (9.4 mg, 0.015 mmol), NaOMe (2.0 mg, 0.038 mmol), MeOH (1.5 mL) and THF (1.5 mL) following the same procedure as used for **28**. Purification by

column chromatography (SiO_2; EtOAc:hexanes = 1:5) gave the pure product **30** (5.1 mg, 65% yield, dr = 16:1) as a yellow solid.

R_f = 0.38 (1:5 EtOAc : hexanes)

TLC Visualization : UV and $KMnO_4$ active

^{1}H-NMR (400 MHz, $CDCl_3$) δ : 7.44-7.38 (4H, m), 7.21-7.16 (4H, m), 6.42 (2H, d, *J* = 15.7 Hz), 6.24 (2H, ddd, J = 7.8, 5.2, 2.1 Hz), 3.73 (6H, s), 3.69-3.62 (2H, m), 3.43-3.42 (2H, m)

3.2.22 Compound 31

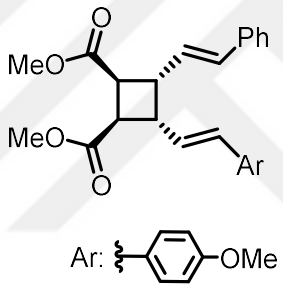

Compound **31** was prepared using **26** (17.1 mg, 0.034 mmol), NaOMe (4.6 mg, 0.085 mmol), MeOH (2 mL) and THF (2 mL) following the same procedure as used for **28**. Purification by column chromatography (SiO_2; EtOAc:hexanes = 1:5) gave the pure product **31** (12.3 mg, 89% yield, dr = 14:1) as a yellow solid.

R_f = 0.38 (1:3 EtOAc : hexanes)

TLC Visualization : UV and $KMnO_4$ active

^{1}H-NMR (400 MHz, $CDCl_3$) δ : 7.35-7.27 (5H, m), 7.23-7.17 (2H,m), 6.82 (2H, d, *J* = 8.7 Hz), 6.49 (1H, d, *J* = 15.9 Hz), 6.82 (1H, d, *J* = 15.8 Hz), 6.28 (1H, dd, *J* = 15.8, 7.4 Hz), 6.14 (1H, d, *J* = 15.8, 7.6 Hz), 3.79 (3H, s), 3.73 (6H, s), 3.71 (2H, app d, *J* = 4.5 Hz), 3.43 (2H, app d, *J* = 5.1 Hz)

FTIR ν_{max} (ATR, film)/cm^{-1} : 3058, 2926, 1760, 1730, 1602, 1366, 1226, 1174

HRMS (APCI +) Calcd for $C_{25}H_{27}O_5$ $[M+H]^+$: 407.1853, found 407.1859.

3.2.23 Compound 32

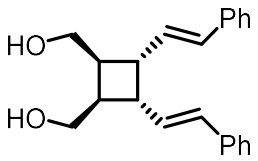

In a round bottom flask, cycloadduct **23** was dissolved in THF (4 mL) under an atmosphere of nitrogen and then this solution was cooled to 0˚C in an ice bath. $LiAlH_4$ (9.5 mg, 0.25 mmol) was added to the cooled solution and reaction mixture was then allowed to stir at 23˚C for 2 h. After full consumption of **23**, reaction was quenched with 10 mL of water and extractions were performed thrice with EtOAc. The organic phases were combined, dried with anhydrous Na_2SO_4, filtered and concentrated in vacuum. Purification by flash coloumn chromatography (SiO_2: 5% MeOH in DCM) afforded the pure product **32** (5.2 mg, 65%) as a pale yellow solid.

R_f **=** 0.52 (5% in DCM)

TLC Visualization : UV and $KMnO_4$ active

^{1}H-NMR (400 MHz, $CDCl_3$) δ : 7.35-7.27 (8H, m), 7.21-7.18 (2H, m), 6.41 (2H, d, *J* = 15.8 Hz), 6.34 (2H, ddd, *J* = 15.9, 4.9, 2.2 Hz), 4.01-3.91 (2H, m), 3.87-3.79 (2H, m), 3.00 (2H, bs), 2.80-2.76 (4H, m)

^{13}C-NMR (100 MHz, $CDCl_3$) δ : 137.4, 130.9, 130.1, 128.7, 127.4, 126.3, 62.5, 42.0, 41.6

FTIR ν_{max} (ATR, film)/cm^{-1} : 3313, 3025, 2853, 1665, 1599, 1492, 1450, 1260

HRMS (APCI +) Calcd for $C_{22}H_{25}O_2$ $[M+H]^+$: 321.1849, found 321.1847.

3.2.24 Compound 33

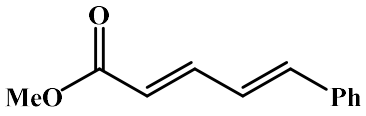

R_f = 0.77 (1:5 EtOAc: hexanes)

TLC Visualization : UV and $KMnO_4$ active

^{1}H-NMR (400 MHz, $CDCl_3$) δ : 7.49-7.45 (3H, m), 7.38-7.31 (3H, m), 6.94-6.75 (2H, m), 6.00 (1H, d, *J* = 15.2 Hz), 3.77 (3H, s)

NMR data for **33** matches the reported data in the literature.[64]

3.3 Reaction Procedures for Chapter 2

3.3.1 Compound 45

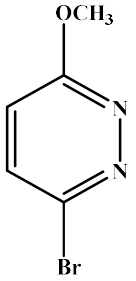

To a solution of 3,6-dibromopyridazine **44** (1002 mg, 4.2 mmol) in 1:1 MeOH: THF (15mL), NaOMe (260 mg, 4.8 mmol) was added at 0 ˚C. The color of the solution turned brown after the addition of NaOMe. The reaction mixture was allowed to stir at 0 ˚C for 1h. The reaction was not going to completion, so the reaction mixture was put in a pre-heated oil bath at 55 ˚C. After 2h, the reaction was not proceeding to completion so NaOMe (57mg, 1.05 mmol) was added. After 30

mins, TLC (1:4 EtOAc: hexanes) indicated full consumption of 3,6-dibromopyridazine. The reaction mixture was diluted with water and extracted with EtOAc. Purification by column chromatography (SiO_2; EtOAc:hexanes = 1:4) gave pure product **45** (639mg, 80% yield) as a white solid.

R_f = 0.53 (1:4 EtOAc: hexanes)

TLC Visualization : UV and $KMnO_4$ active

^{1}H-NMR (400 MHz, $CDCl_3$) δ : 7.45 (1H, d, *J* = 9.2 Hz), 6.84 (1H, d, *J* = 9.0 Hz), 4.06 (s, 3H)

^{13}C-NMR (100 MHz, $CDCl_3$) δ : 164.8, 141.7, 134.0, 120.0, 55.3

FTIR ν_{max} (ATR, film)/cm^{-1} : 3058, 2990, 2851, 1679, 1583, 1575, 1461, 1397

3.3.2 Compound 46

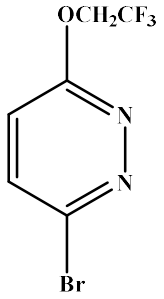

3,6-dibromopyridazine **44** (100 mg, 0.42 mmol) was dissolved in THF (2 mL) at 0 ˚C under nitrogen. To this solution, trifluoroethanol (42 µL, 0.588 mmol) and potassium tert-butoxide (66 mg, 0.588 mmol) were added sequentially. The reaction mixture was stirred at 23 ˚C for 75 minutes. All the organics were directly evaporated. Then the reaction mixture was diluted with water and extracted with EtOAc. Purification by column chromatography (SiO_2; EtOAc:hexanes = 1:4) gave pure product **46** (63 mg, 58%) as a black solid.

R_f **=** 0.69 (1:4 EtOAc: hexanes)

TLC Visualization : UV and $KMnO_4$ active

^{1}H-NMR (400 MHz, $CDCl_3$) δ : 7.59 (1H, d, *J* = 9.7 Hz), 7.02 (1H, d, *J* = 9.7 Hz), 4.89 (2H, q, *J* = 8.1 Hz)

^{13}C-NMR (100 MHz, $CDCl_3$) δ : 163.0, 143.2, 134.9, 123.8 (q, *J* = 277.0 Hz) 119.8, 63.8 (q, *J* = 36.7 Hz)

^{19}F NMR (376 MHz; $CDCl_3$) δ: -73.06 (s)

FTIR ν_{max} (ATR, film)/cm^{-1} : 3066, 2963, 2919, 1579, 1420, 1325

3.3.3 Characterization of Compound 47

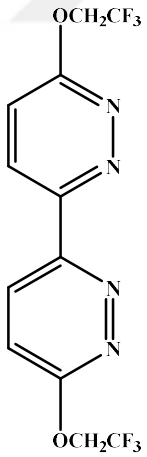

R_f **=** 0.69 (1:4 EtOAc: hexanes)

TLC Visualization : UV and $KMnO_4$ active

^{1}H-NMR (400 MHz, $CDCl_3$) δ : 8.70 (1H, d, *J* = 9.3 Hz), 7.30 (1H, d, *J* = 9.2 Hz), 5.03 (2H, q, *J* = 8.3 Hz)

^{13}C-NMR (100 MHz, $CDCl_3$) δ : 164.0, 153.6, 128.4, 118.4, 63.7 (q, J = 36.7 Hz)

^{19}F NMR (376 MHz; $CDCl_3$) δ: -72.52 (s)

NMR SPECTRA

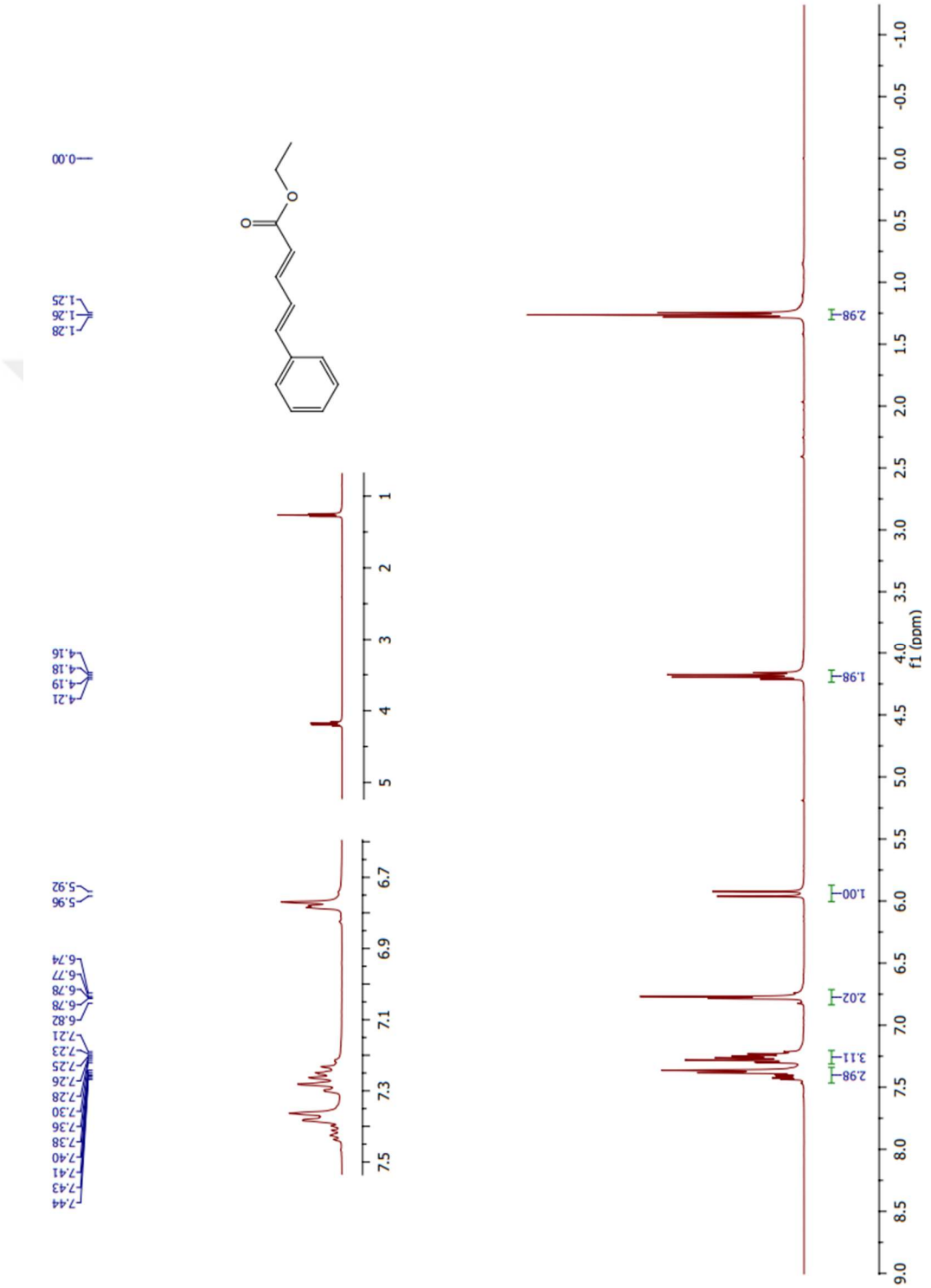

Figure 19. ^{1}H-NMR spectrum of **10** in $CDCl_3$

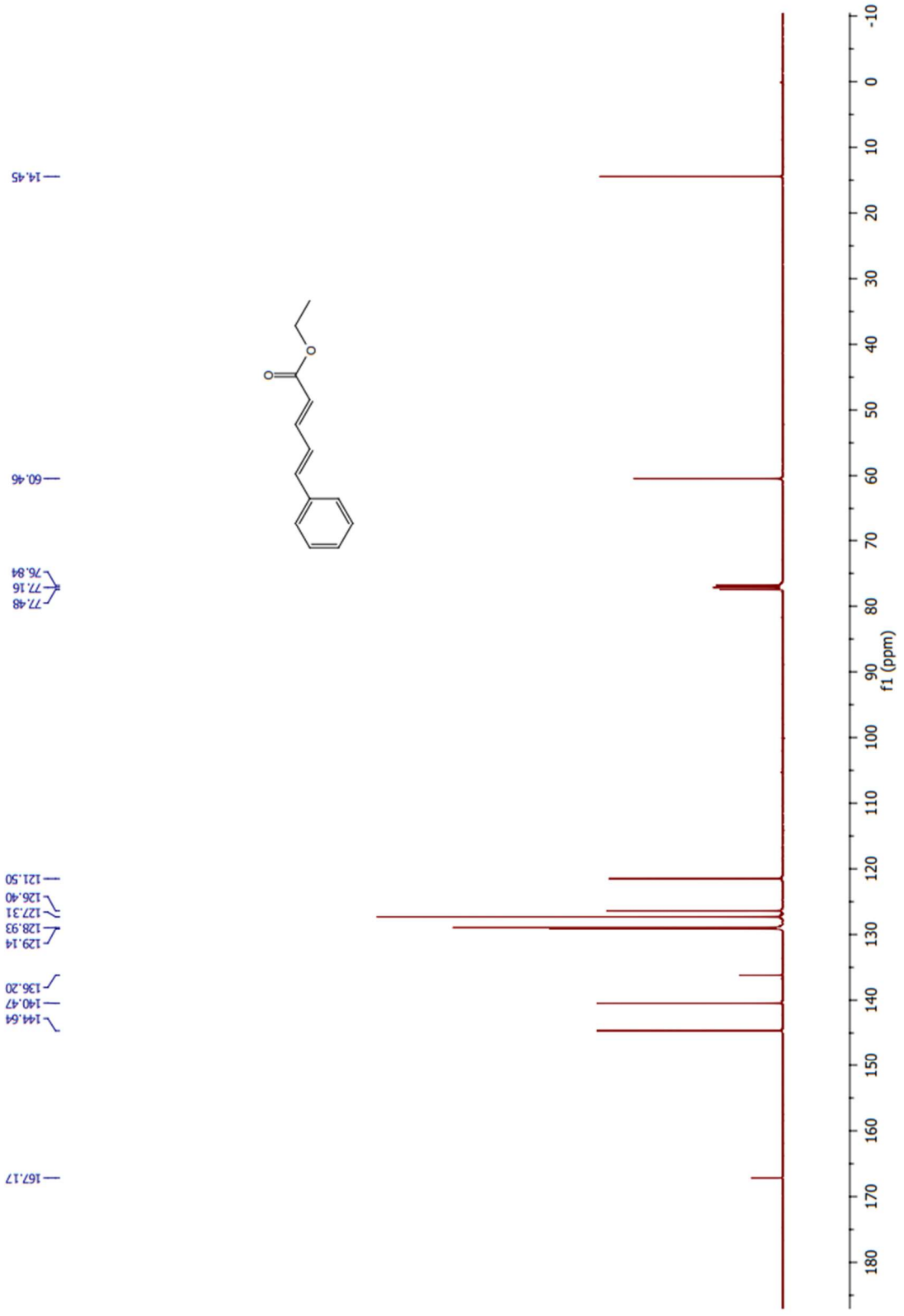

Figure 20. ^{13}C-NMR spectrum of **10** in $CDCl_3$

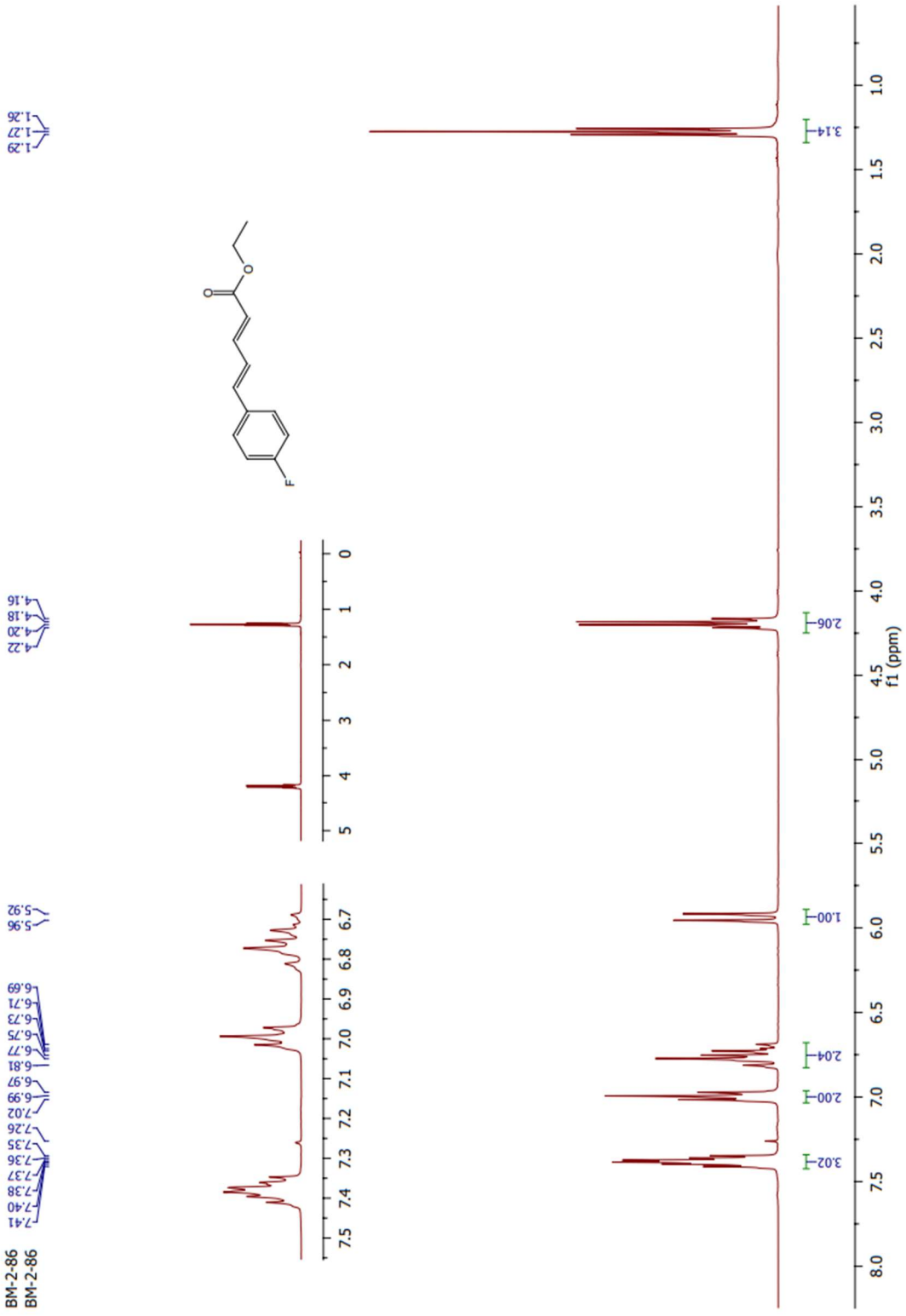

Figure 21. ^{1}H-NMR spectrum of **11** in $CDCl_3$

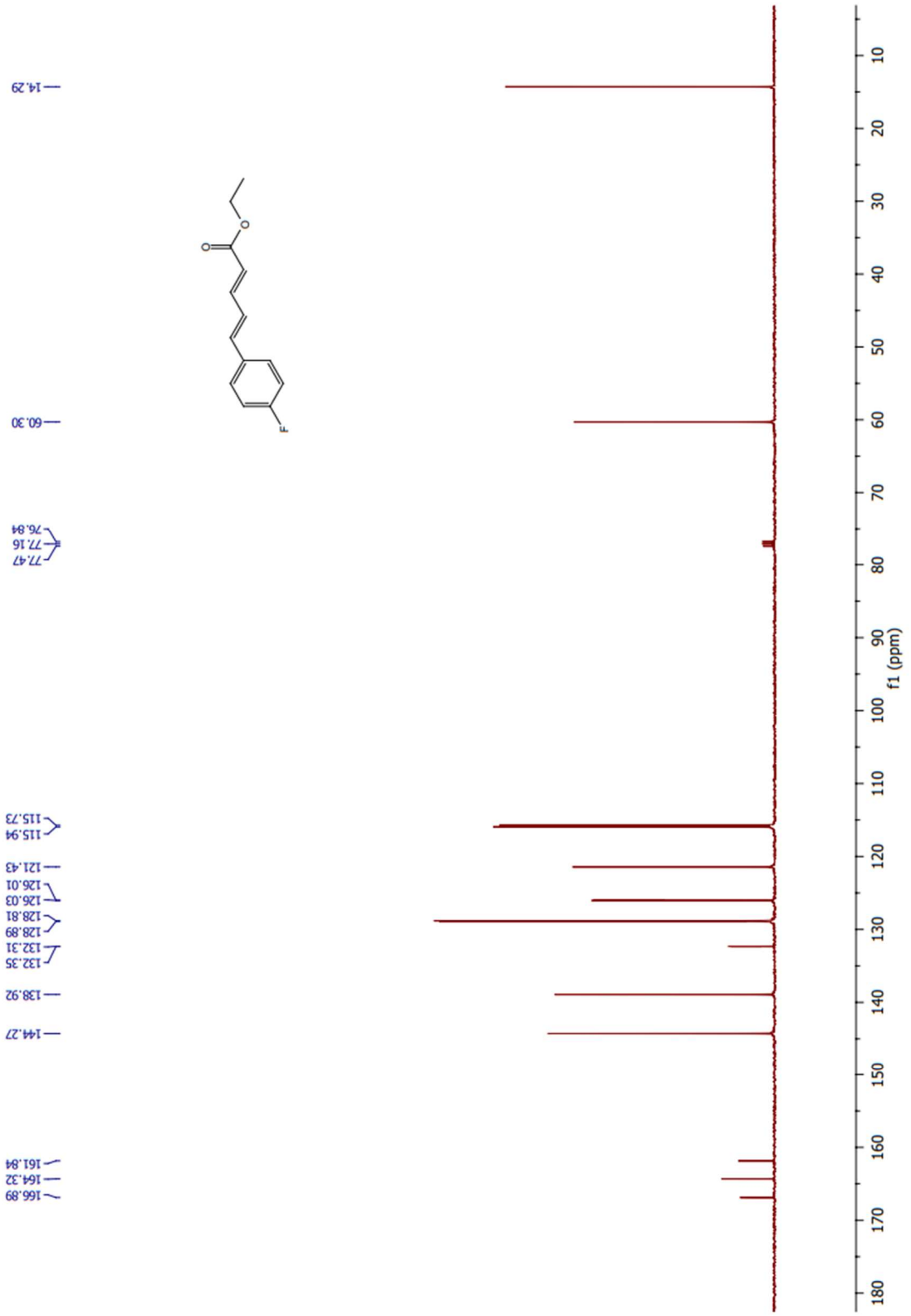

Figure 22. ^{13}C-NMR spectrum of **11** in $CDCl_3$

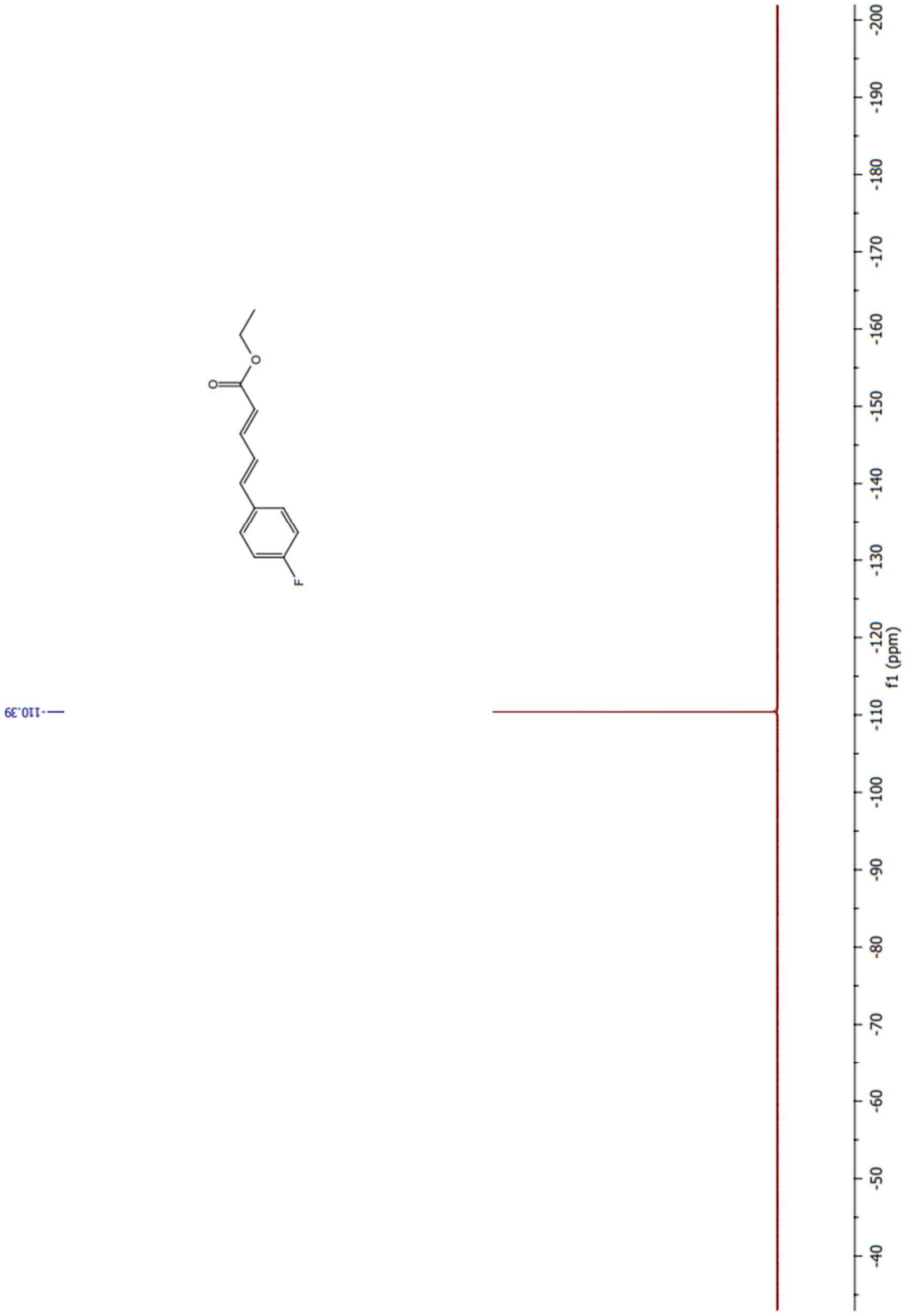

Figure 23. ^{19}F-NMR spectrum of **11** in $CDCl_3$

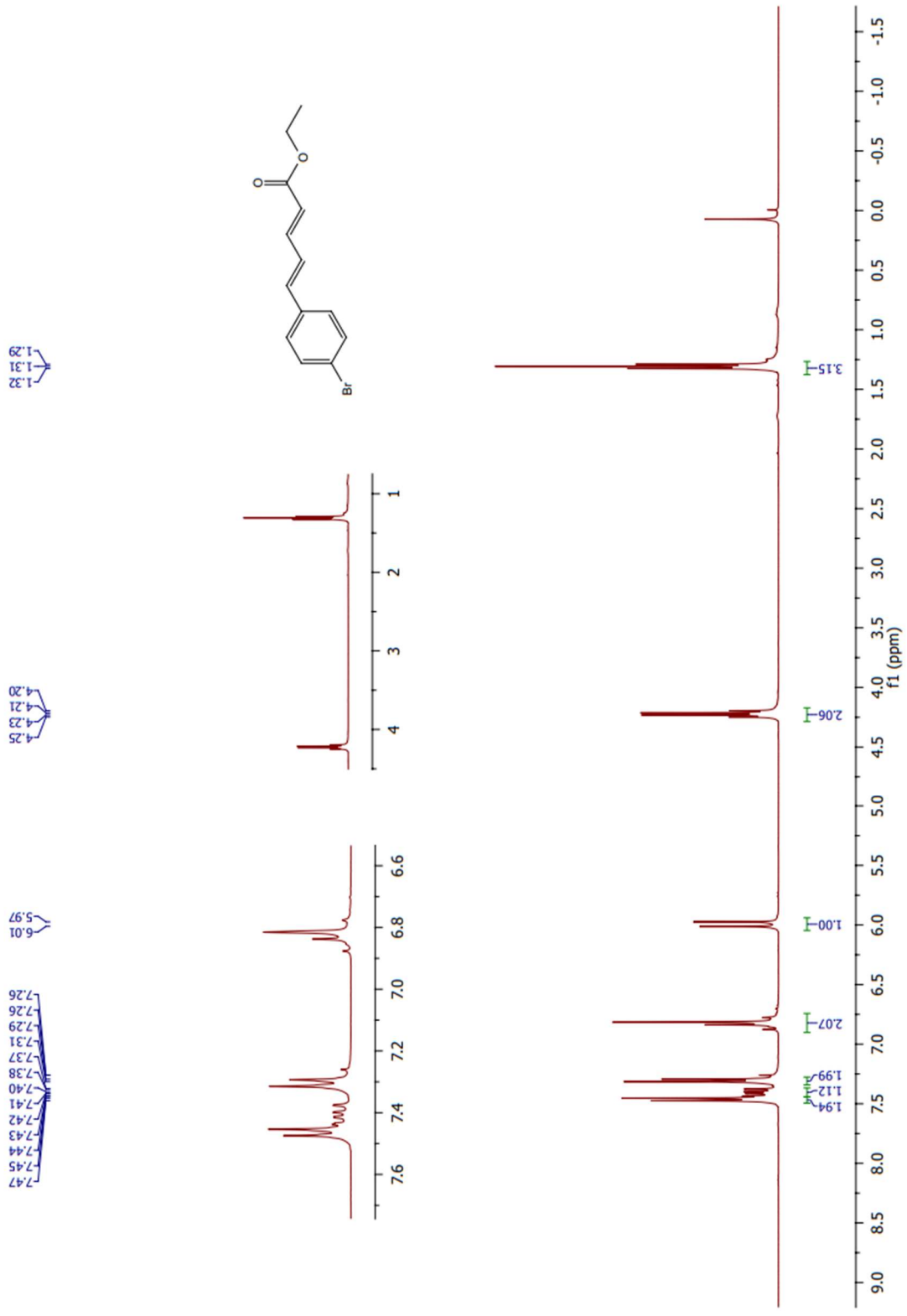

Figure 24. ^{1}H-NMR spectrum of **12** in $CDCl_3$

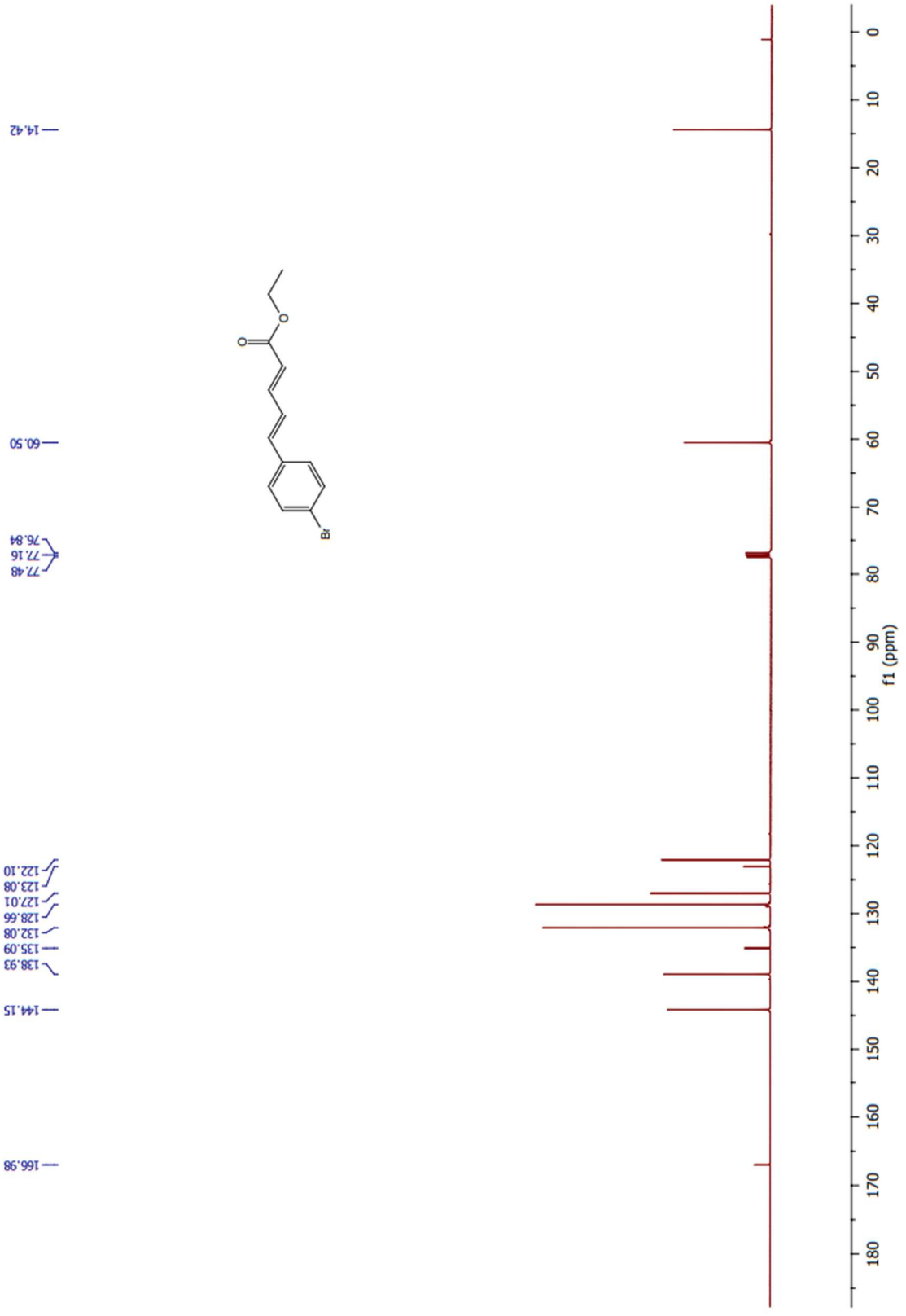

Figure 25. ^{13}C-NMR spectrum of **12** in $CDCl_3$

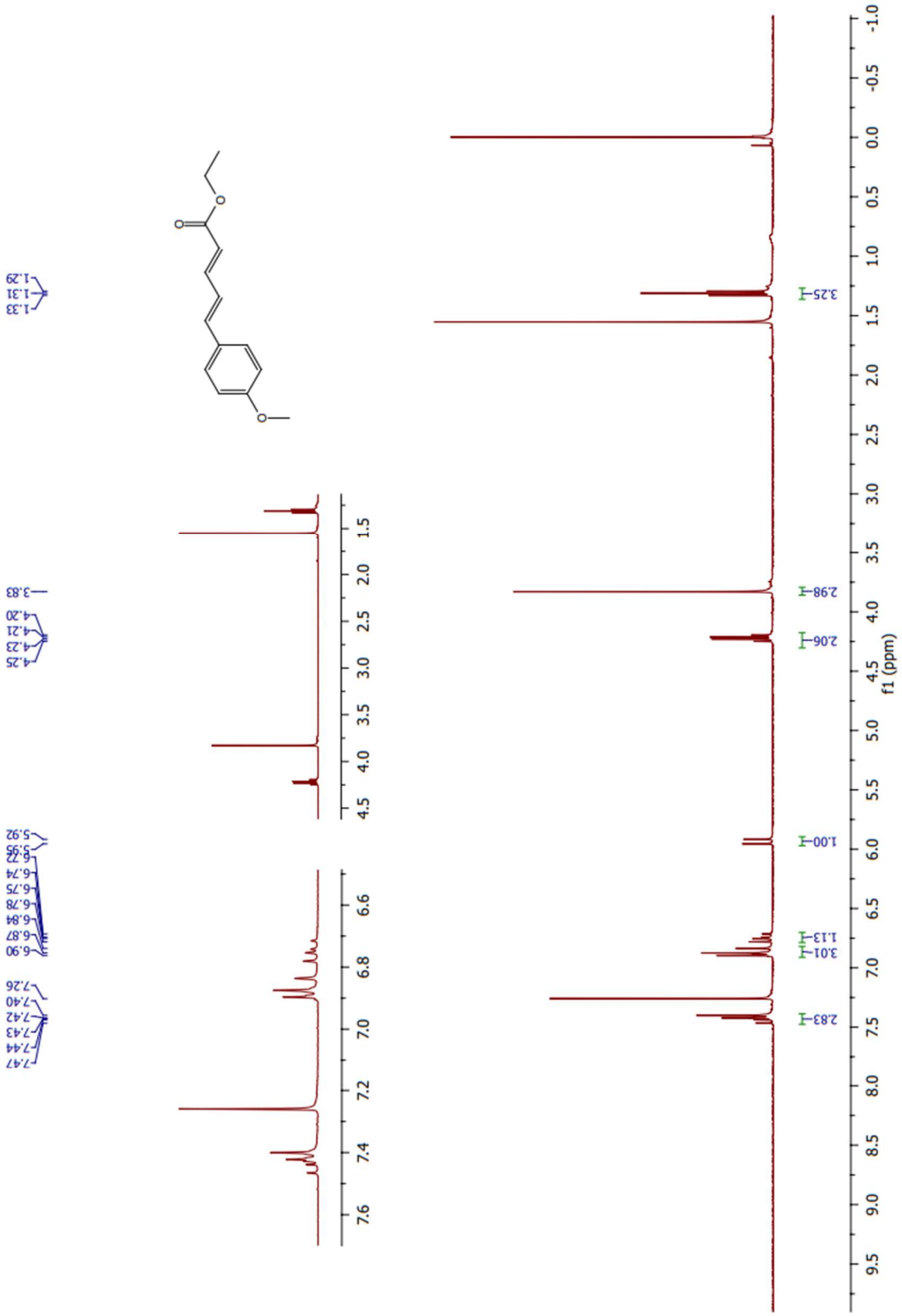

Figure 26. ^{1}H-NMR spectrum of **13** in $CDCl_3$

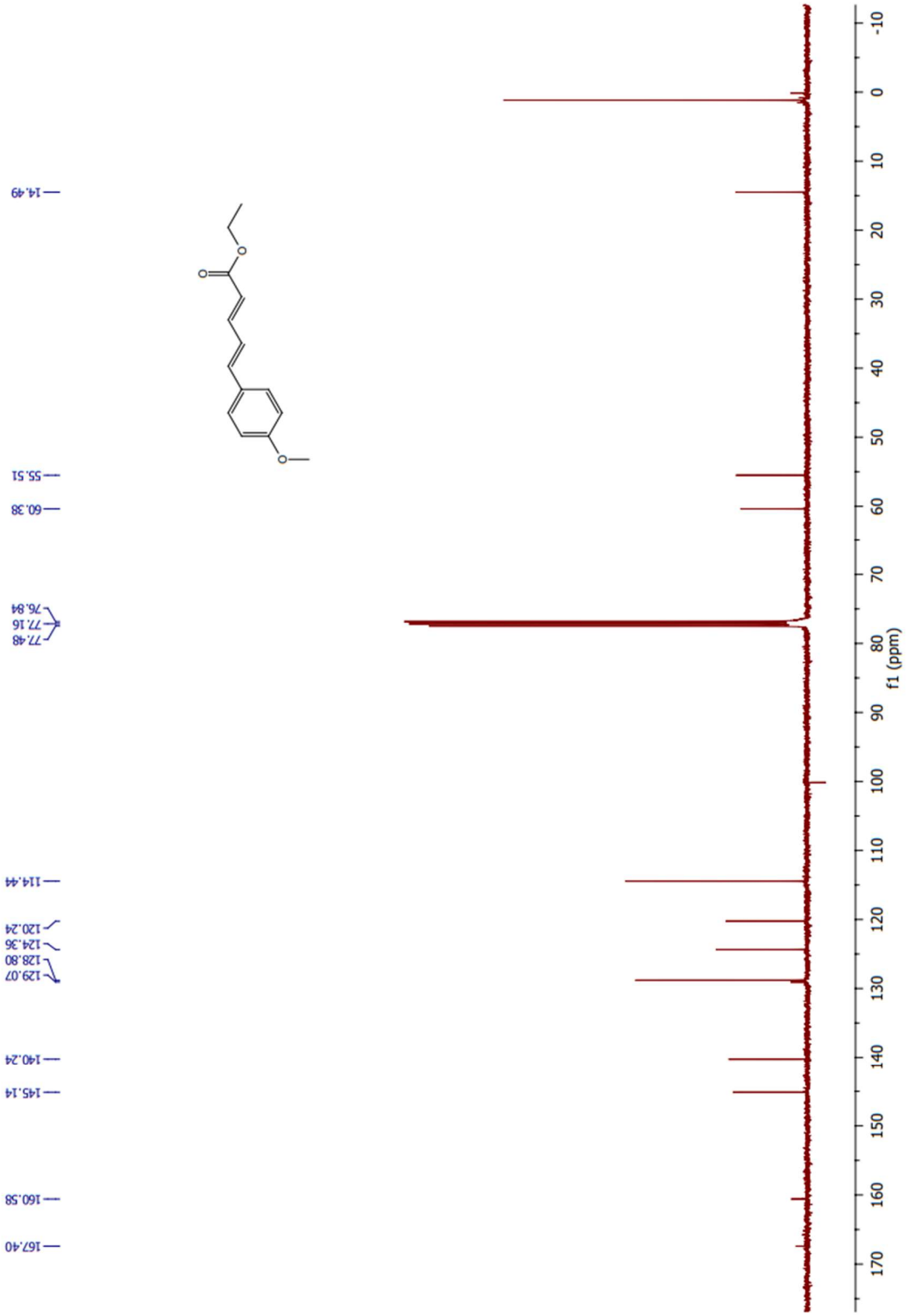

Figure 27. ^{13}C-NMR spectrum of **13** in $CDCl_3$

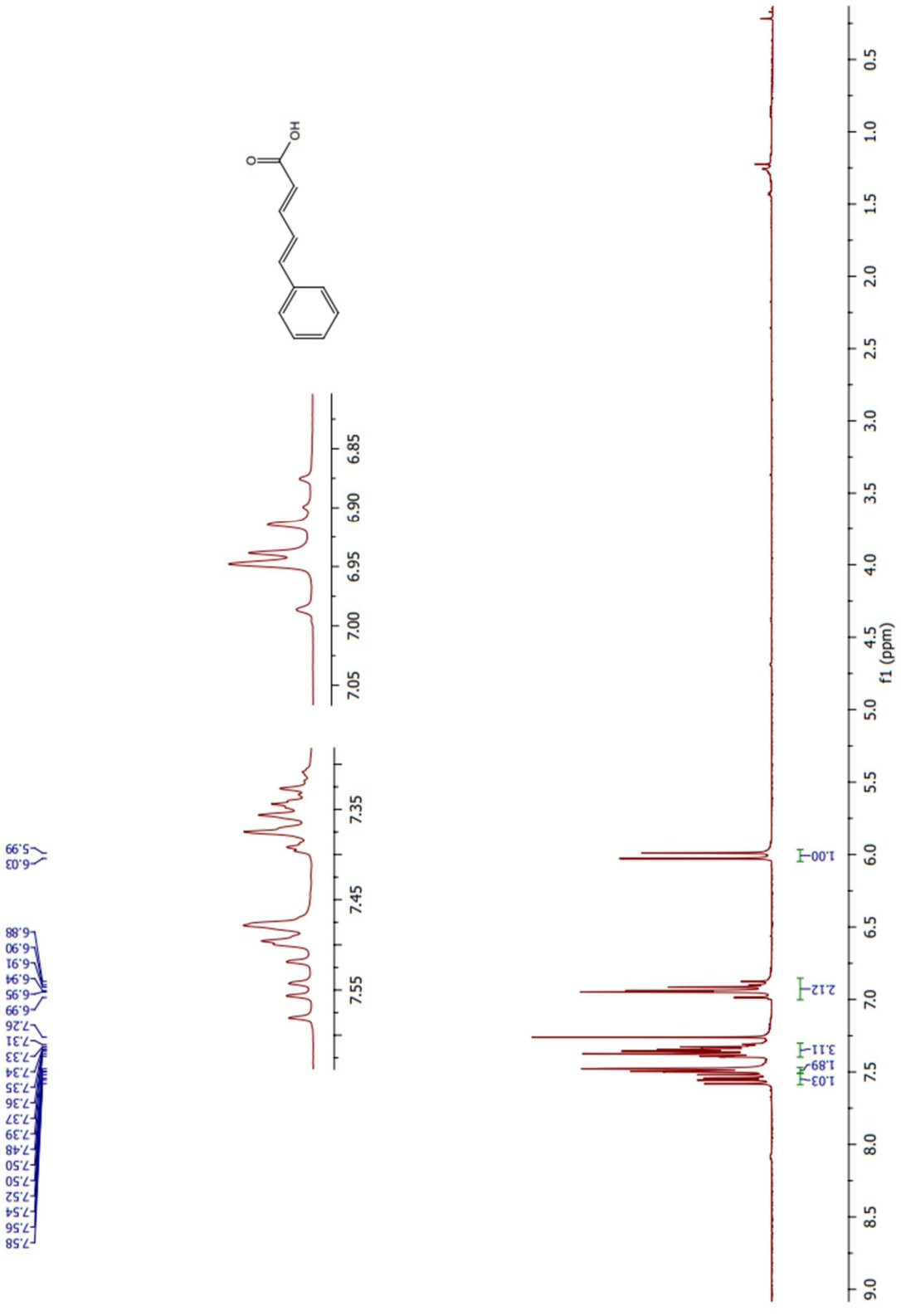

Figure 28. ^{1}H-NMR spectrum of **2** in $CDCl_3$

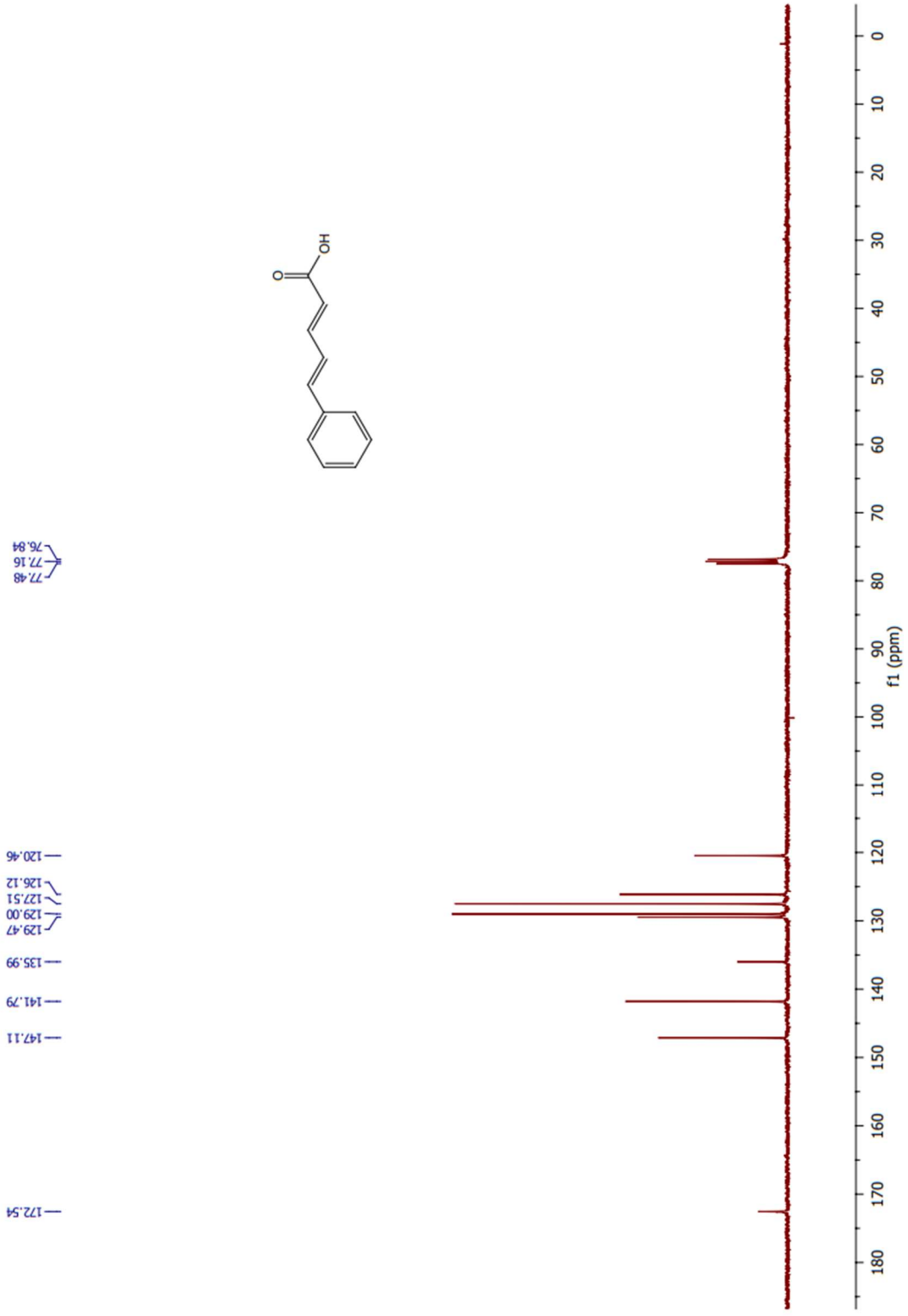

Figure 29. ^{13}C-NMR spectrum of **2** in $CDCl_3$

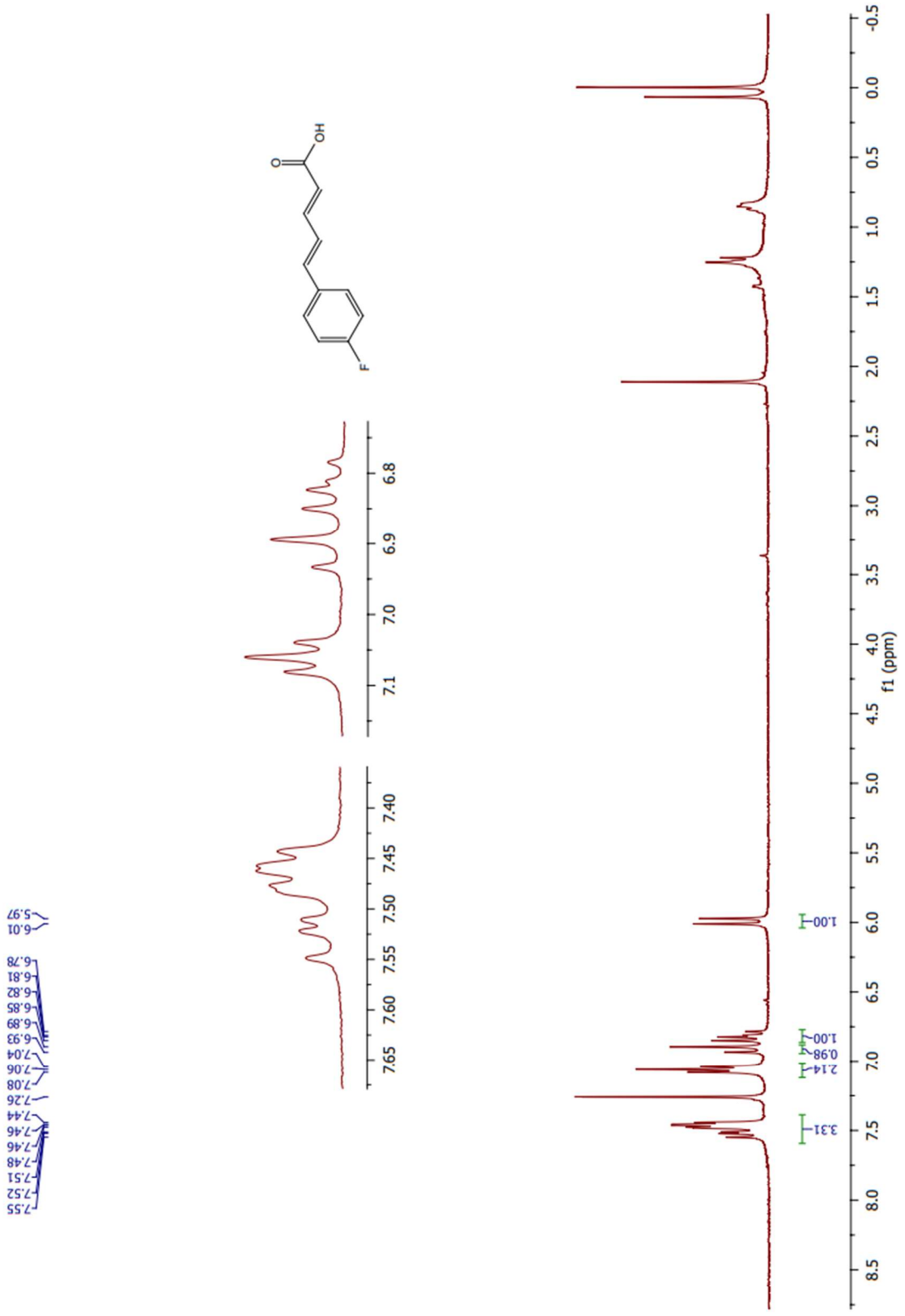

Figure 30. ^{1}H-NMR spectrum of **14** in $CDCl_3$

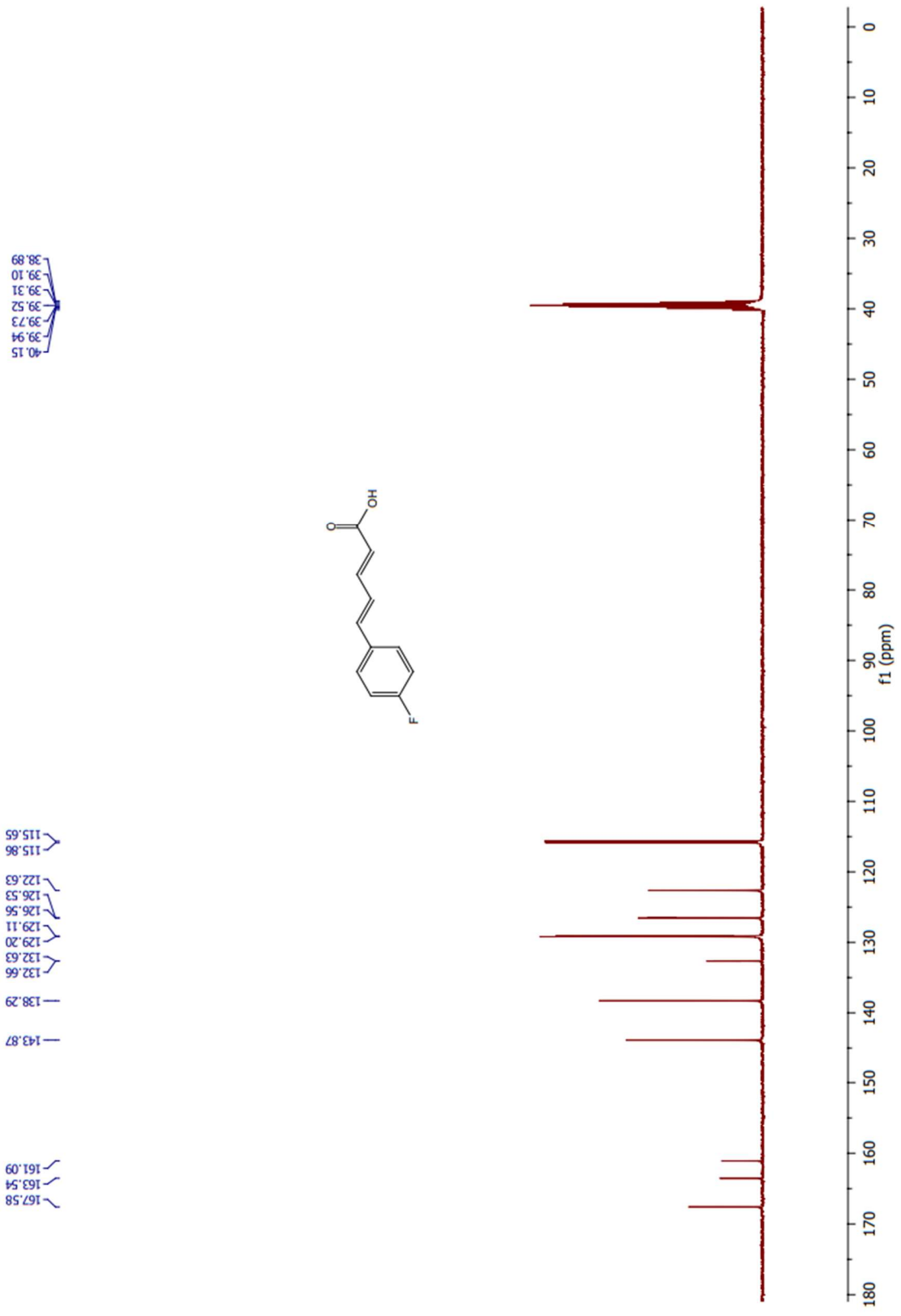

Figure 31. ^{13}C-NMR spectrum of **14** in DMSO-*d*6

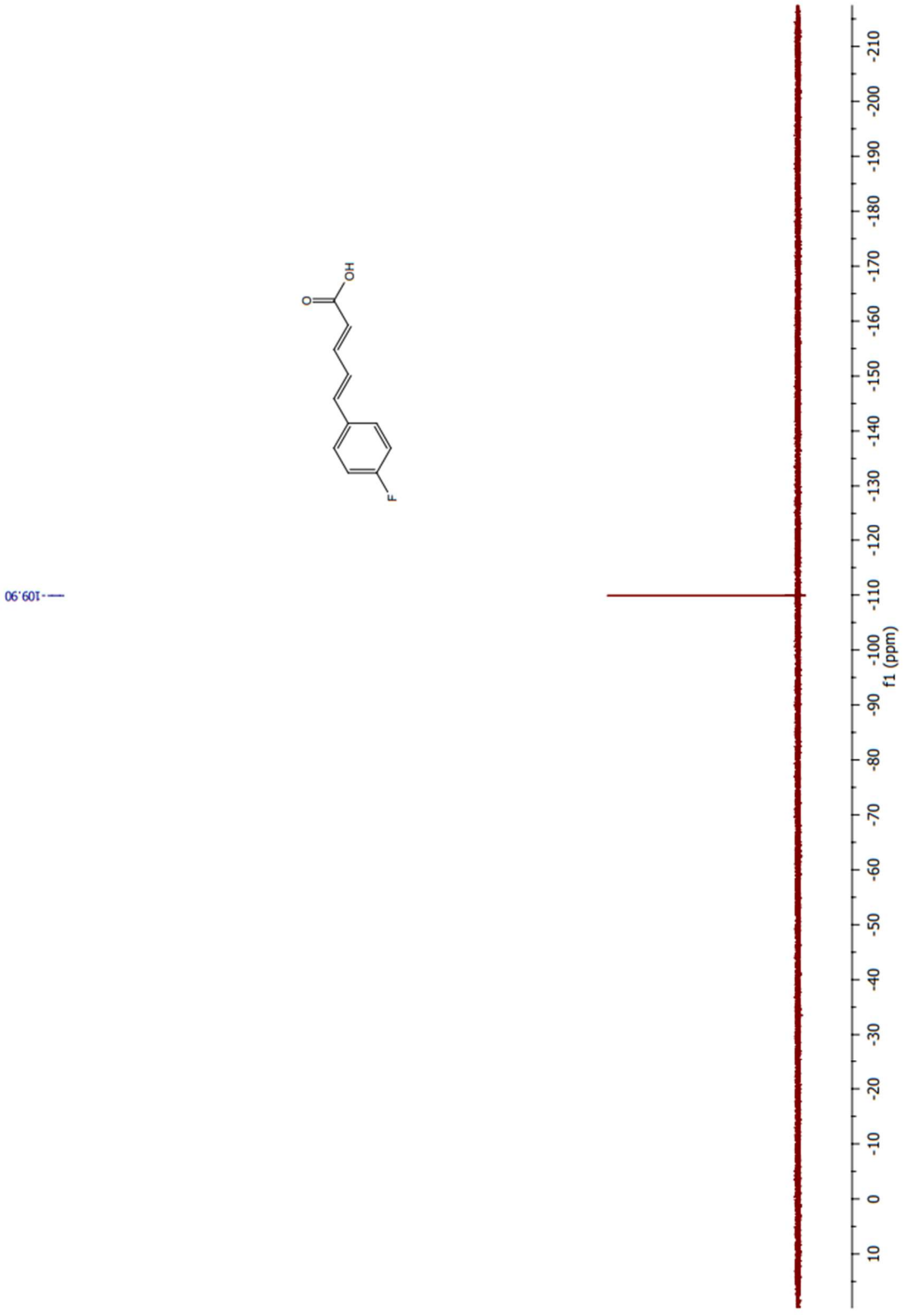

Figure 32. ^{19}F-NMR spectrum of **14** in $CDCl_3$

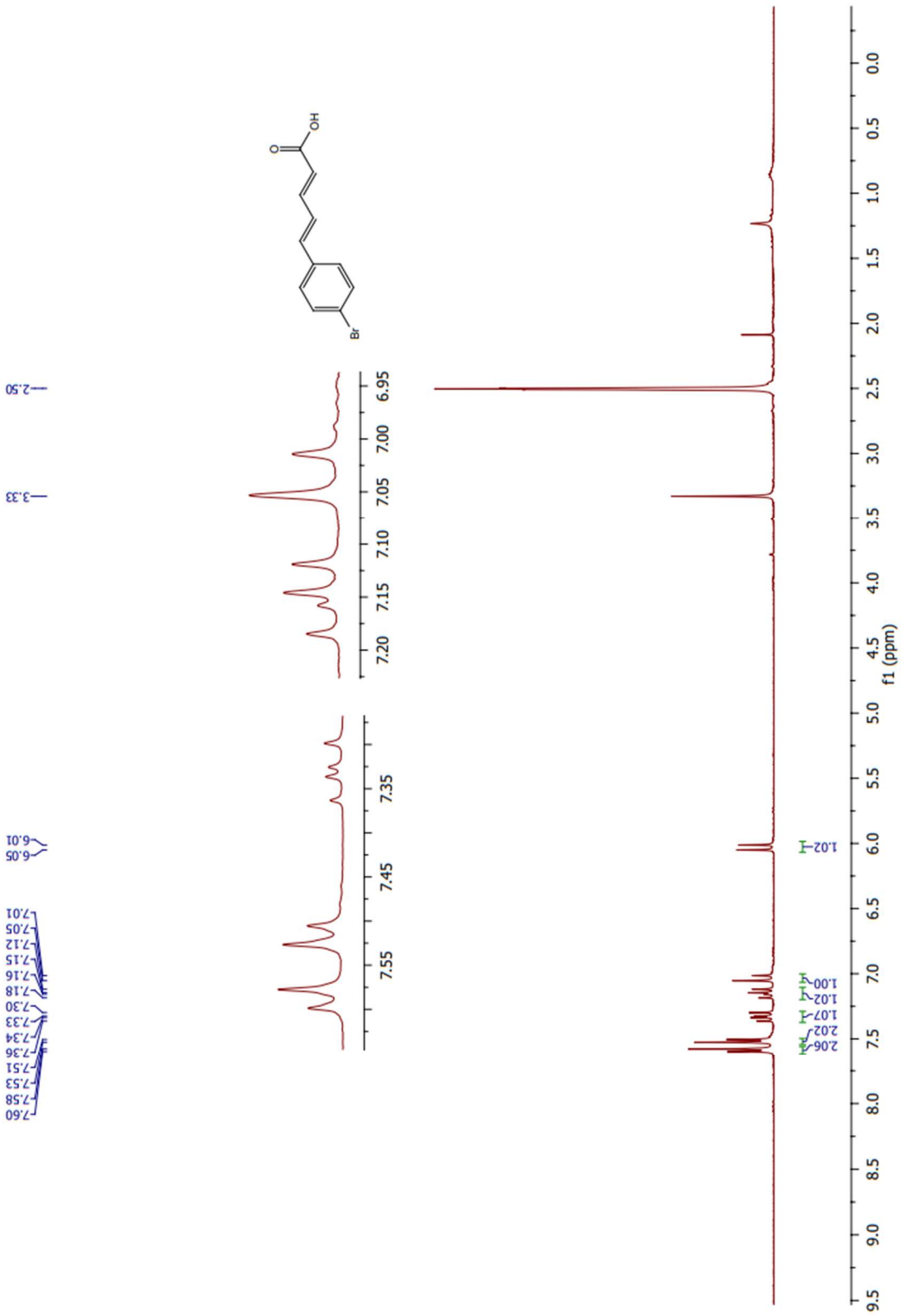

Figure 33. [1]H-NMR spectrum of **15** in DMSO-*d*6

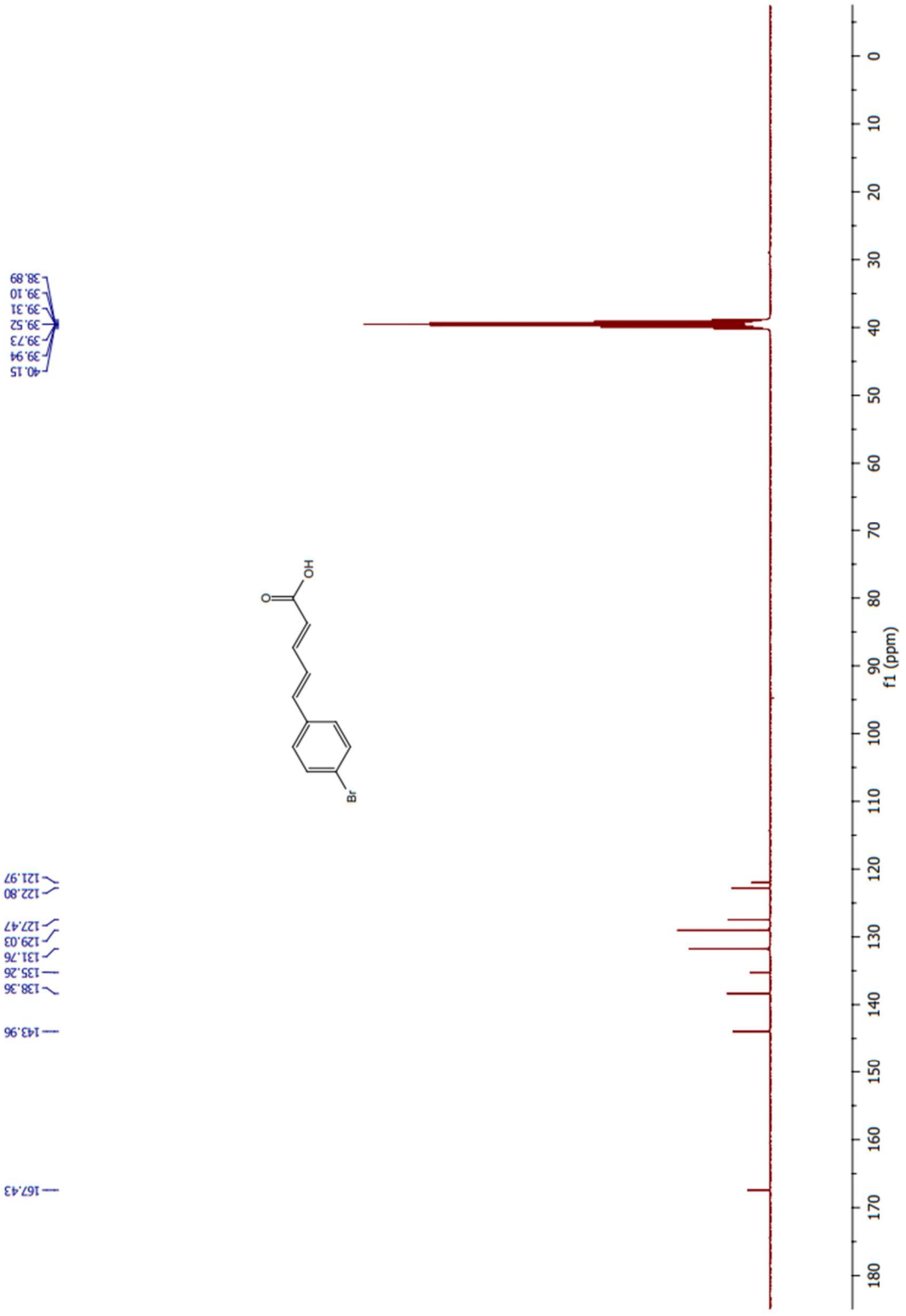

Figure 34. ^{13}C-NMR spectrum of **15** in DMSO-*d*6

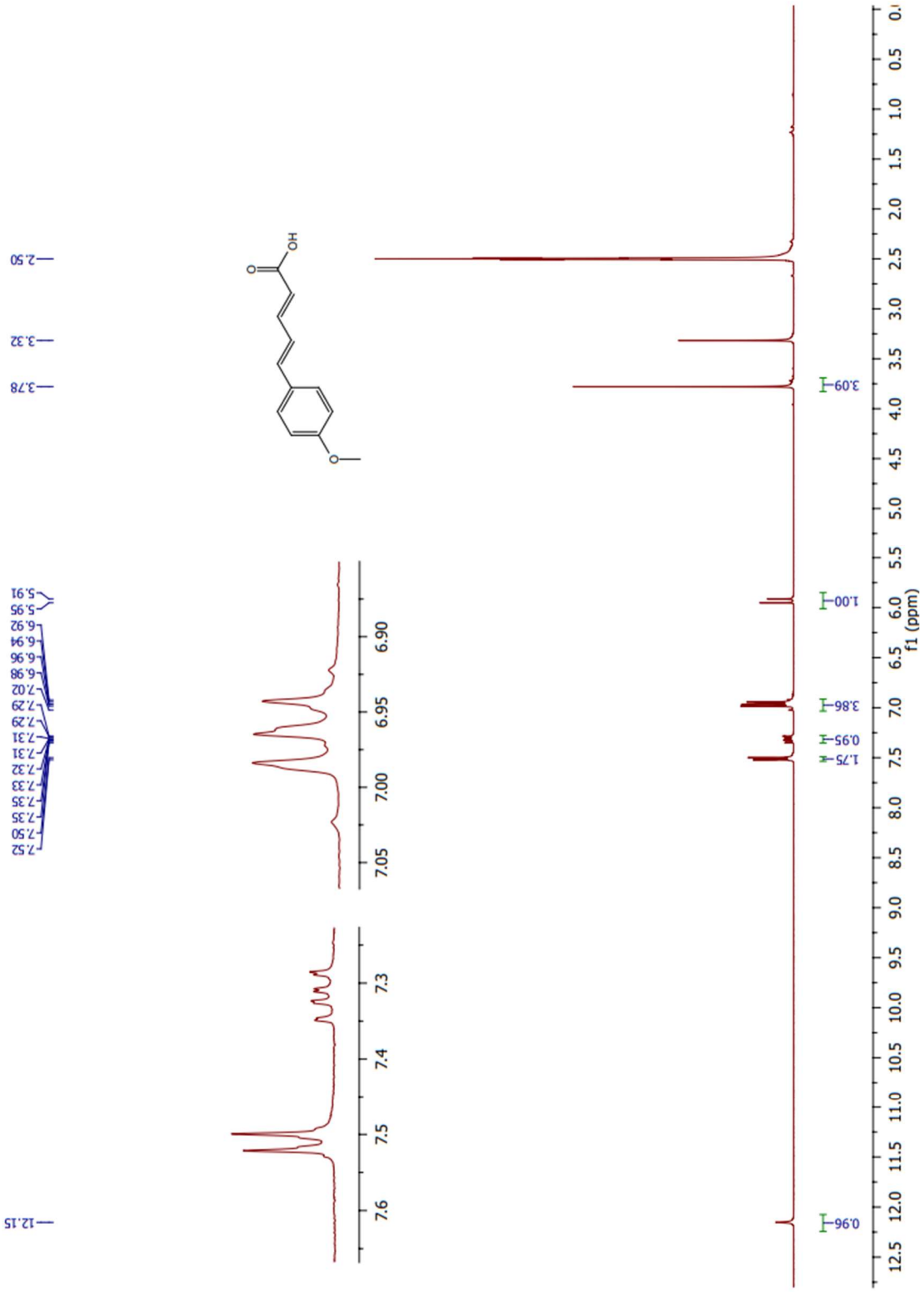

Figure 35. [1]H-NMR spectrum of **16** in DMSO-*d*6

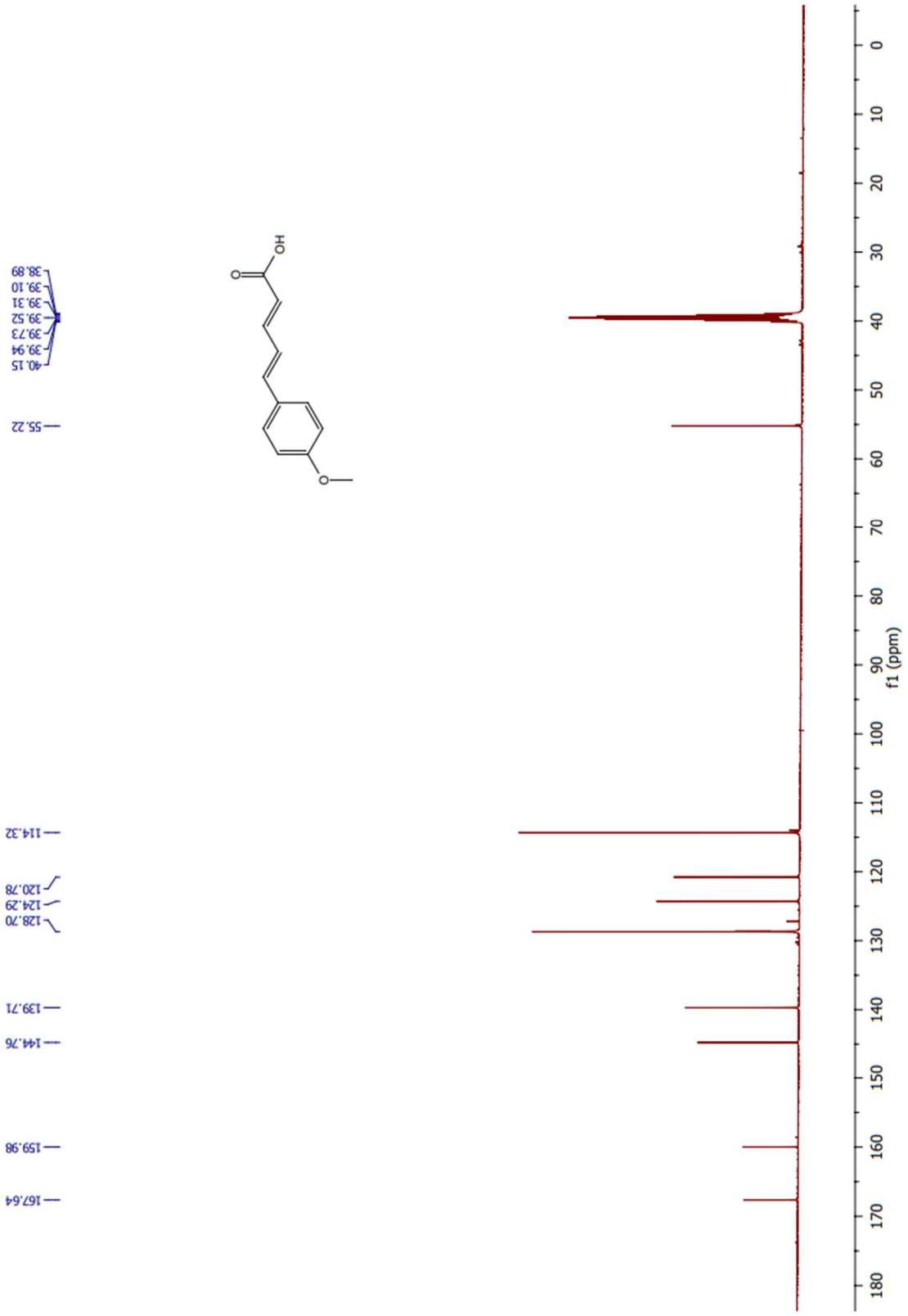

Figure 36. ^{13}C-NMR spectrum of **16** in DMSO-*d*6

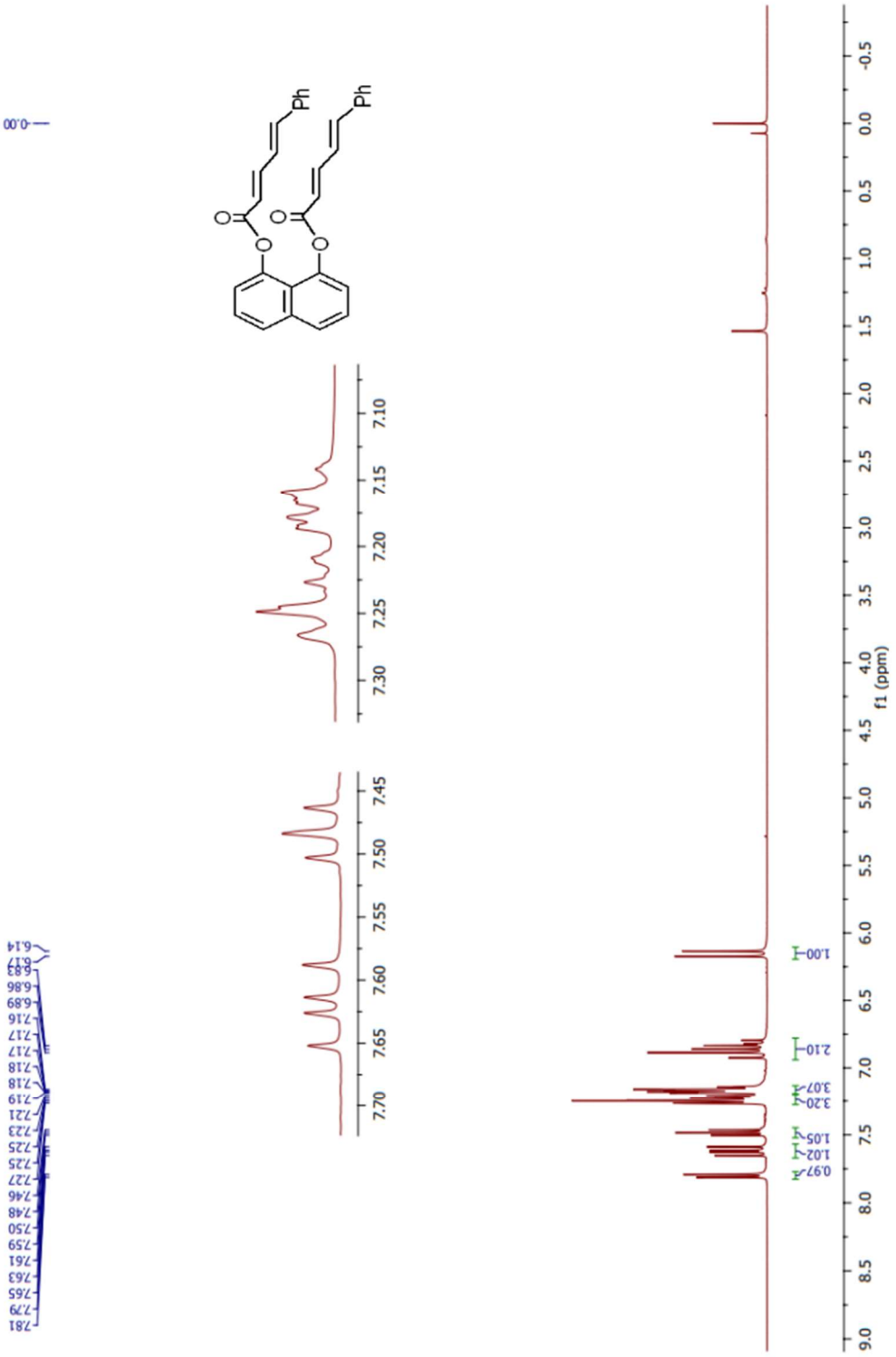

Figure 37. ^{1}H-NMR spectrum of **17** in $CDCl_3$

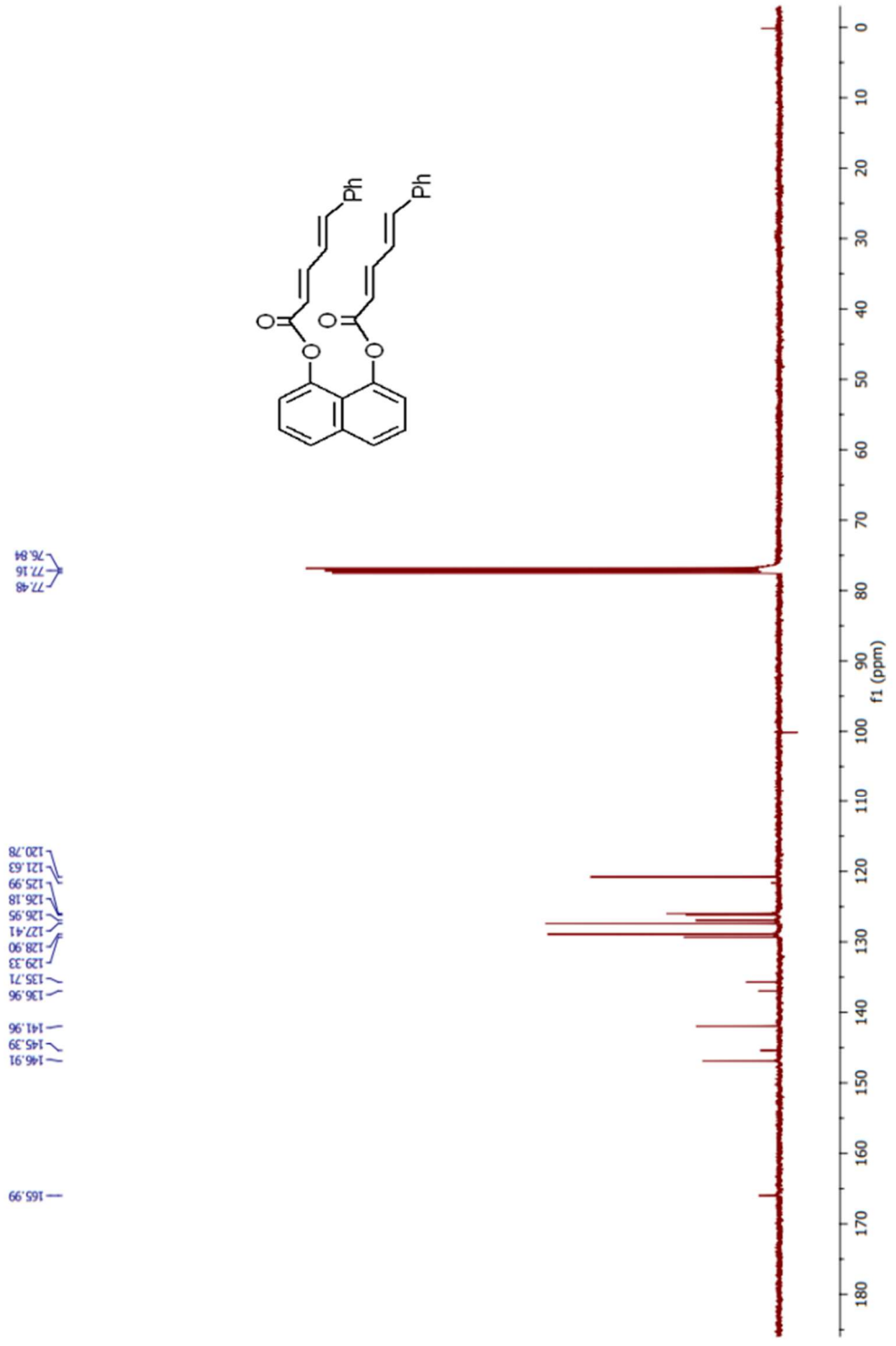

Figure 38. ^{13}C-NMR spectrum of **17** in $CDCl_3$

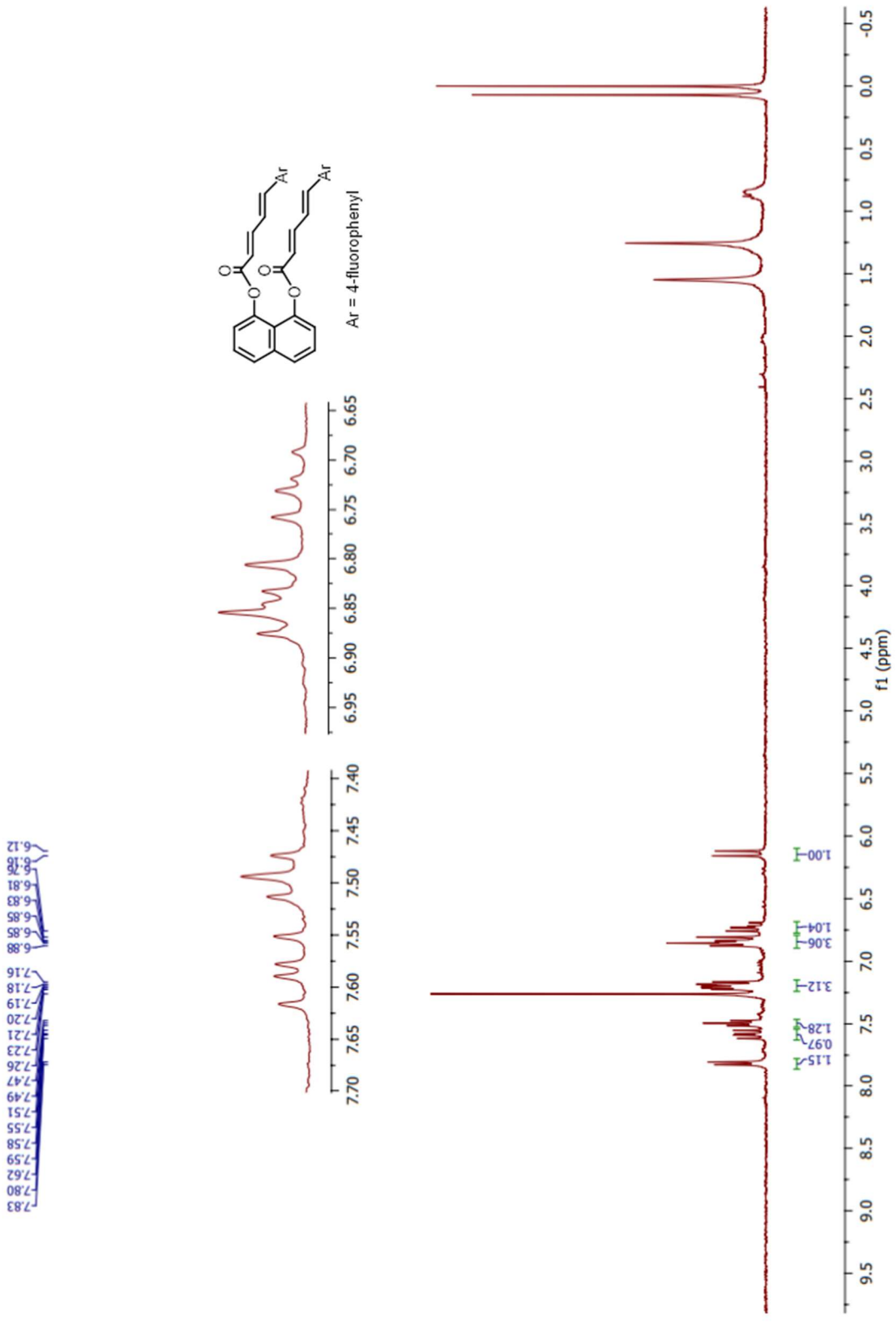

Figure 39. ^{1}H-NMR spectrum of **18** in $CDCl_3$

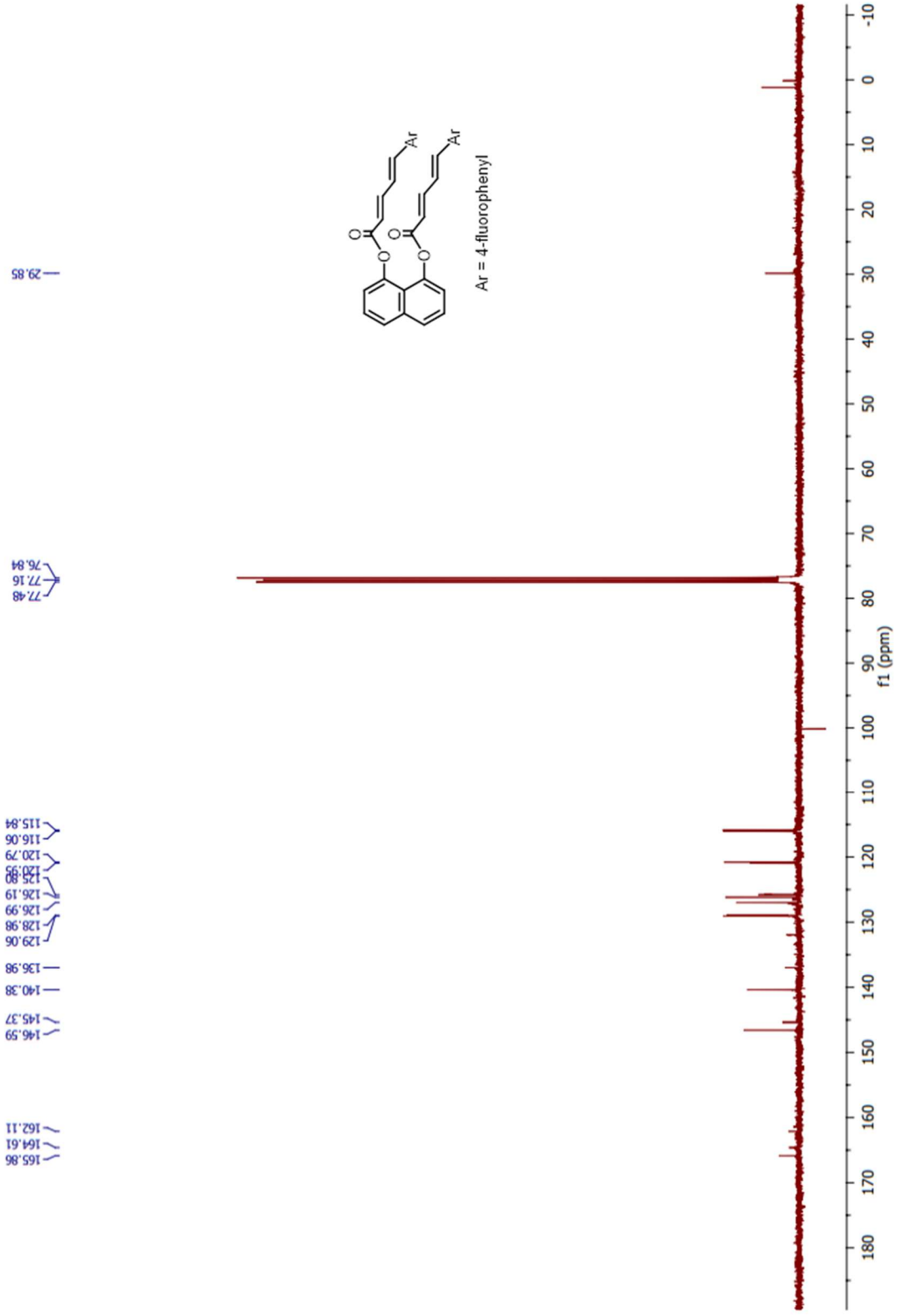

Figure 40. ^{13}C-NMR spectrum of **18** in $CDCl_3$

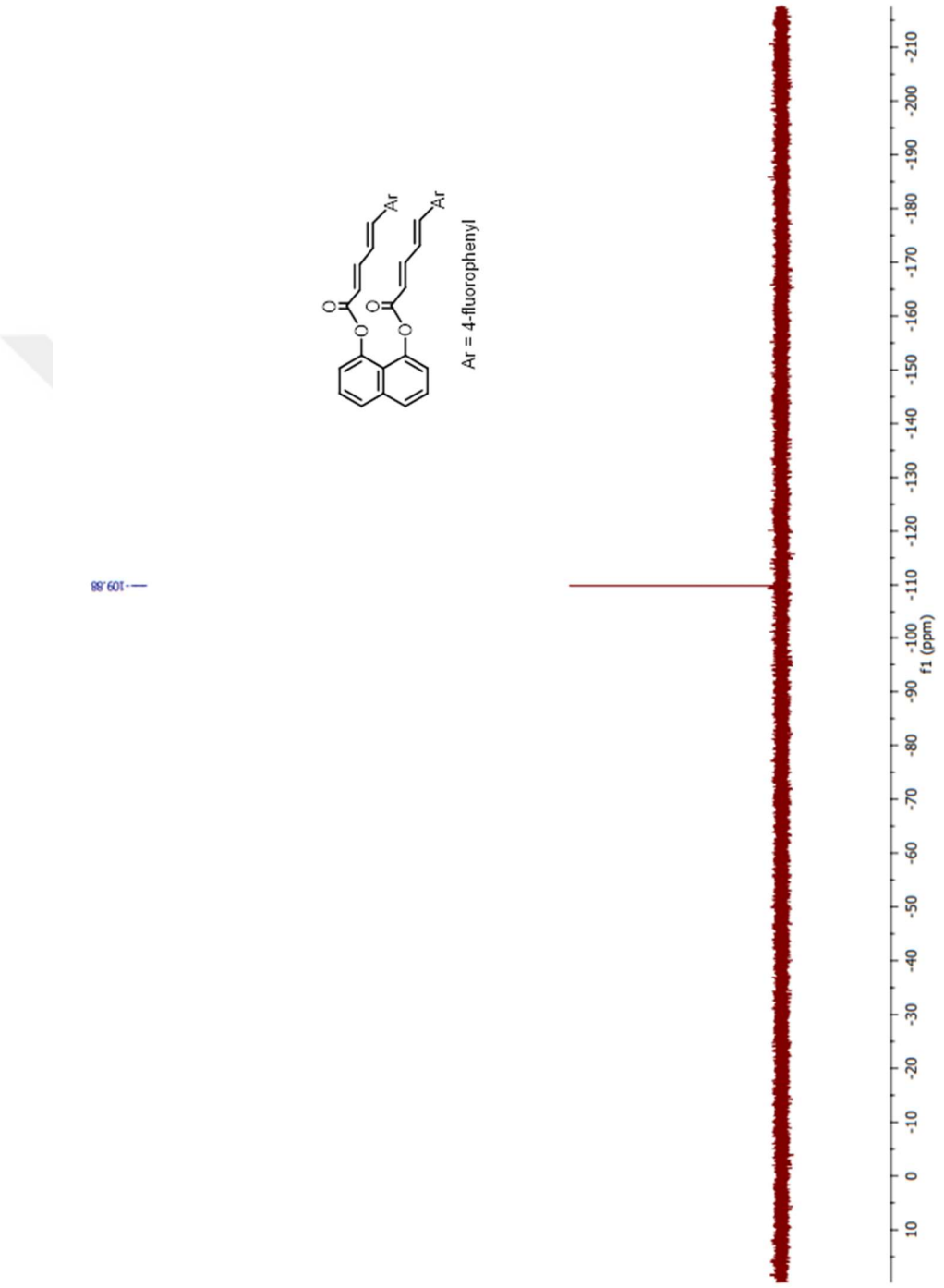

Figure 41. ^{19}F-NMR spectrum of **18** in $CDCl_3$

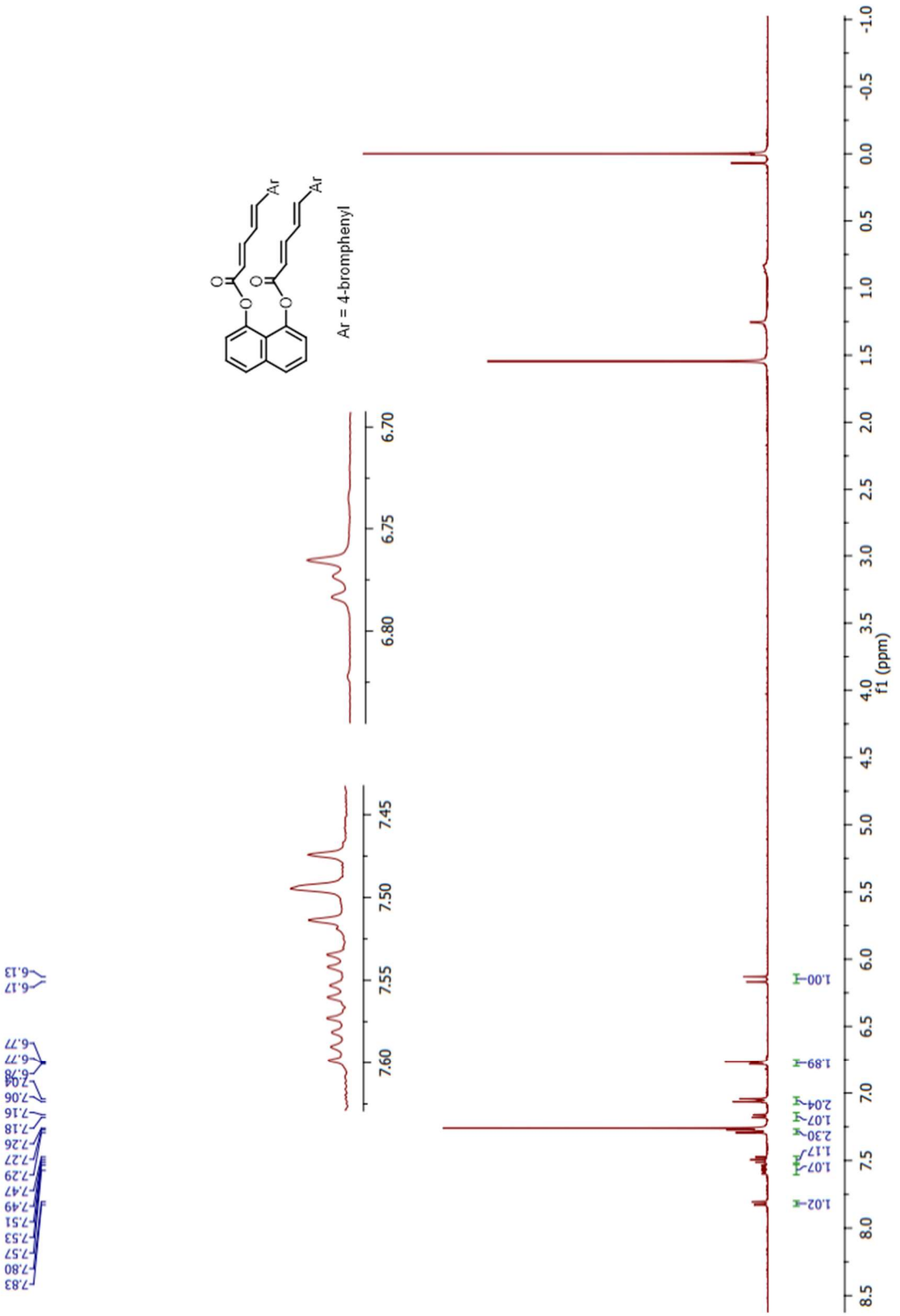

Figure 42. ^{1}H-NMR spectrum of **19** in $CDCl_3$

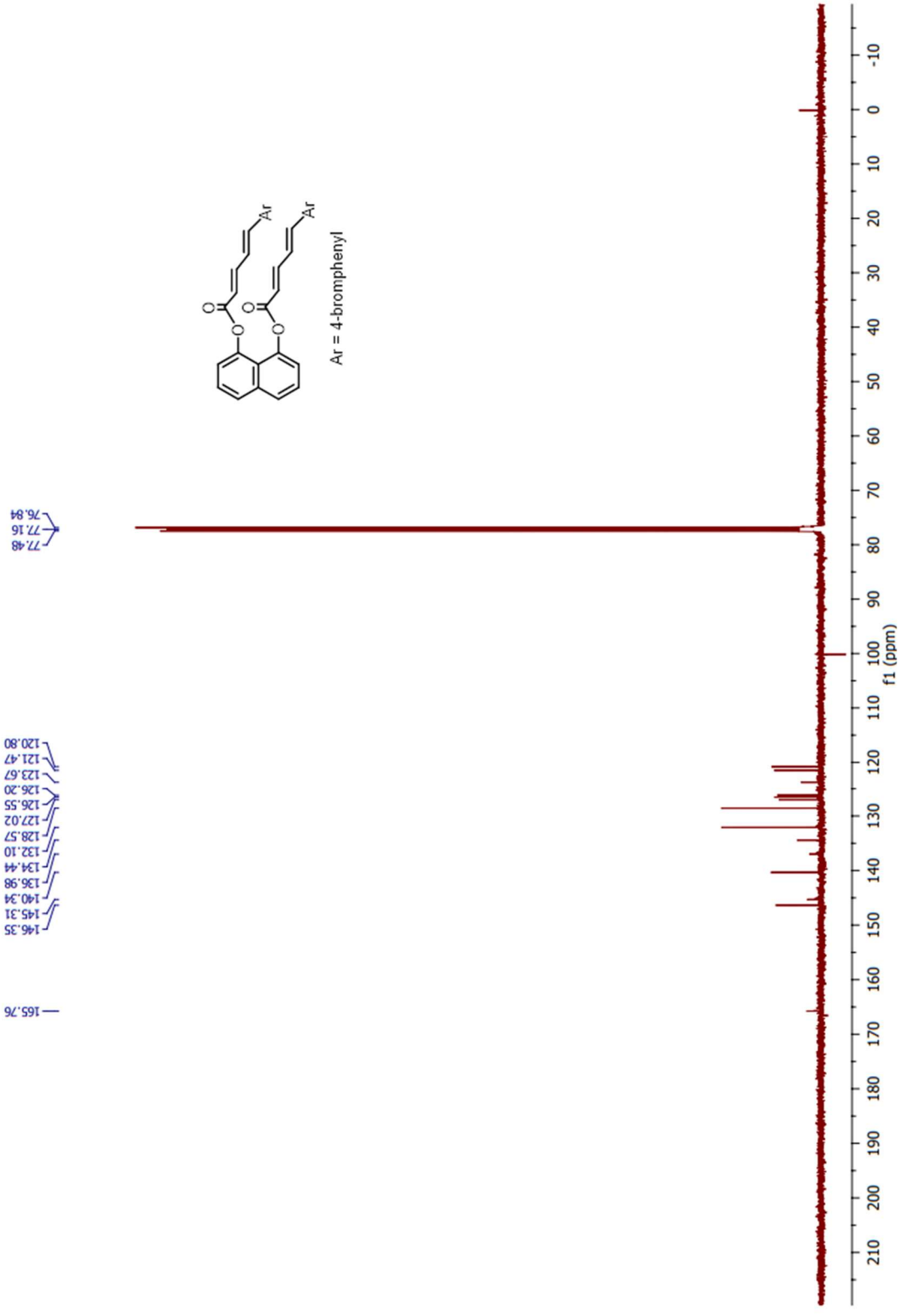

Figure 43. ^{13}C-NMR spectrum of **19** in $CDCl_3$

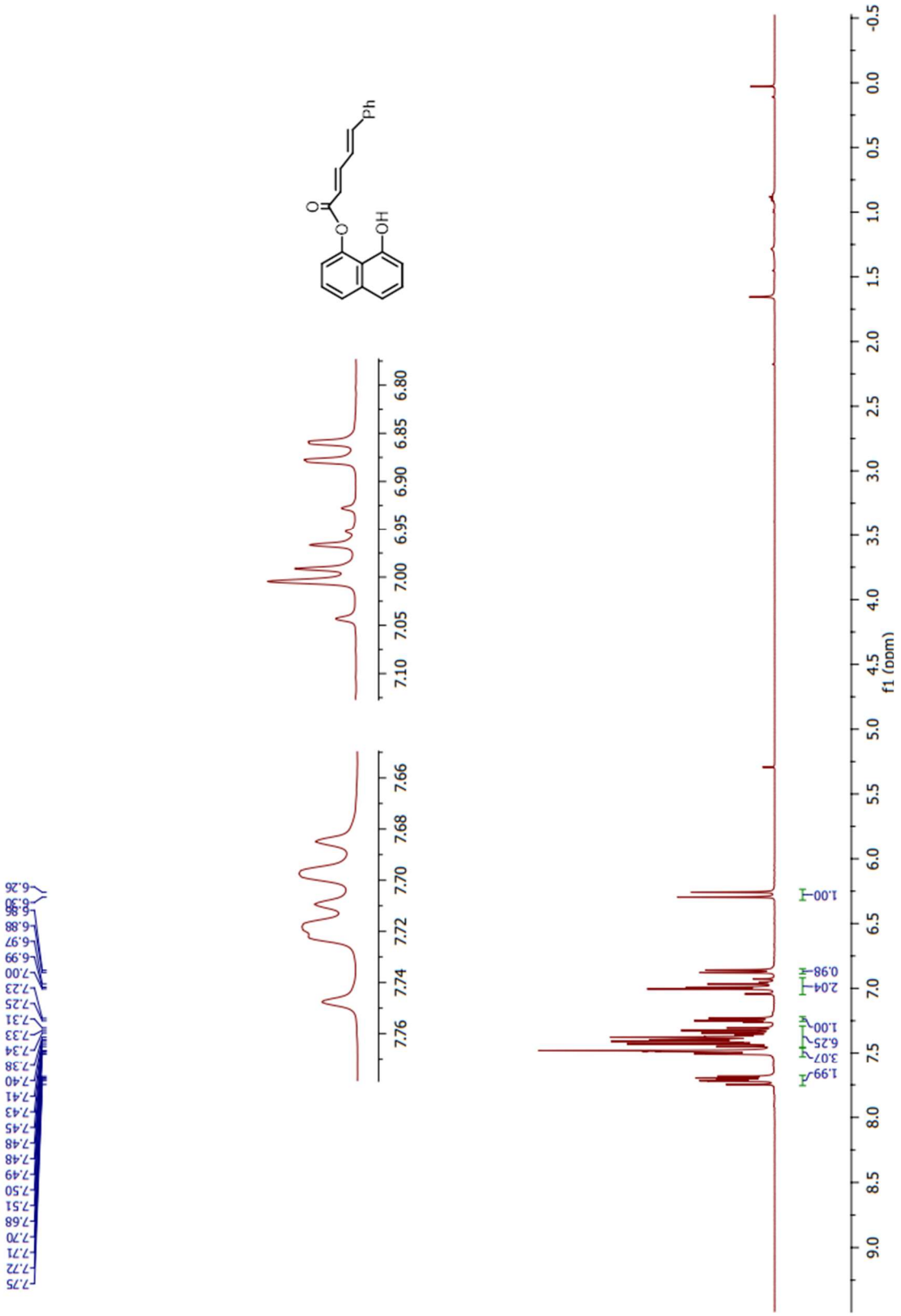

Figure 44. ^{1}H-NMR spectrum of **21** in $CDCl_3$

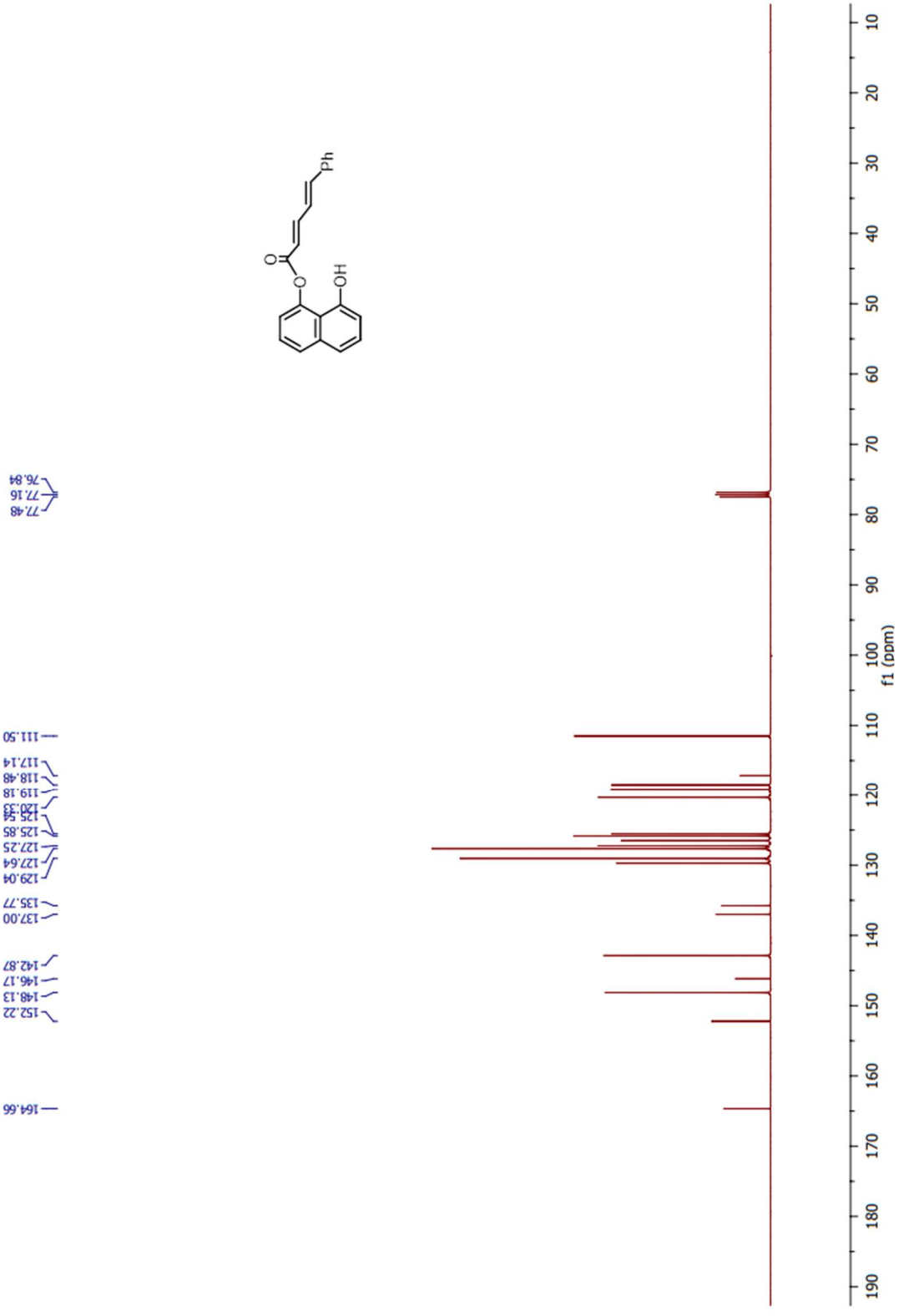

Figure 45. ^{13}C-NMR spectrum of **21** in $CDCl_3$

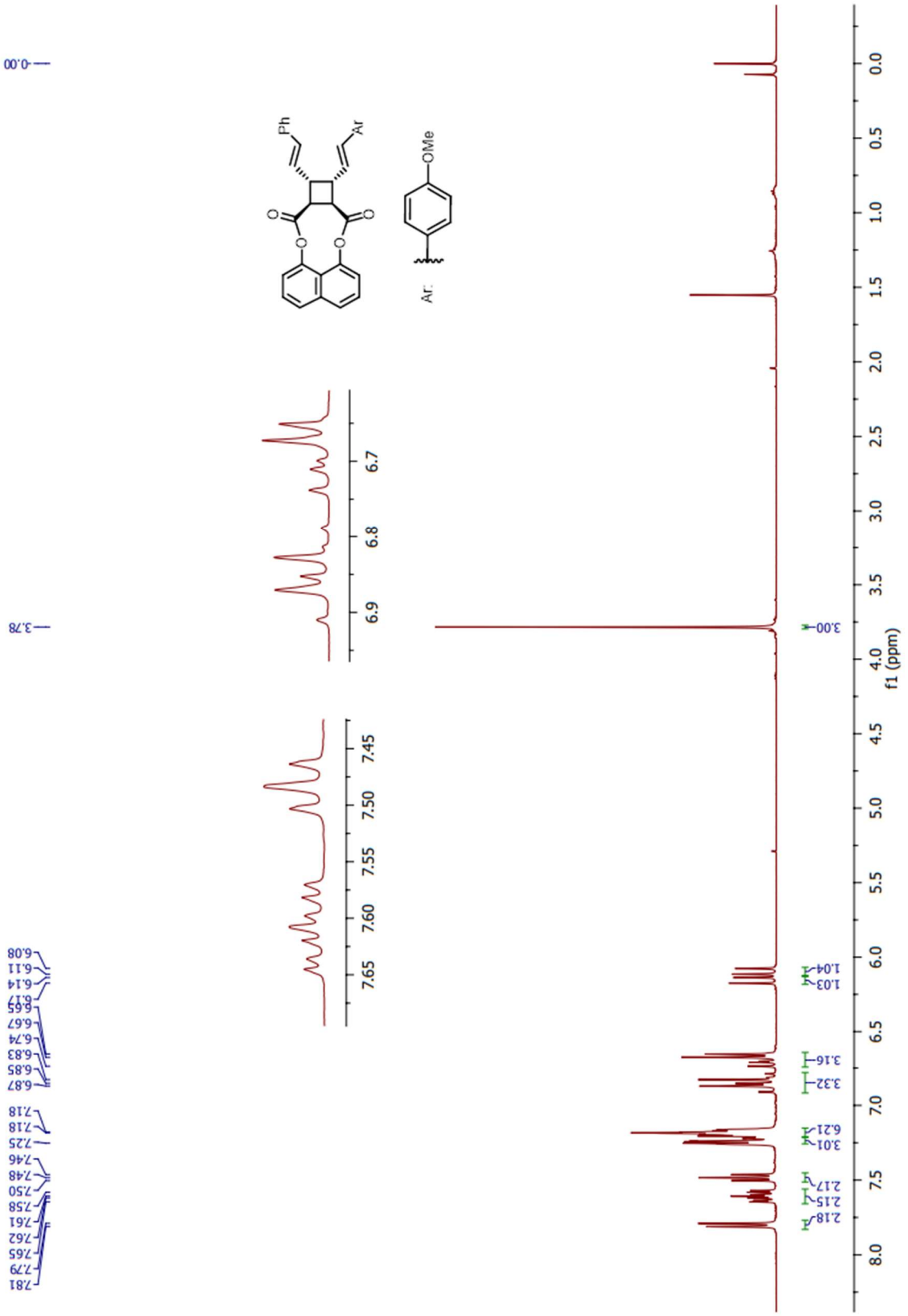

Figure 46. ^{1}H-NMR spectrum of **22** in $CDCl_3$

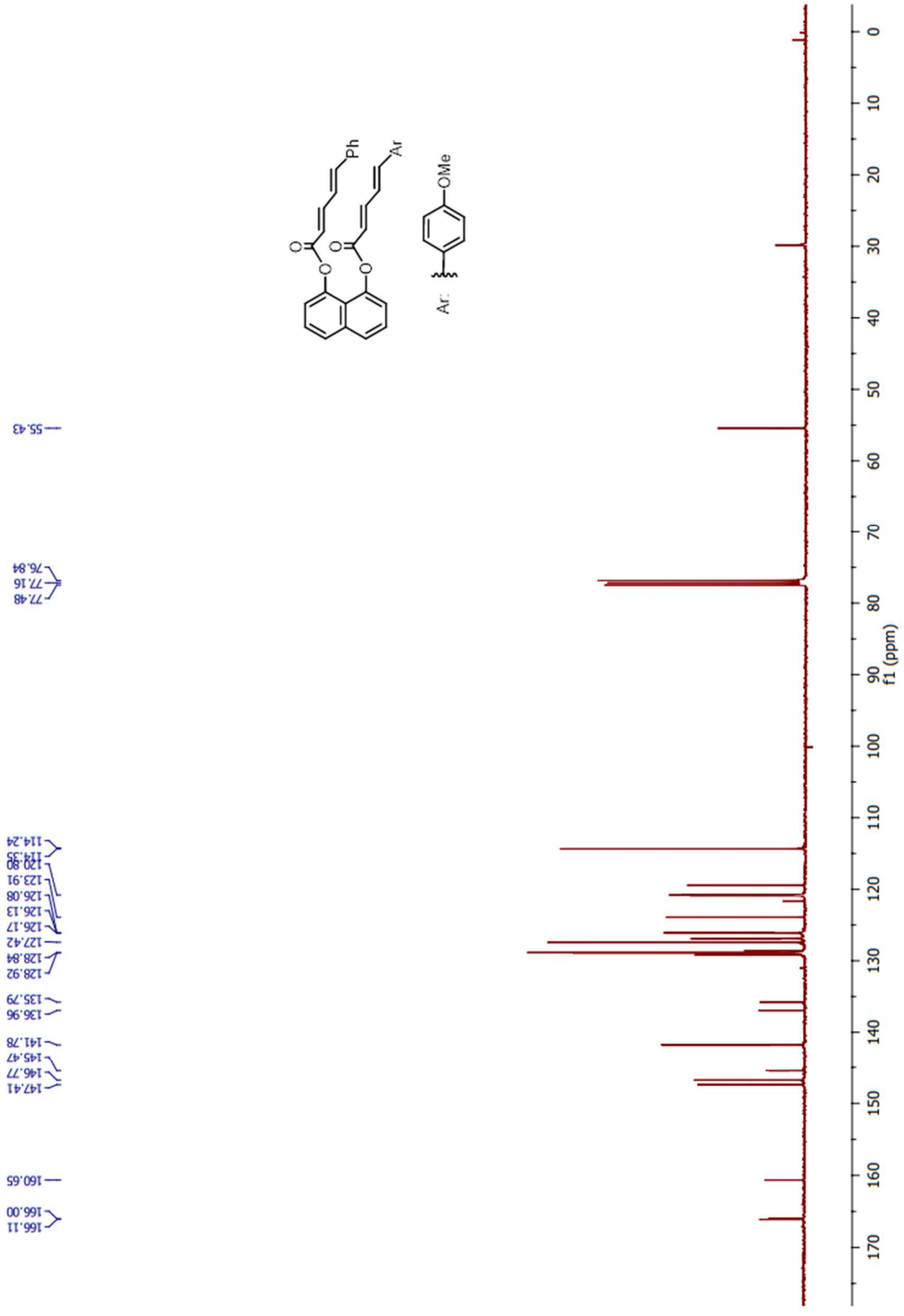

Figure 47. ^{13}C-NMR spectrum of **22** in $CDCl_3$

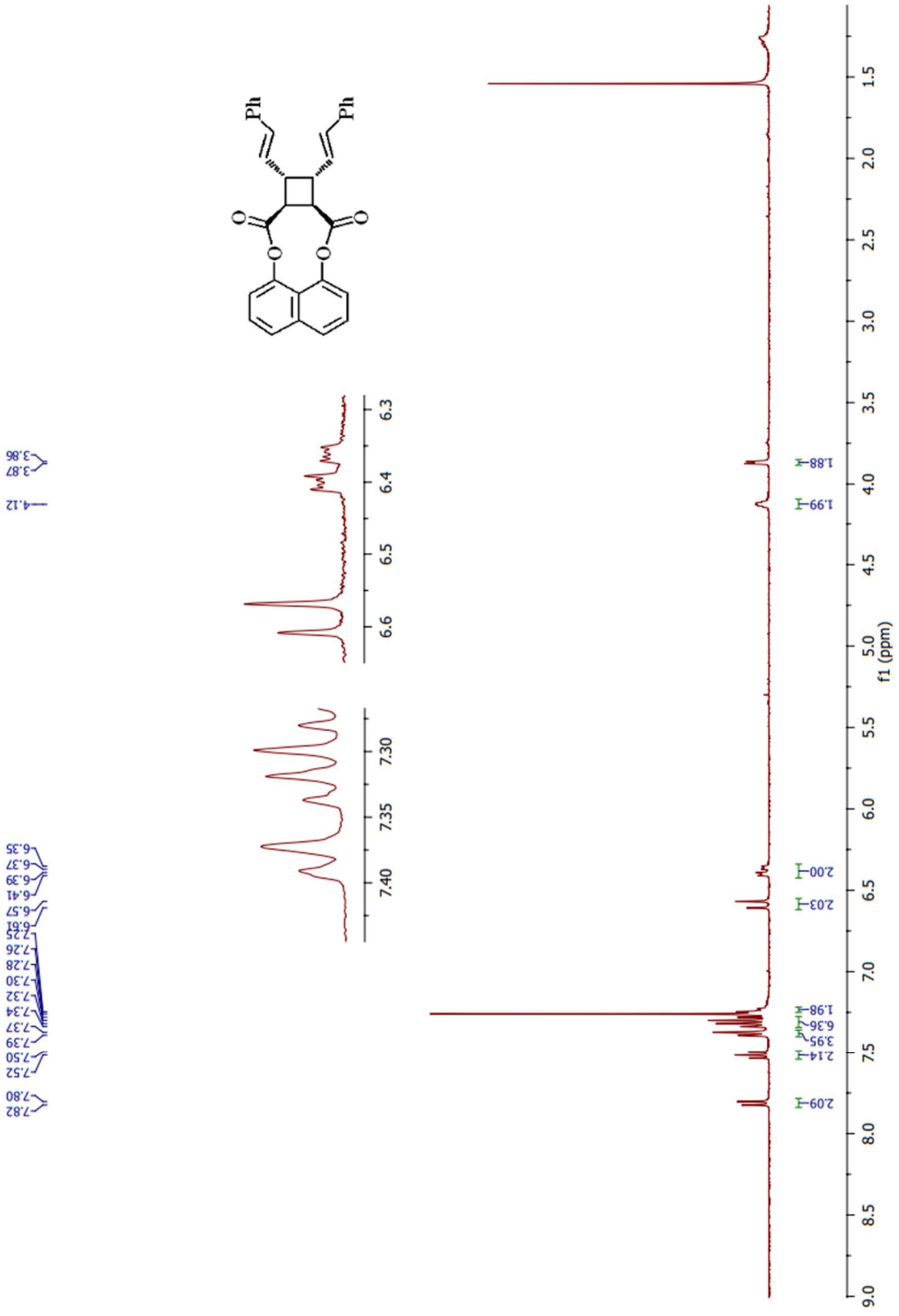

Figure 48. ^{1}H-NMR spectrum of **23** in $CDCl_3$

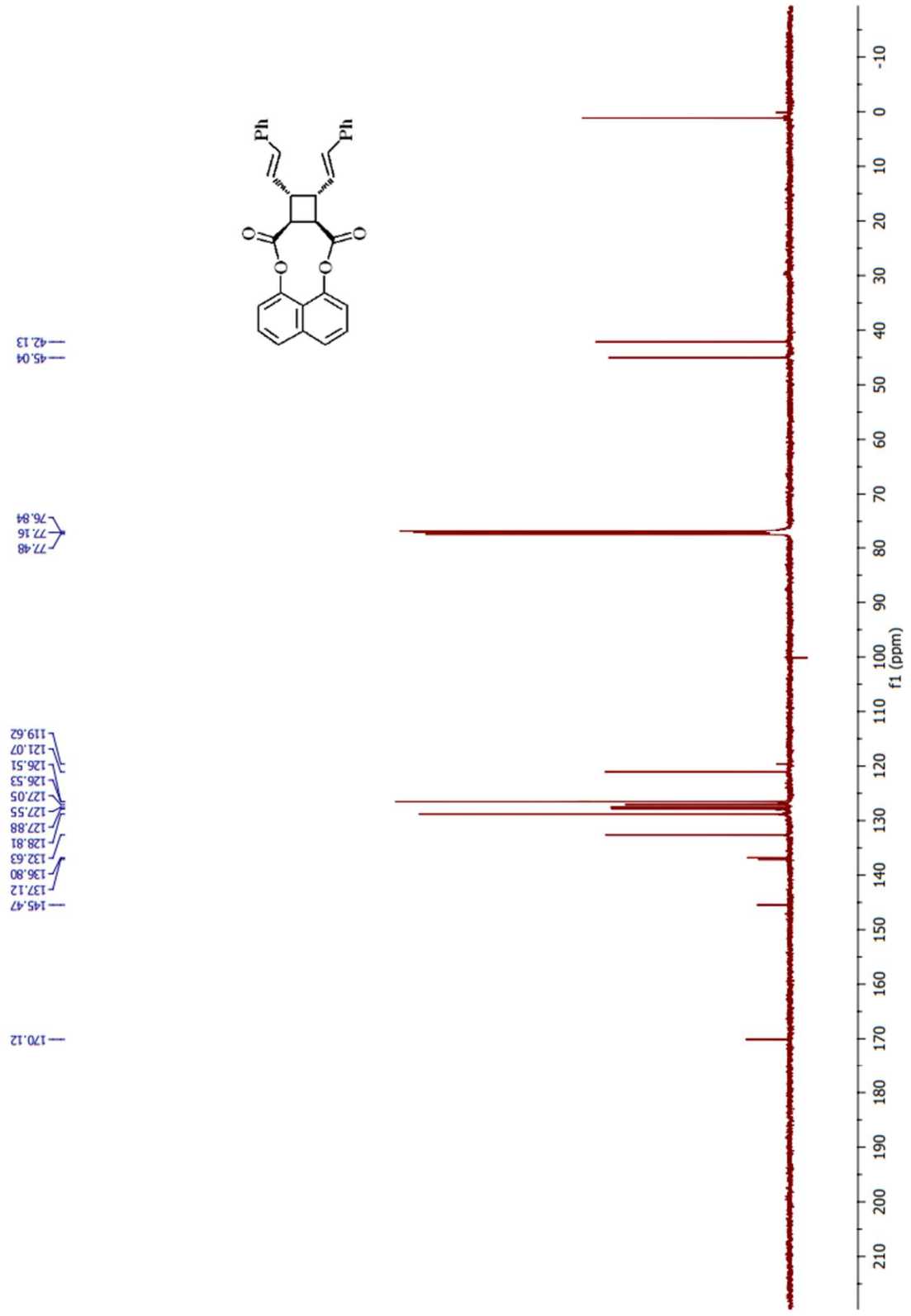

Figure 49. ^{13}C-NMR spectrum of **23** in $CDCl_3$

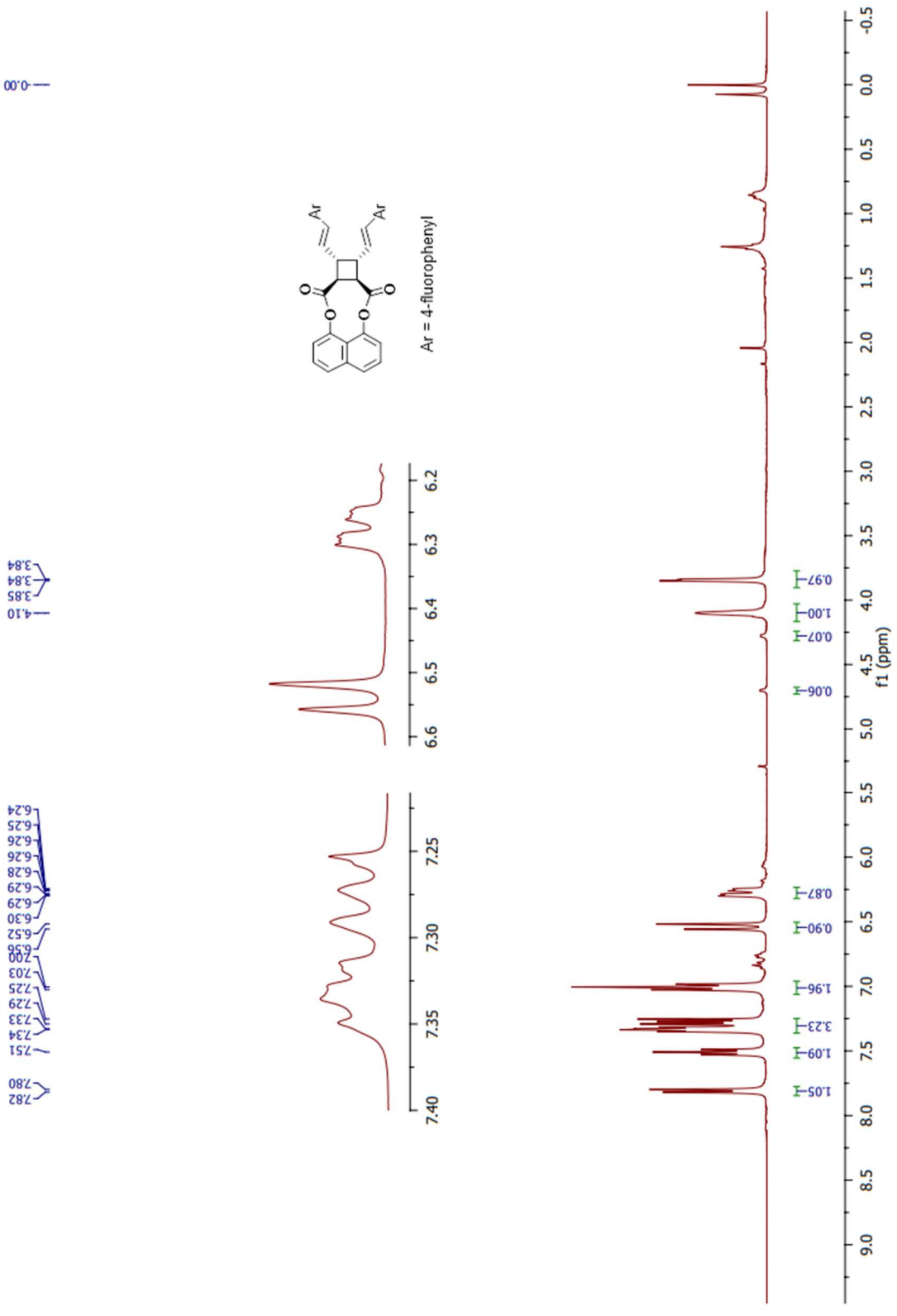

Figure 50. ^{1}H-NMR spectrum of **24** in $CDCl_3$

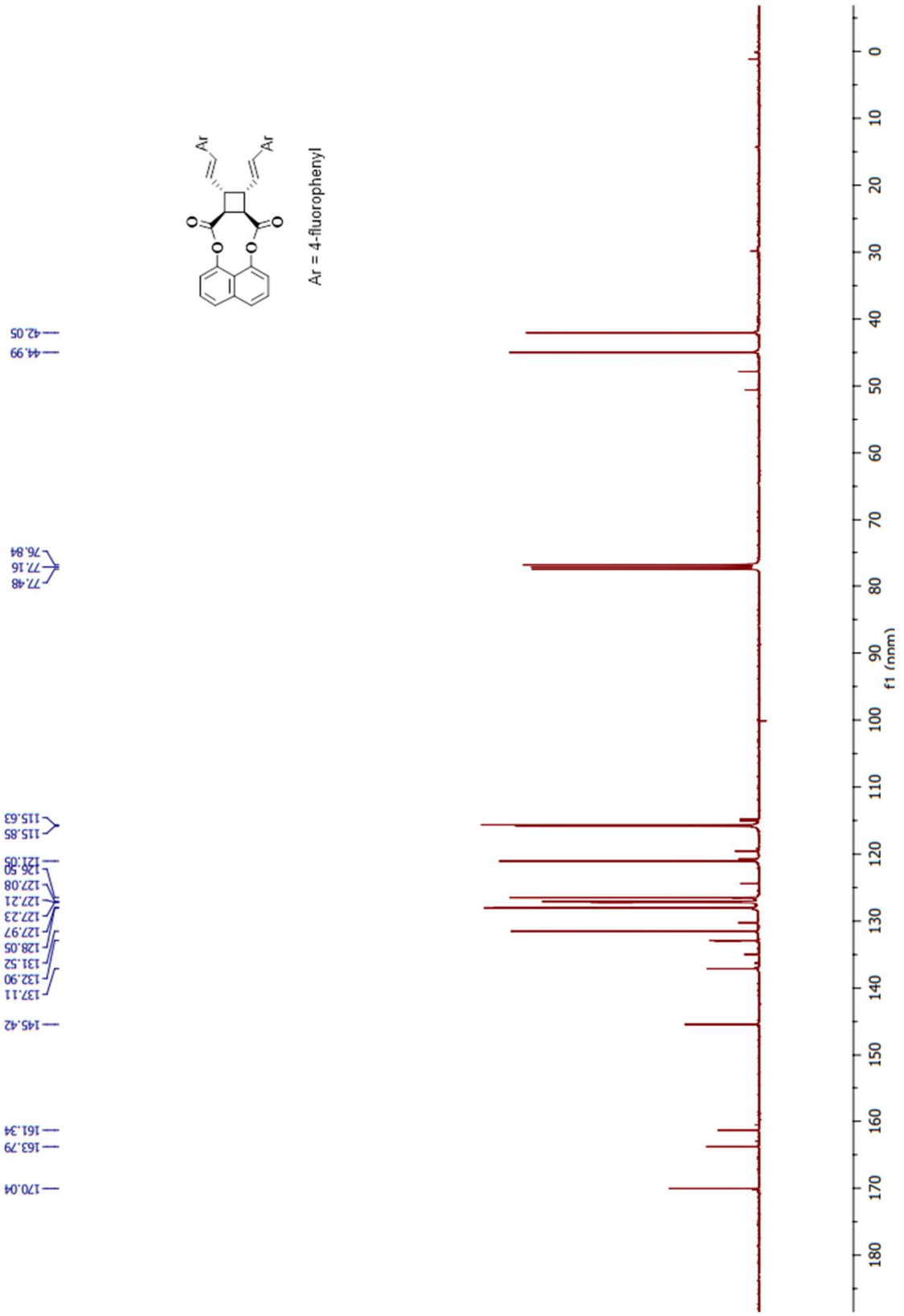

Figure 51. ^{13}C-NMR spectrum of **24** in $CDCl_3$

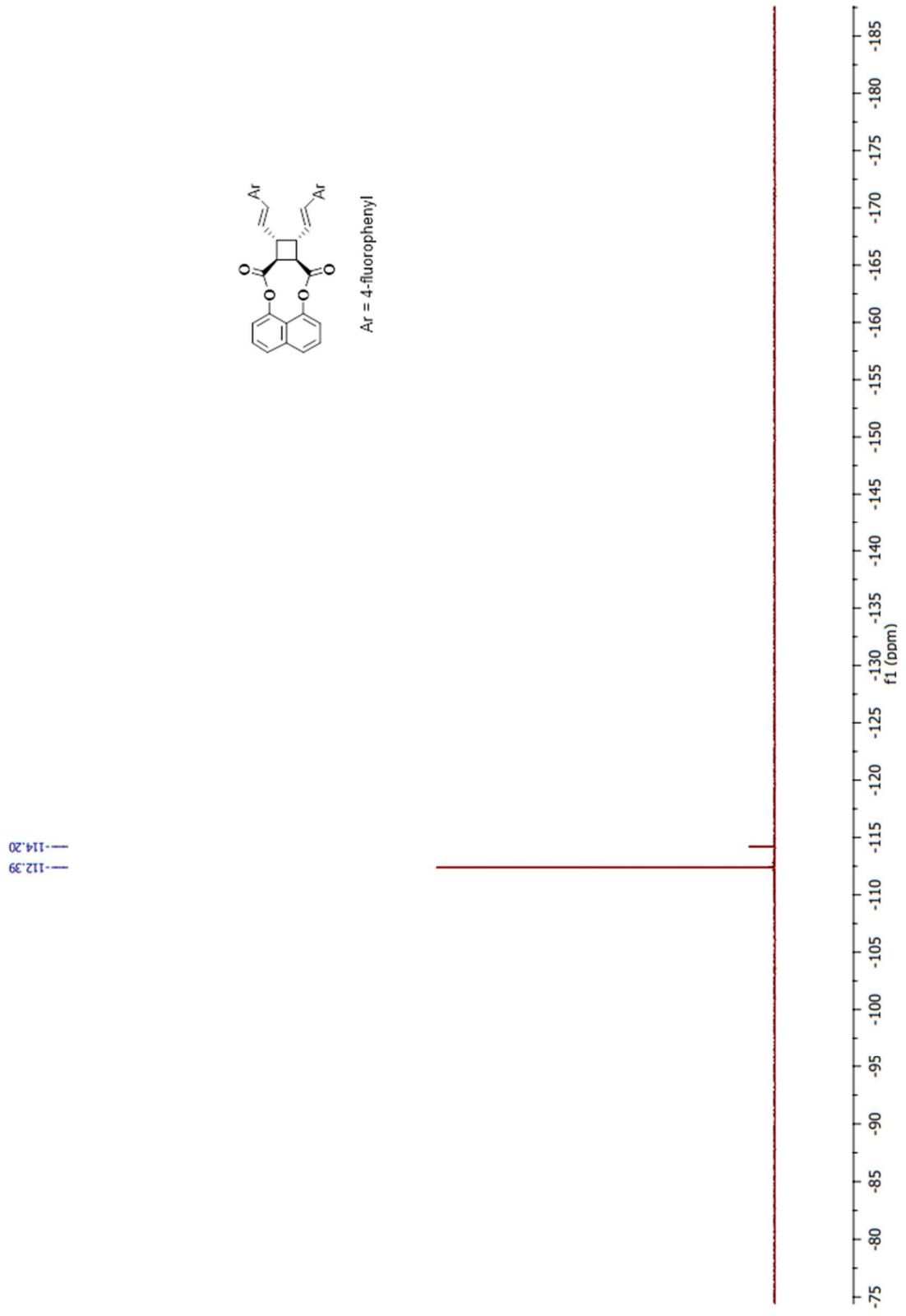

Figure 52. ^{19}F-NMR spectrum of **24** in $CDCl_3$

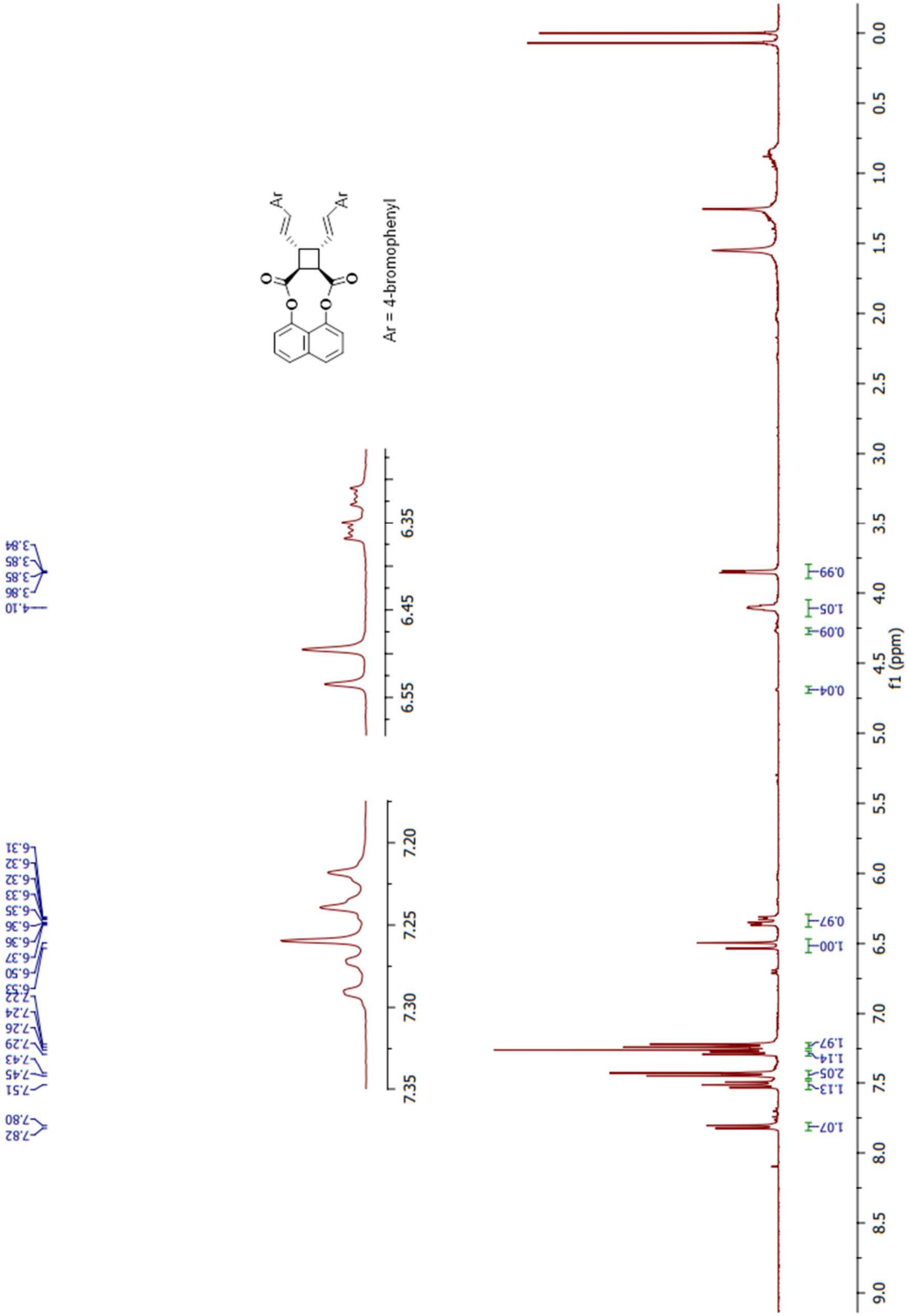

Figure 53. ^{1}H-NMR spectrum of **25** in $CDCl_3$

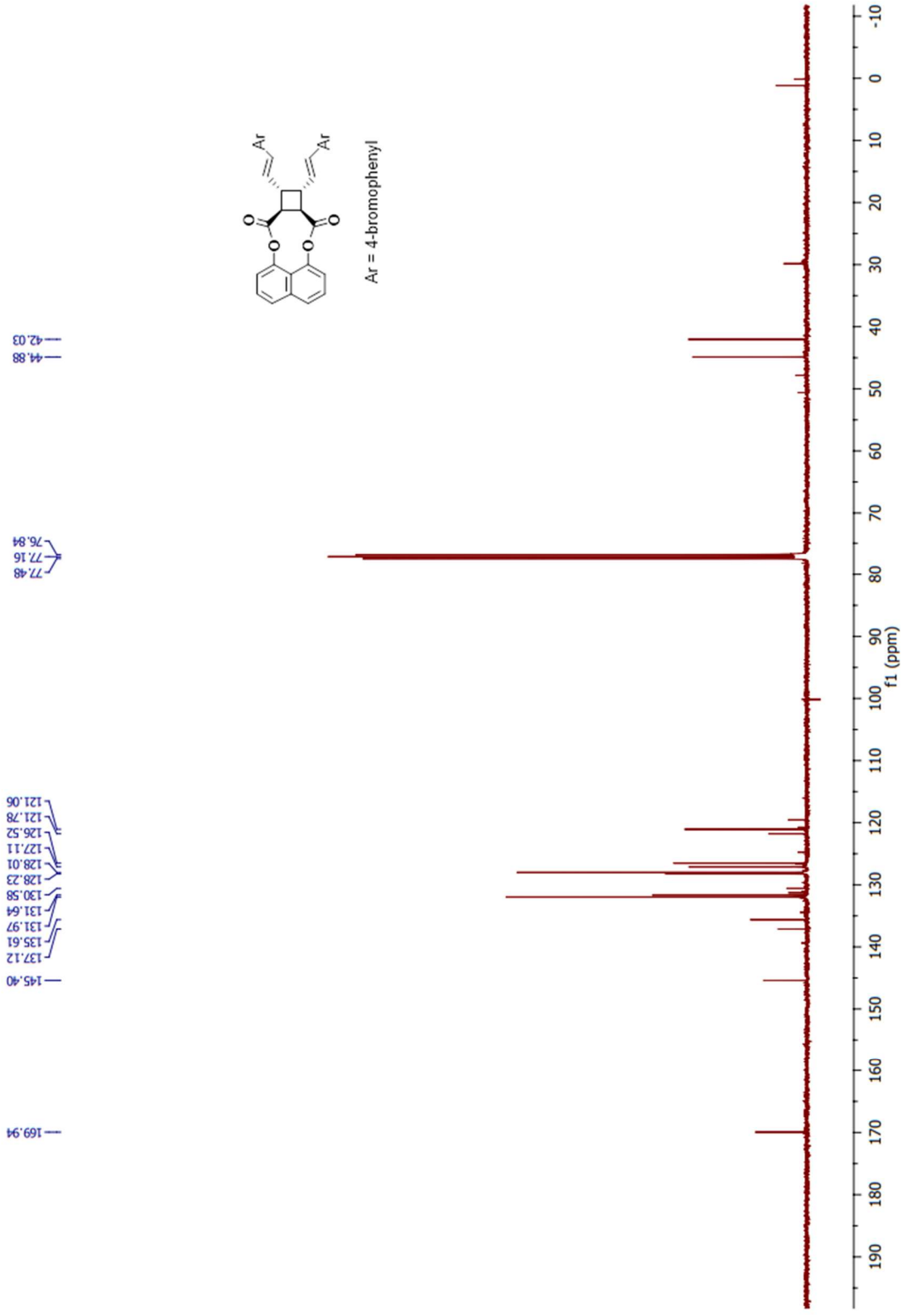

Figure 54. ^{13}C-NMR spectrum of **25** in $CDCl_3$

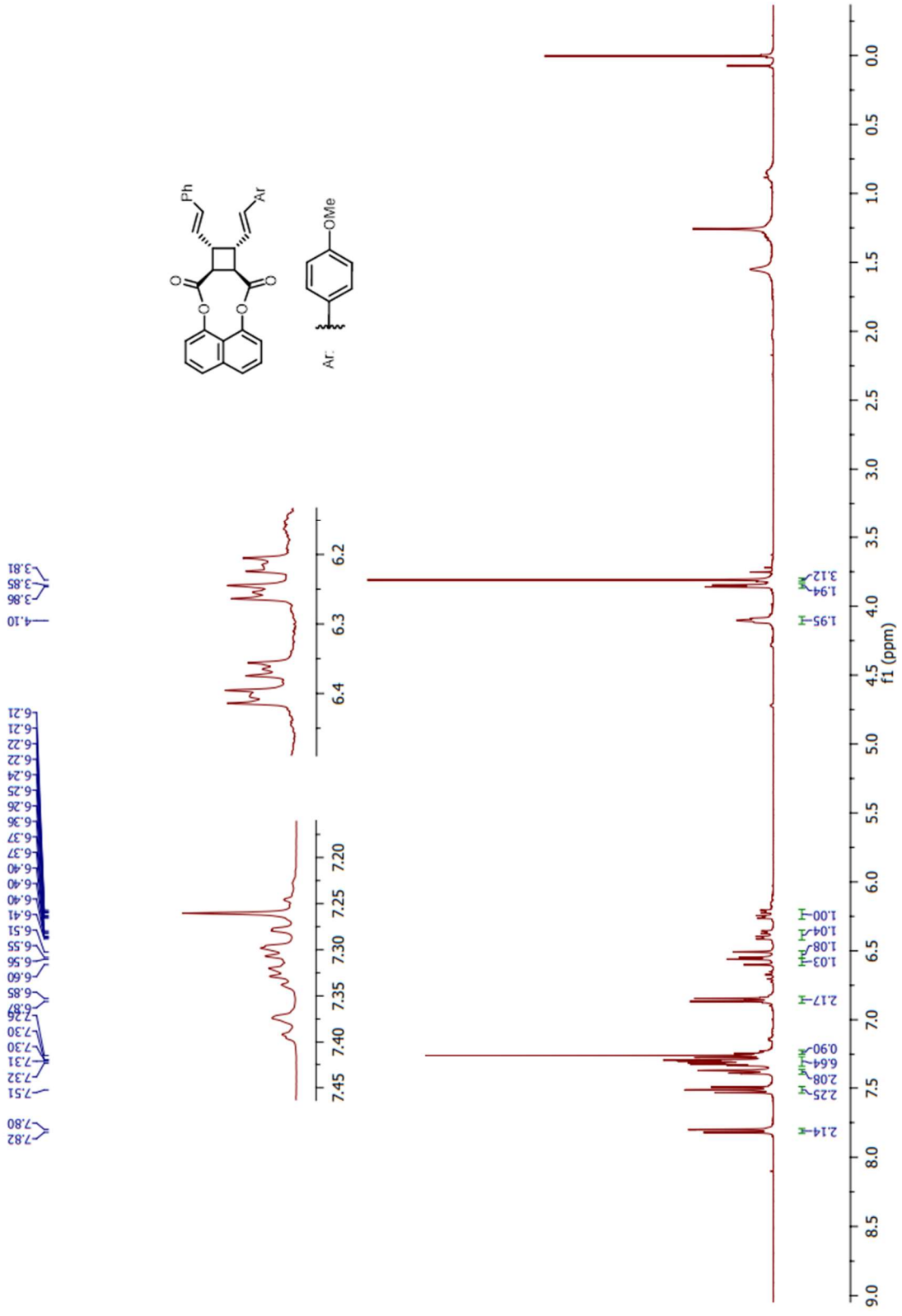

Figure 55. ^{1}H-NMR spectrum of **26** in $CDCl_3$

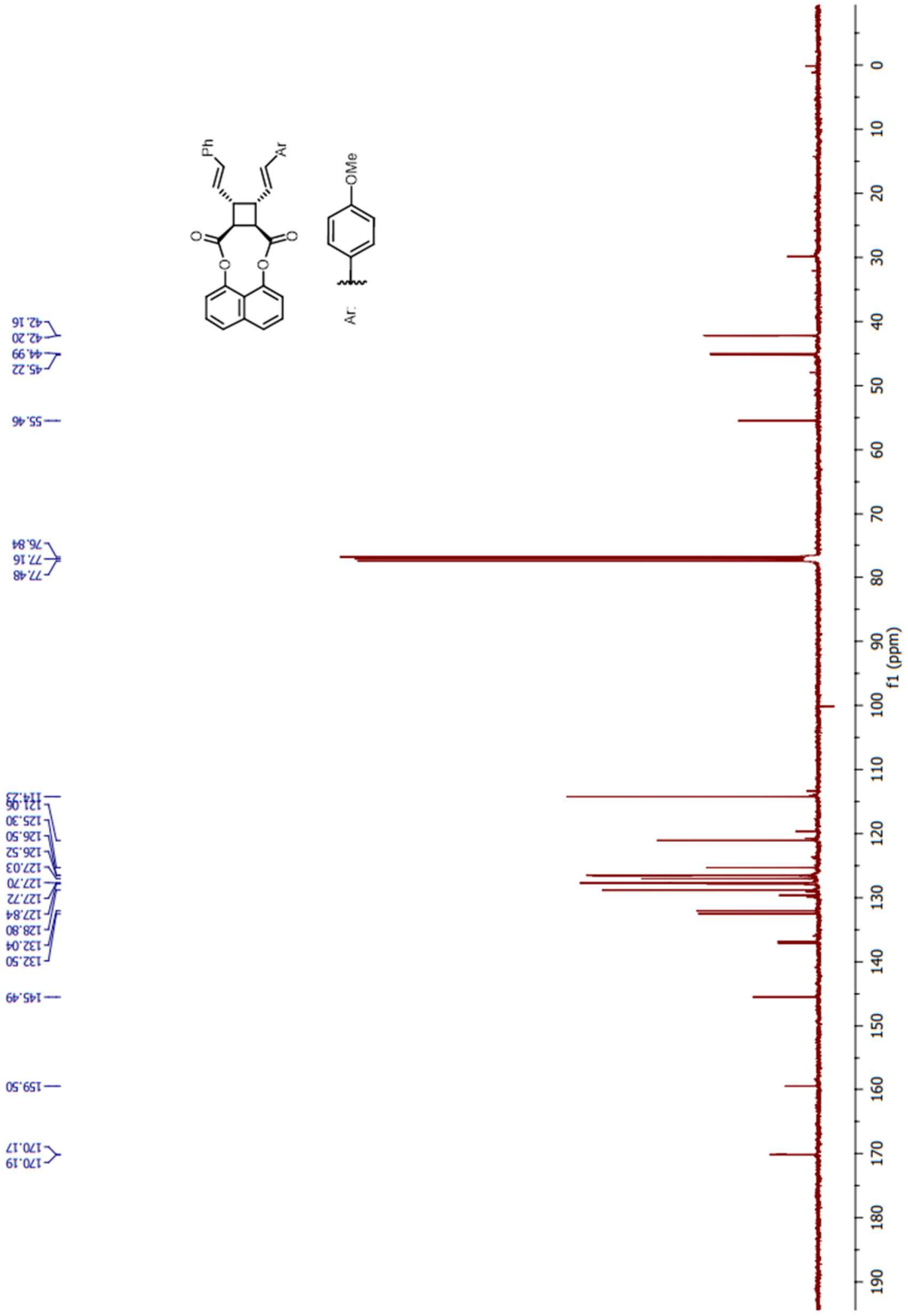

Figure 56. ^{13}C-NMR spectrum of **26** in $CDCl_3$

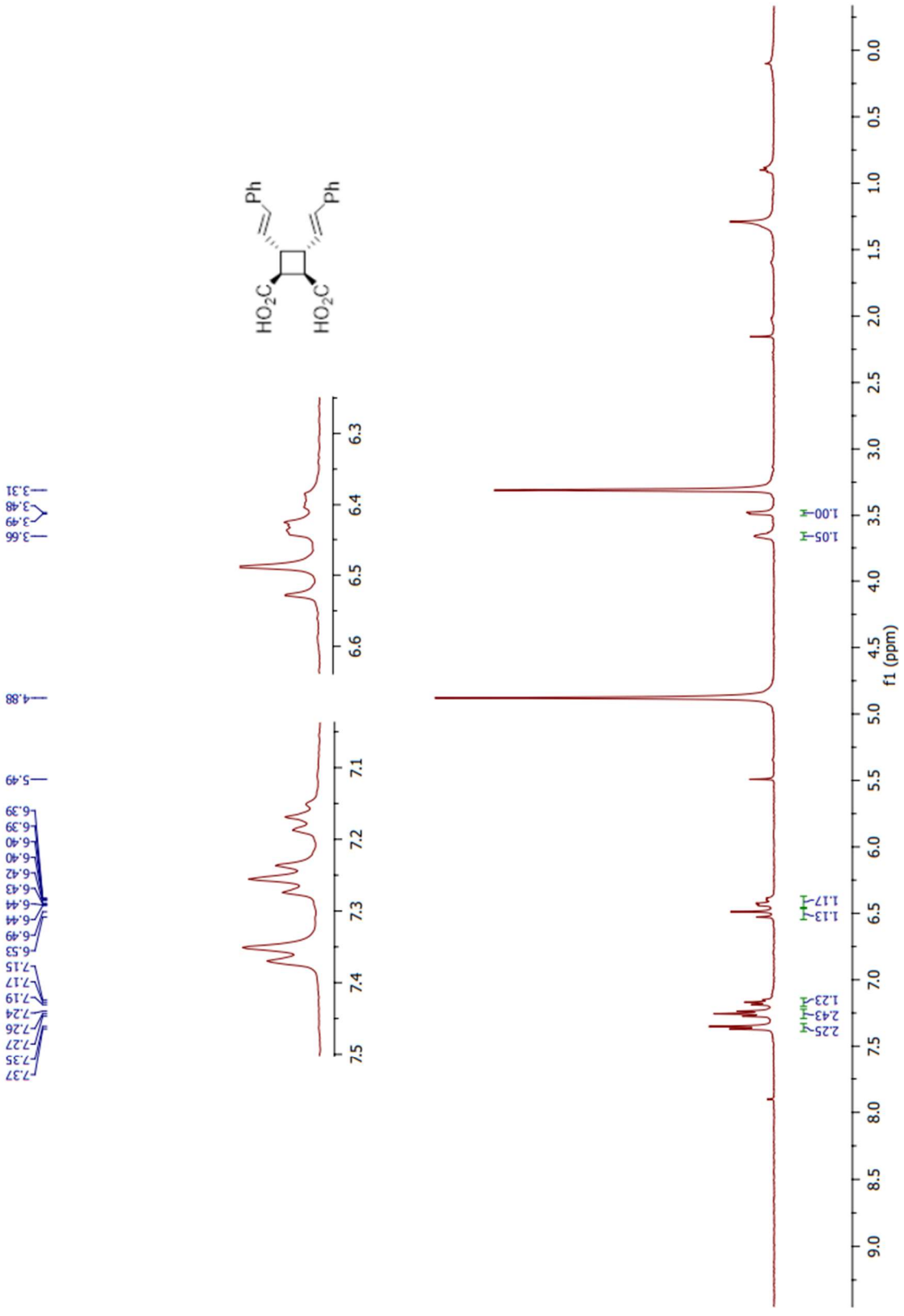

Figure 57. ^{1}H-NMR spectrum of **27** in CD_3OD

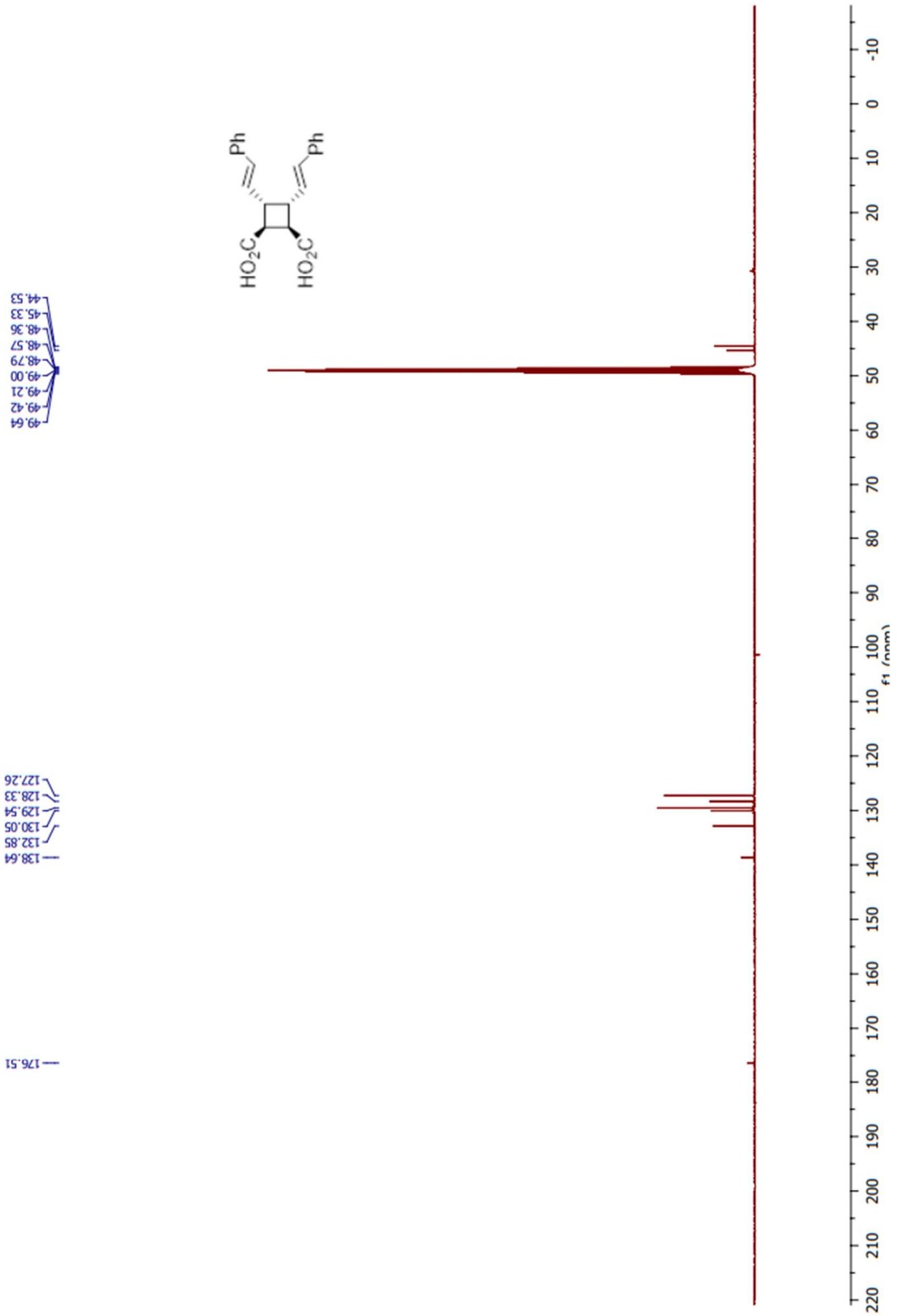

Figure 58. ^{13}C-NMR spectrum of **27** in CD_3OD

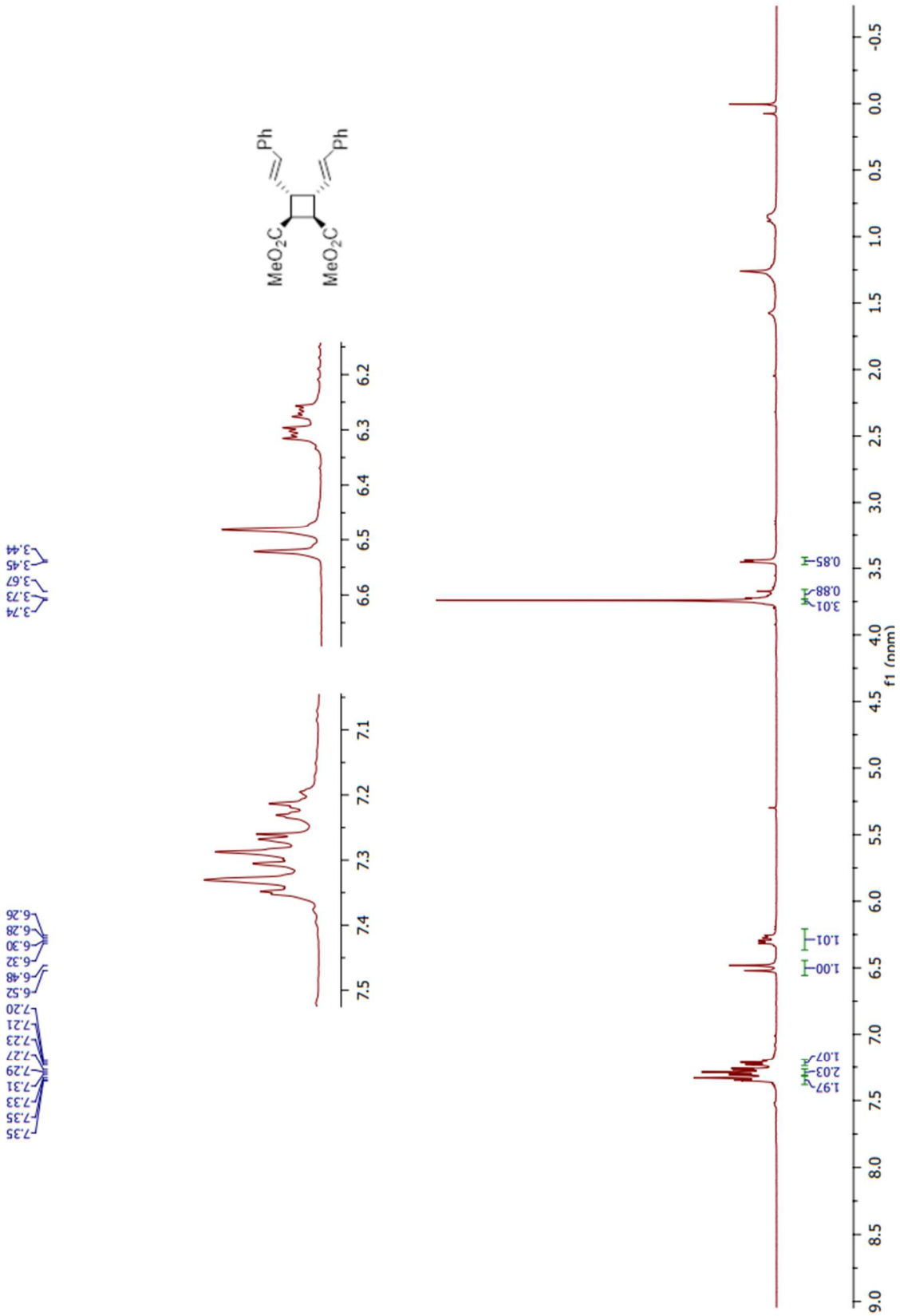

Figure 59. ^{1}H-NMR spectrum of **28** in $CDCl_3$

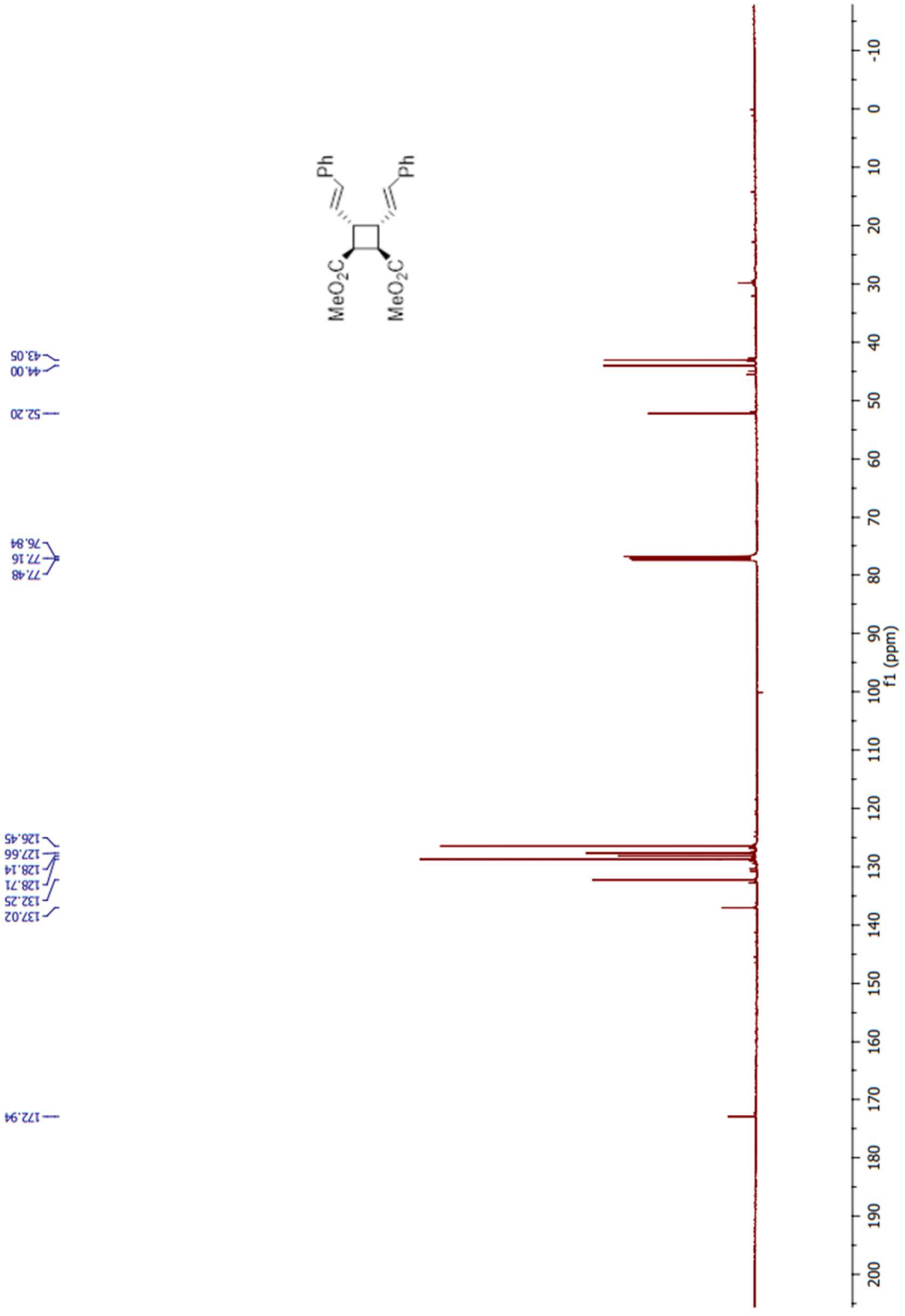

Figure 60. ^{13}C-NMR spectrum of **28** in $CDCl_3$

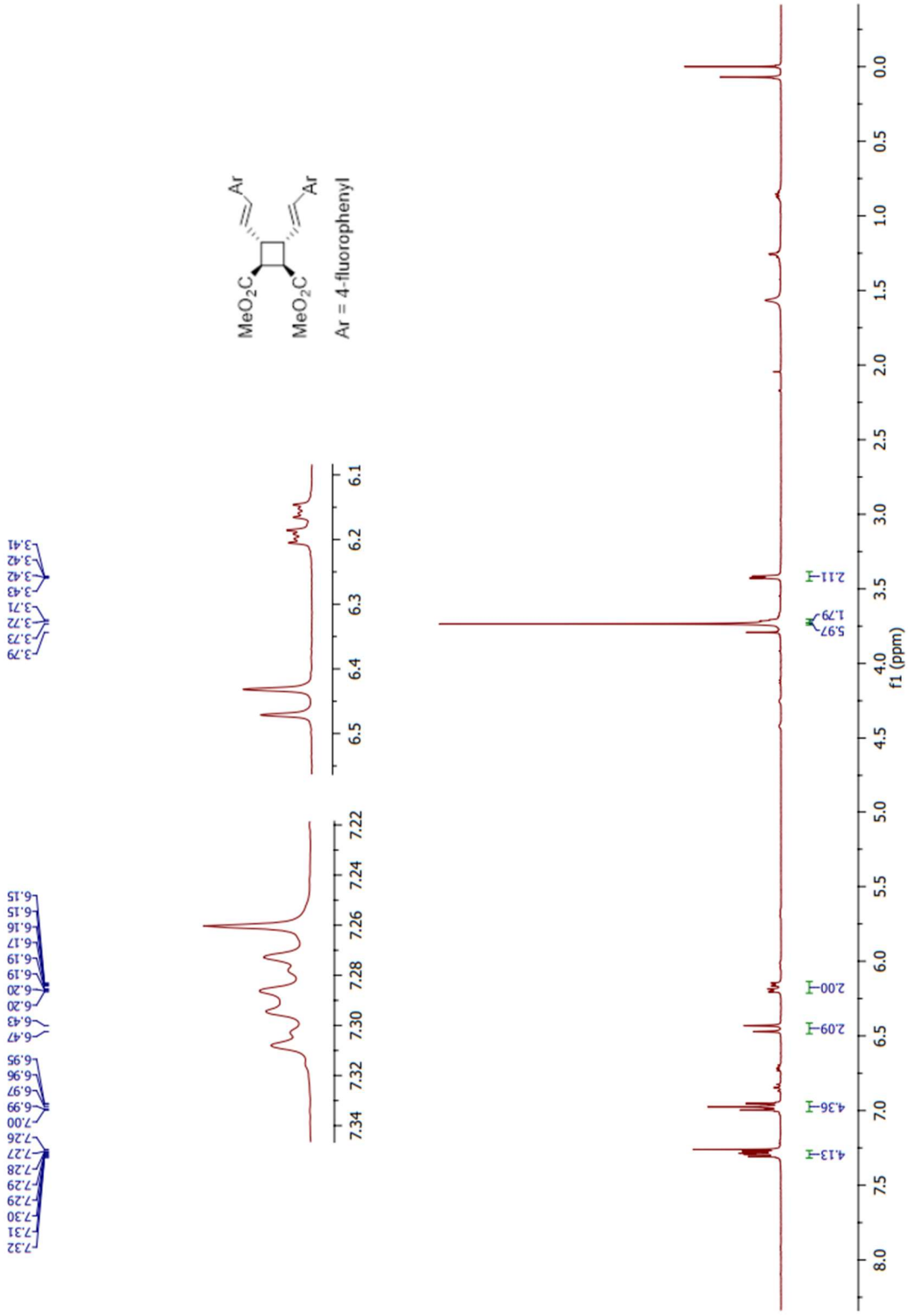

Figure 61. ^{1}H-NMR spectrum of **29** in $CDCl_3$

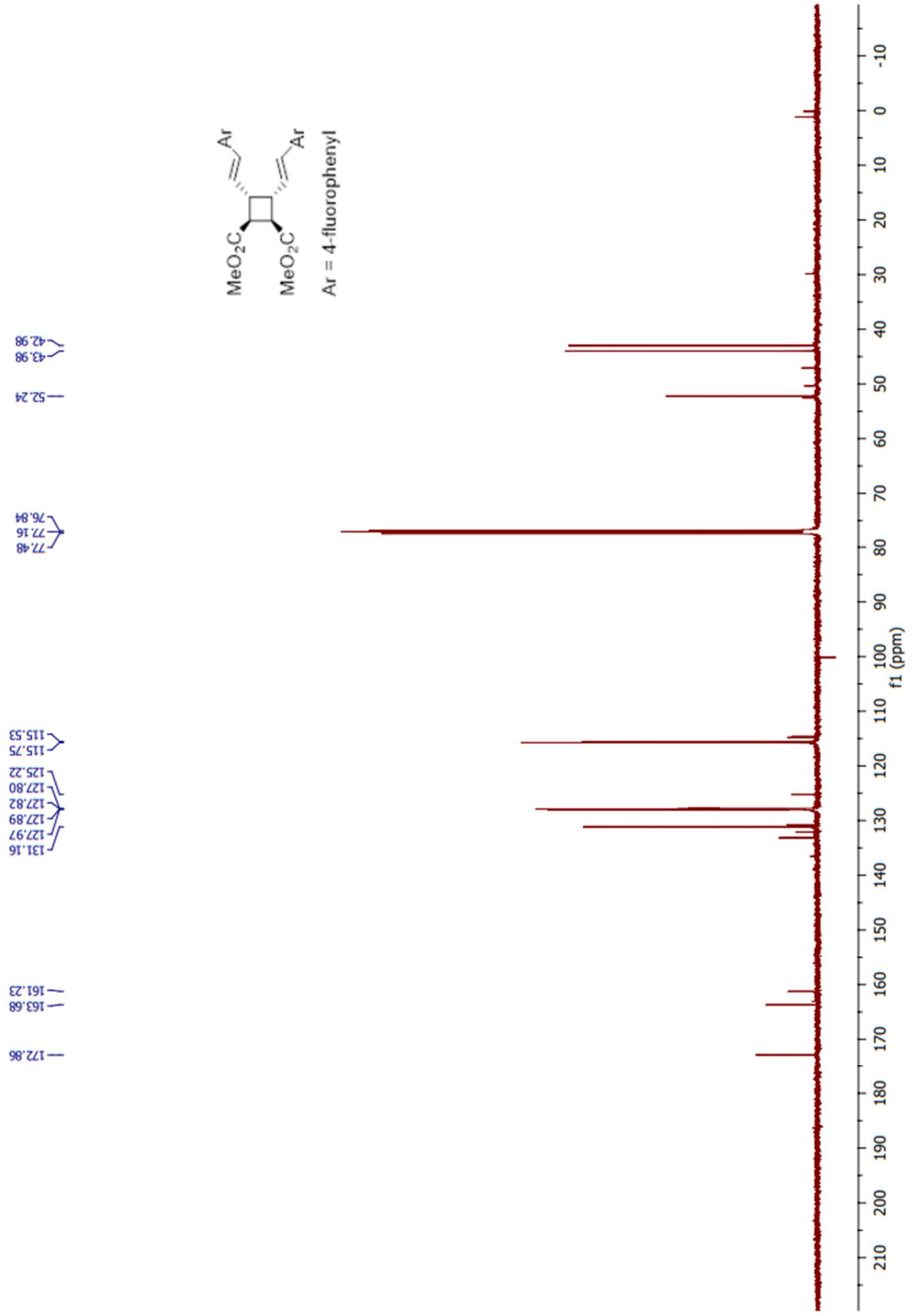

Figure 62. ^{13}C-NMR spectrum of **29** in $CDCl_3$

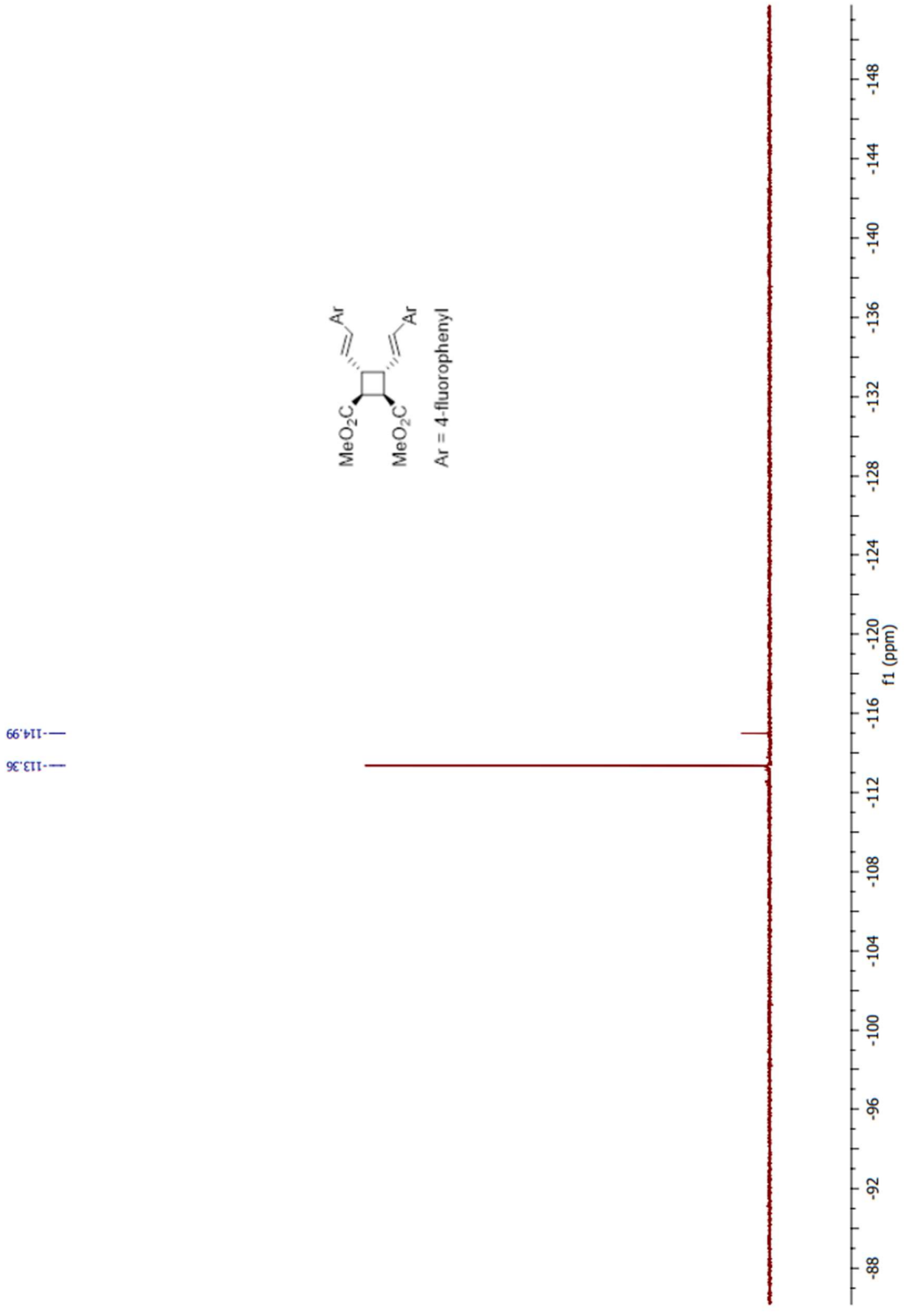

Figure 63. ^{19}F-NMR spectrum of **29** in $CDCl_3$

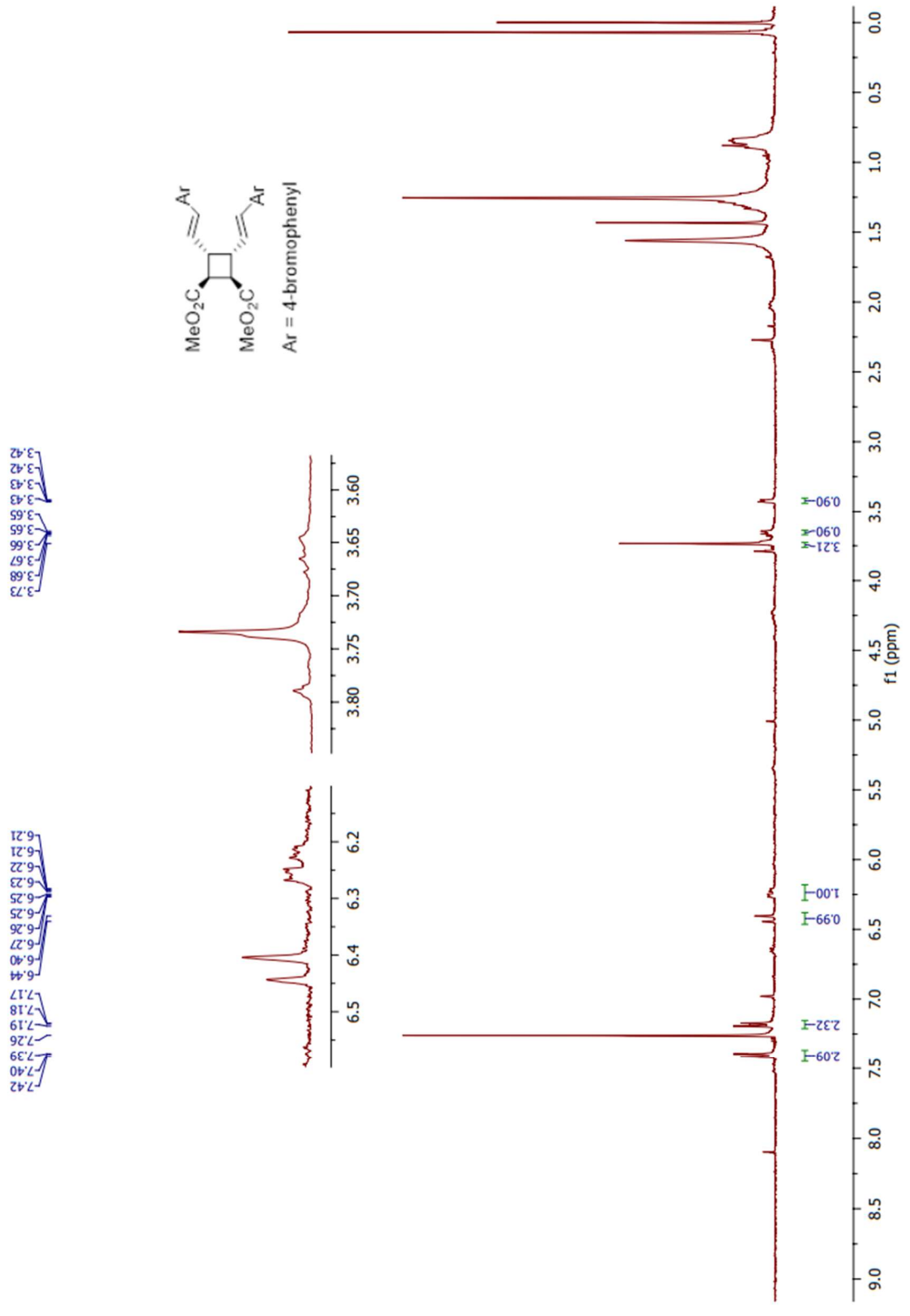

Figure 64. ^{1}H-NMR spectrum of **30** in $CDCl_3$

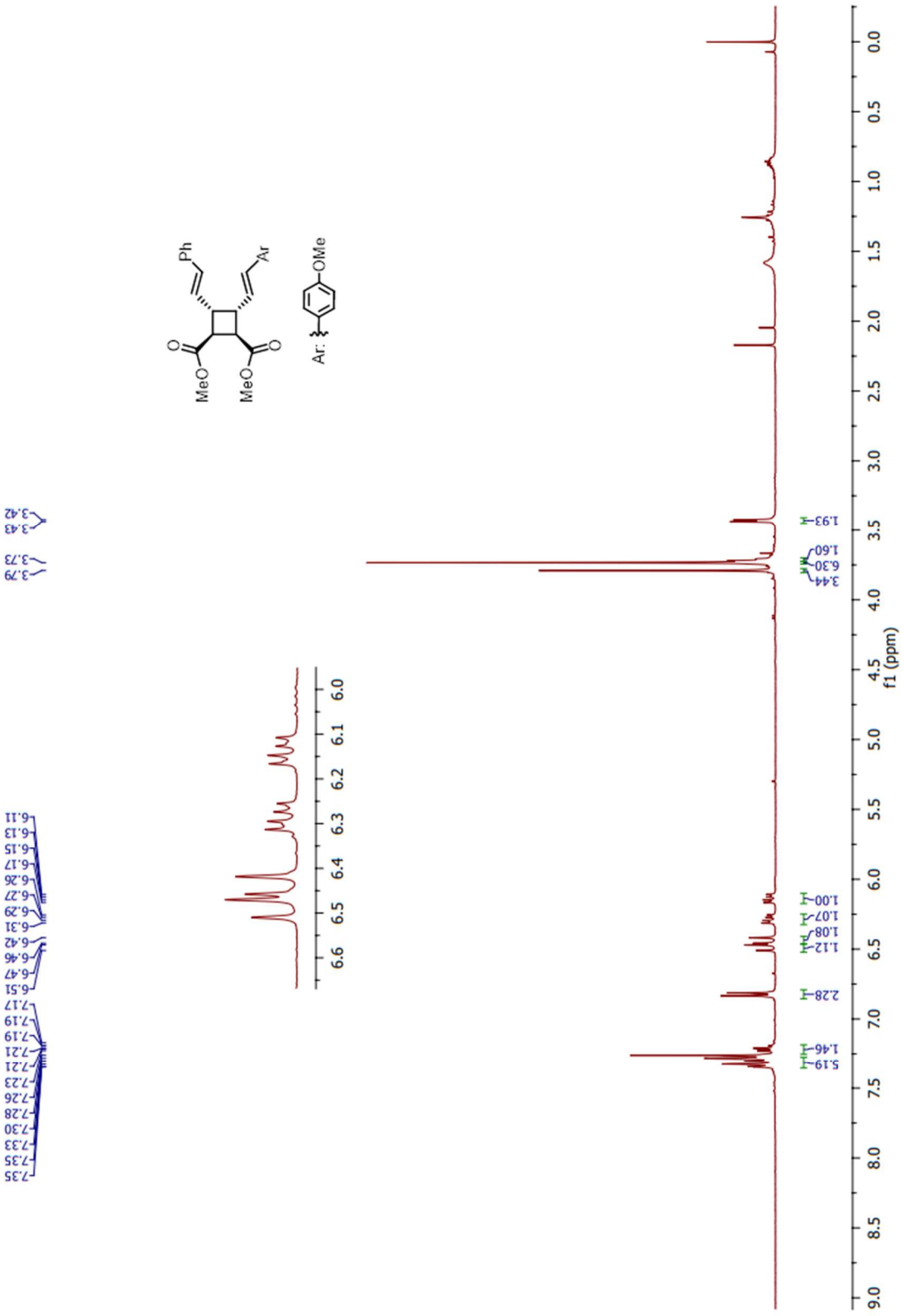

Figure 65. ^{1}H-NMR spectrum of **31** in $CDCl_3$

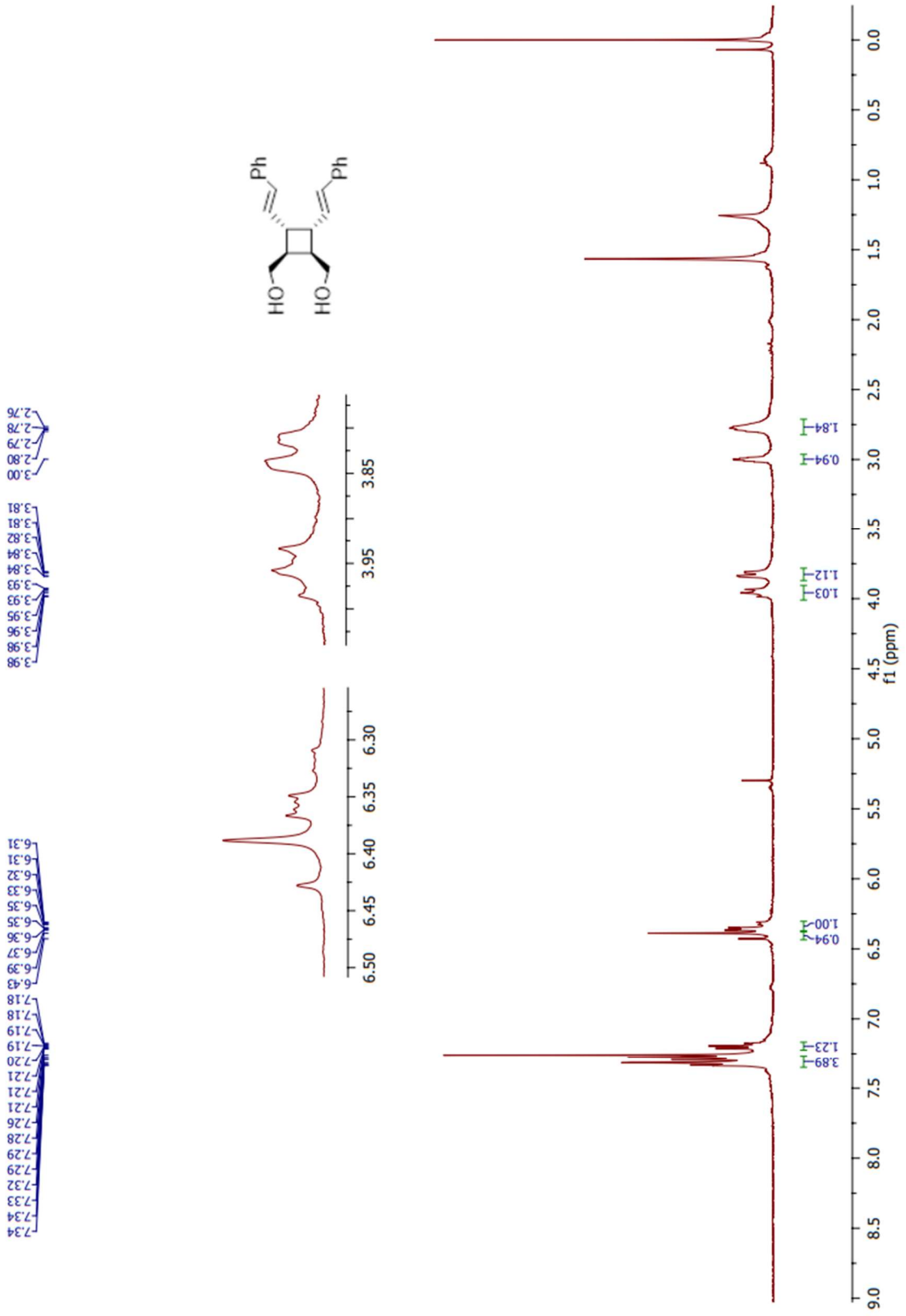

Figure 66. ^{1}H-NMR spectrum of **32** in $CDCl_3$

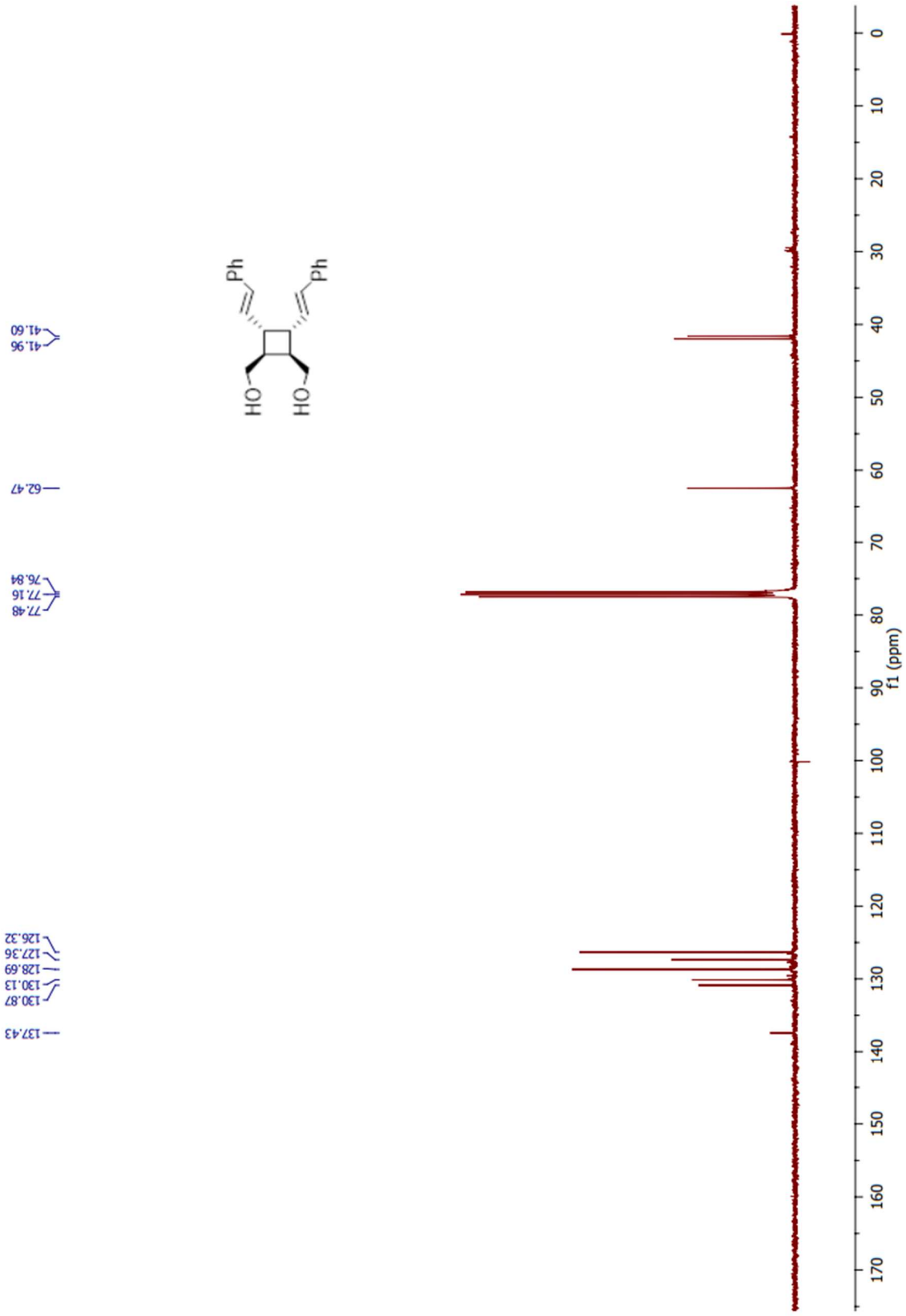

Figure 67. ^{13}C-NMR spectrum of **32** in $CDCl_3$

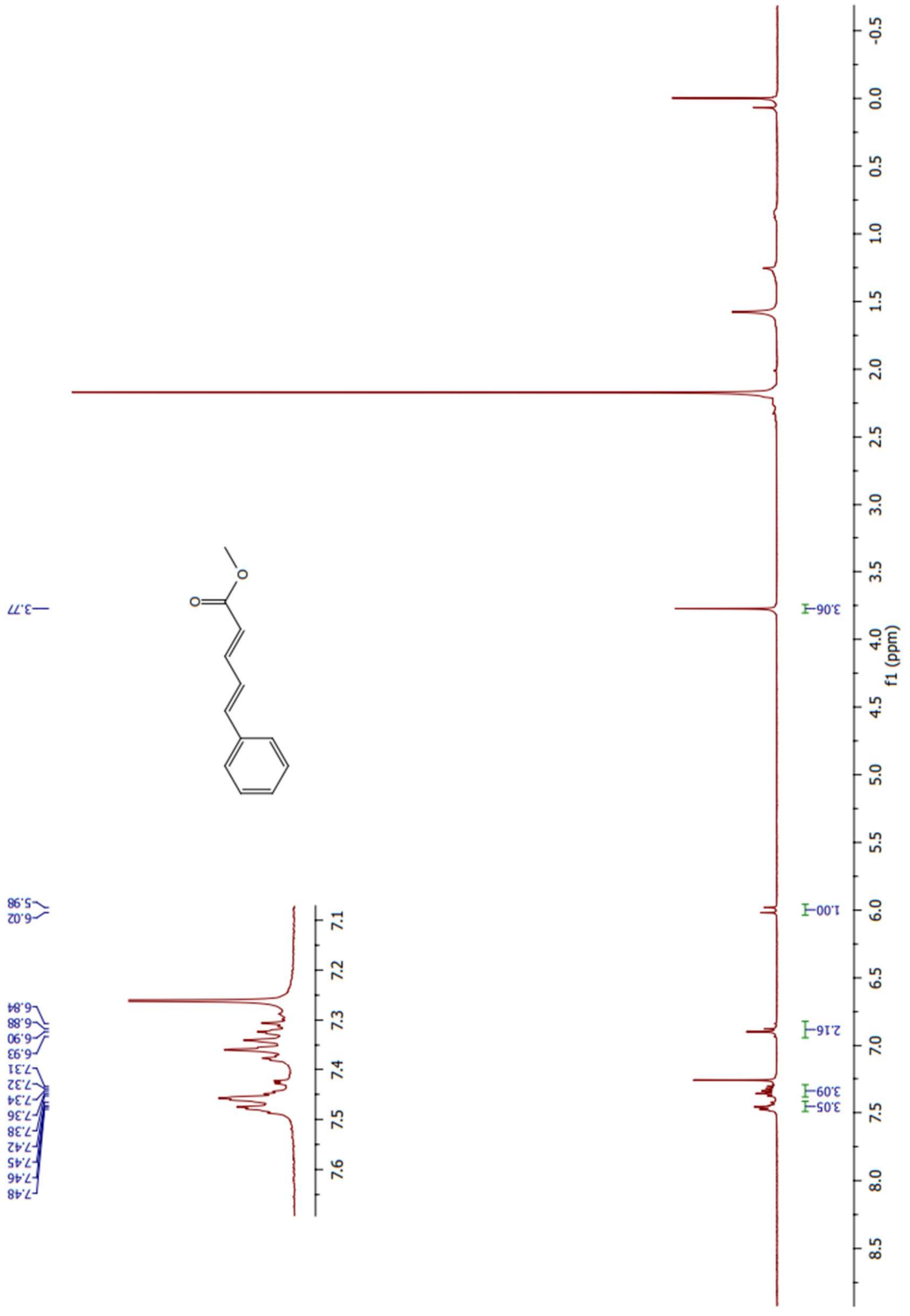

Figure 68. ^{1}H-NMR spectrum of **33** in $CDCl_3$

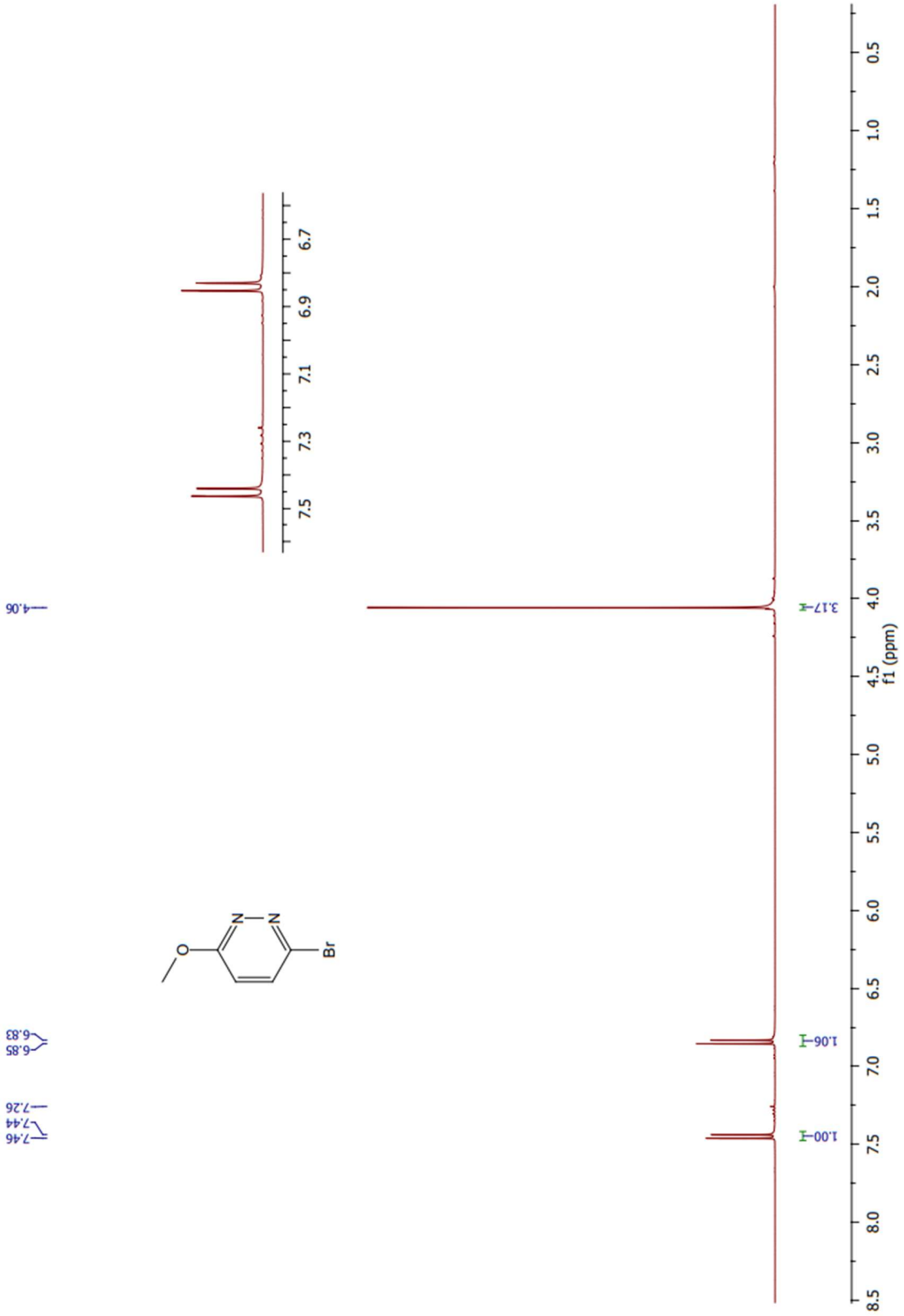

Figure 69. ^{1}H-NMR spectrum of **45** in $CDCl_3$

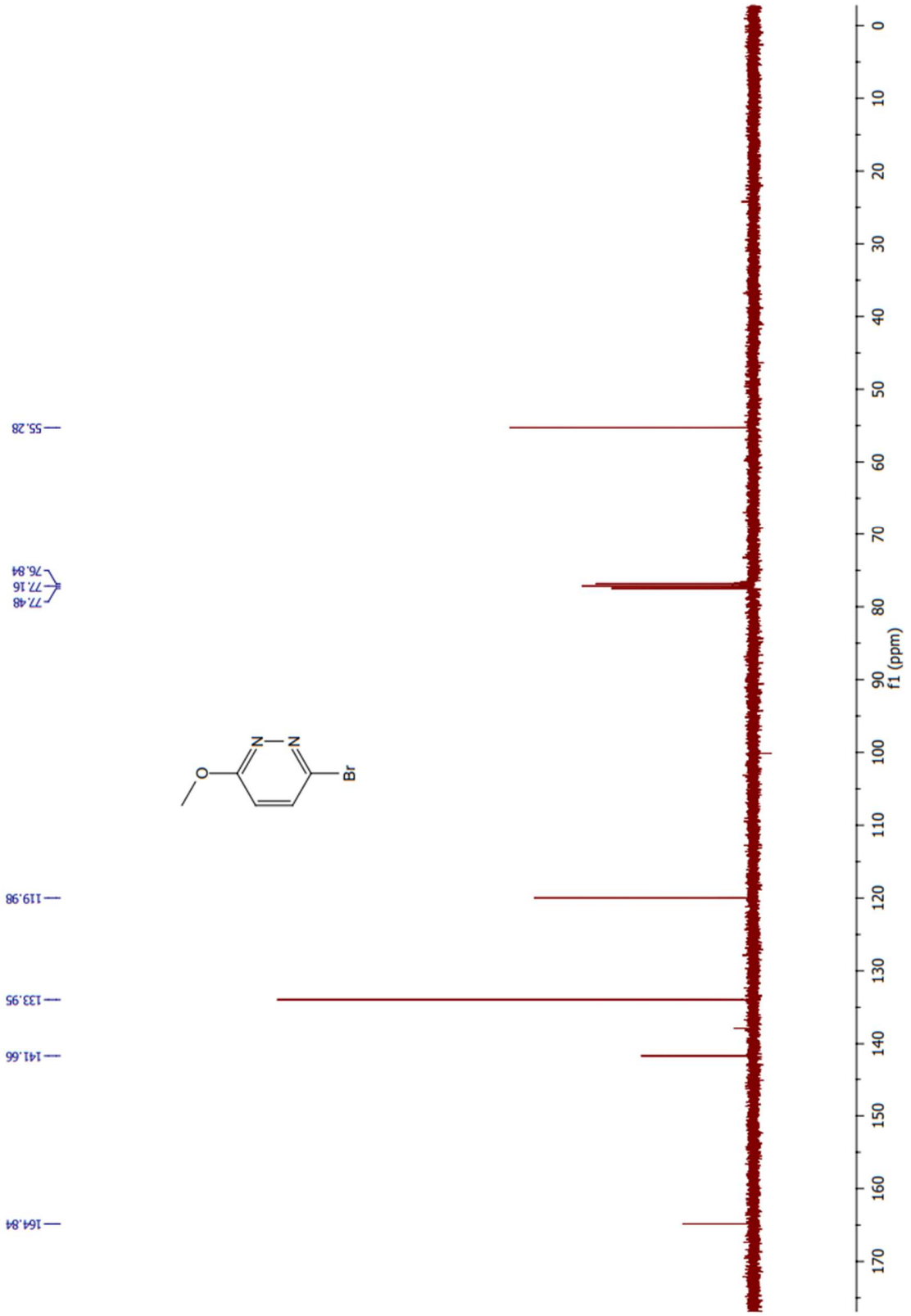

Figure 70. ^{13}C-NMR spectrum of **45** in $CDCl_3$

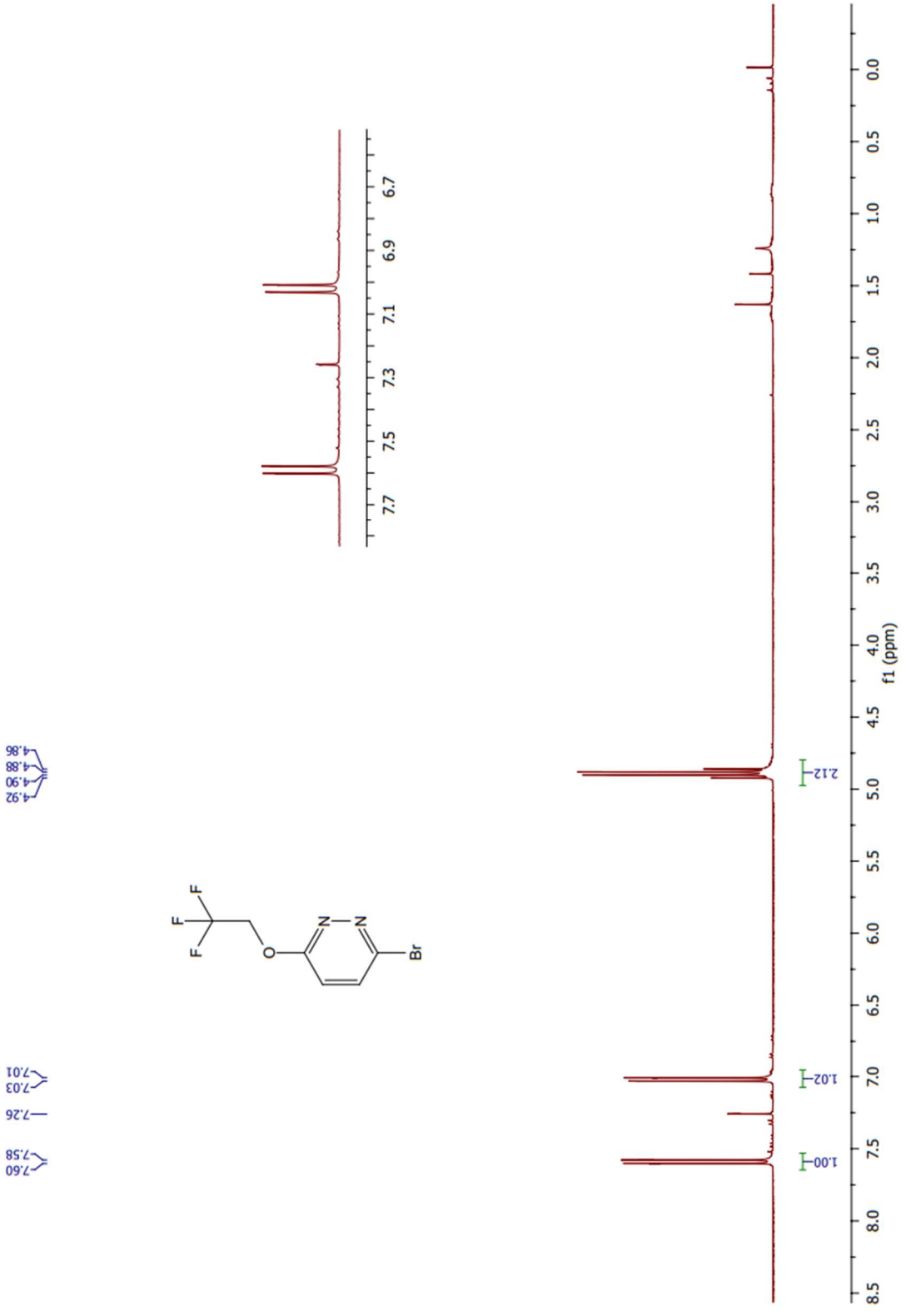

Figure 71. ^{1}H-NMR spectrum of **46** in $CDCl_3$

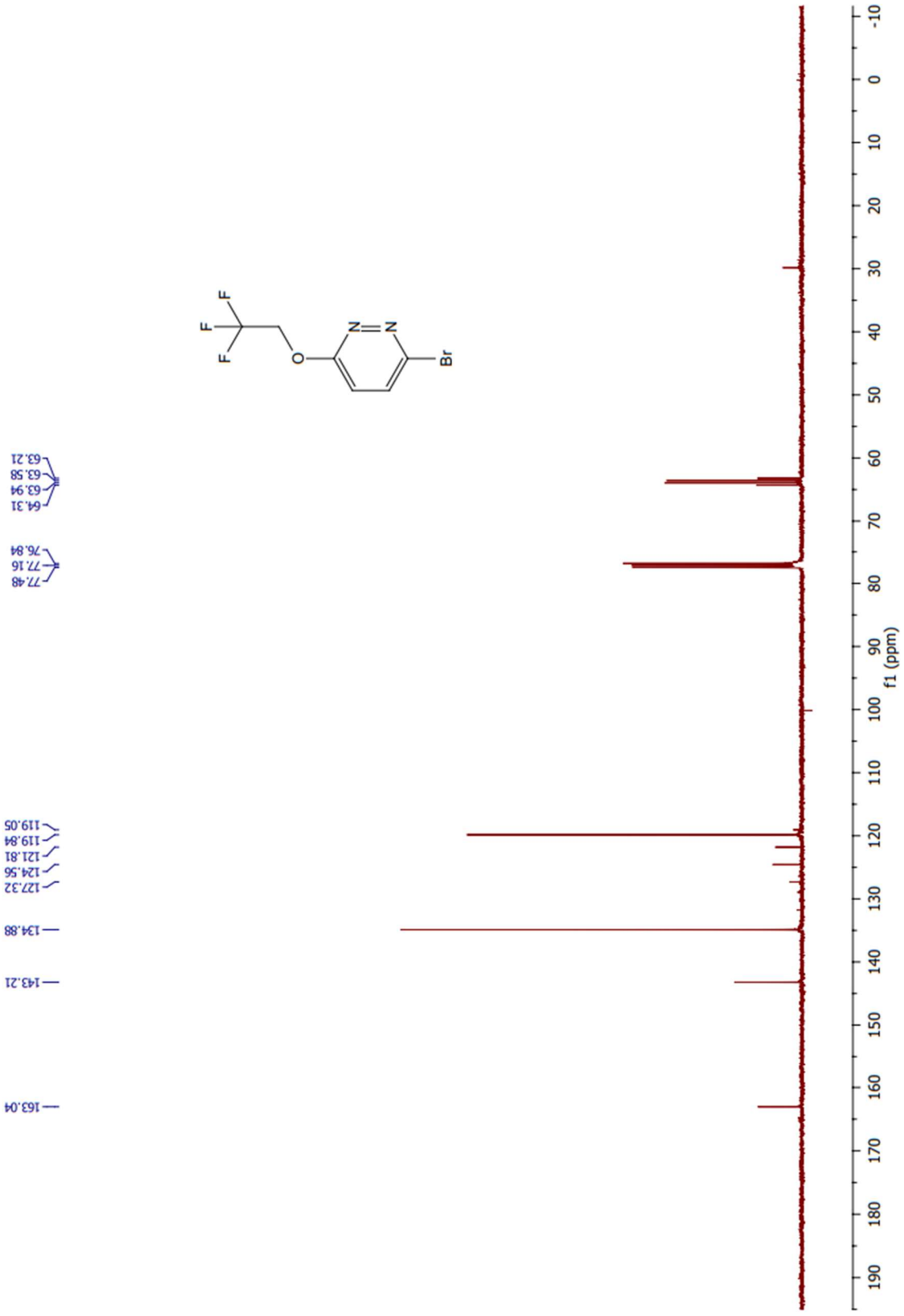

Figure 72. ^{13}C-NMR spectrum of **46** in $CDCl_3$

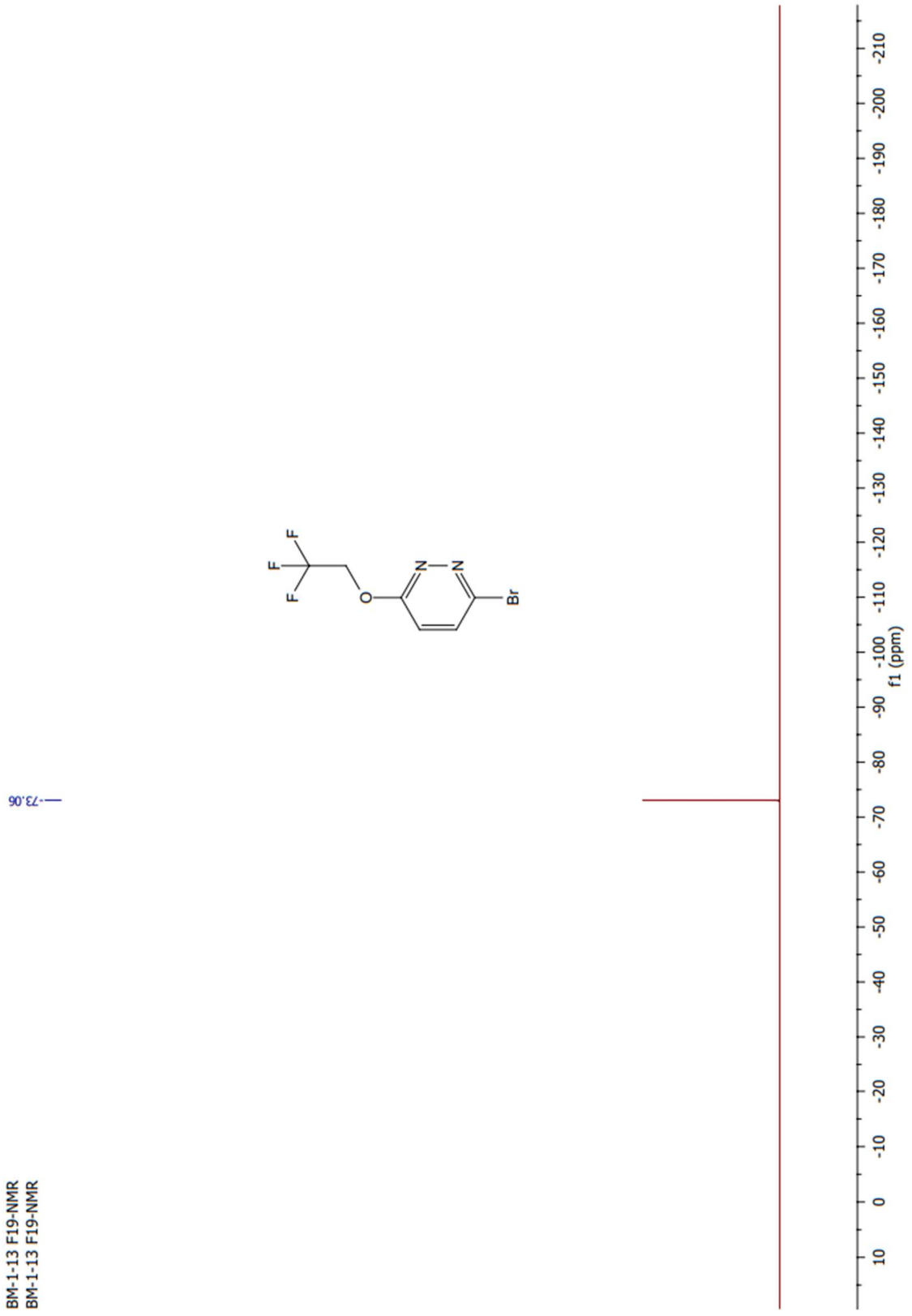

Figure 73. ^{19}F-NMR spectrum of **46** in $CDCl_3$

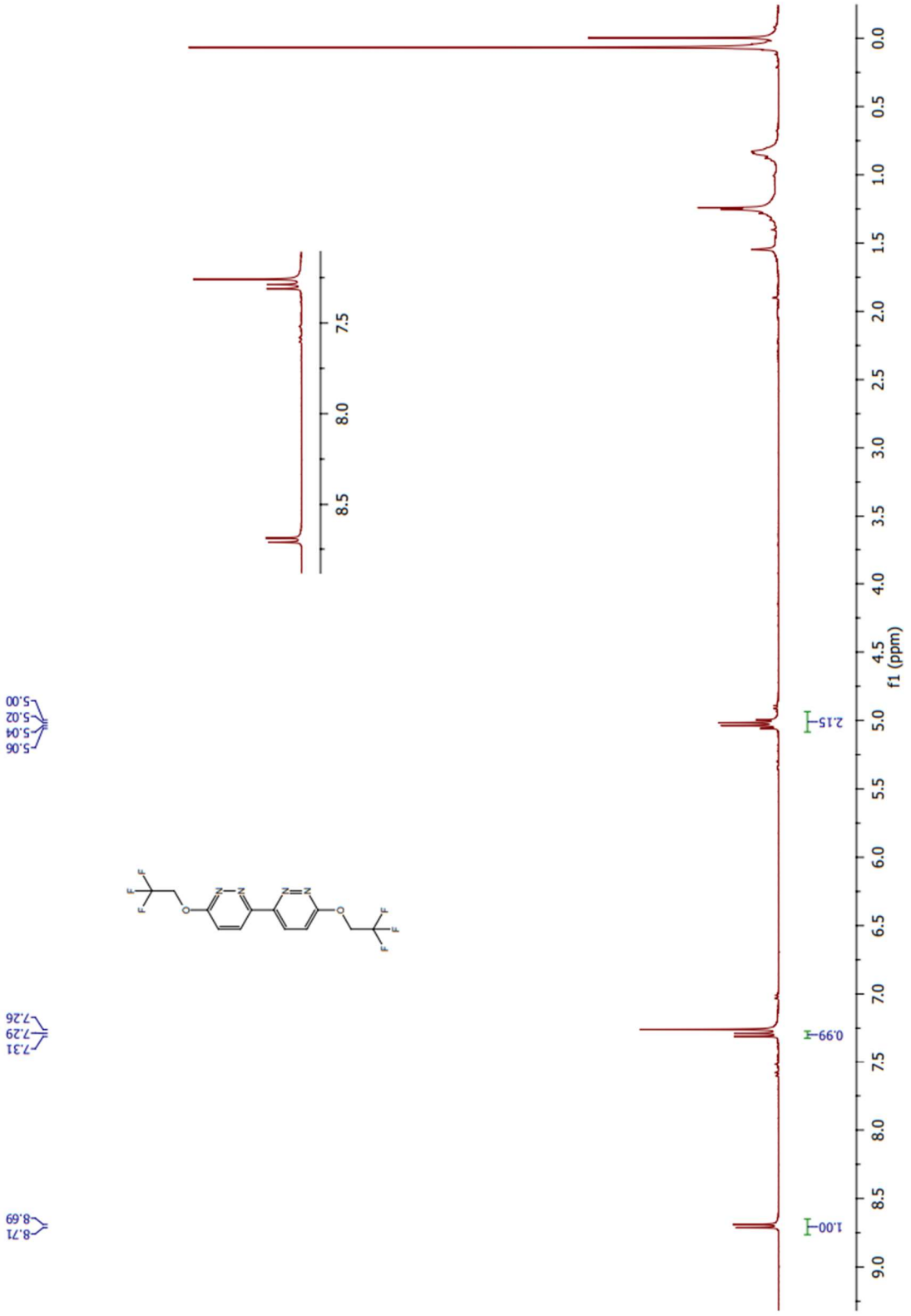

Figure 74. ^{1}H-NMR spectrum of **47** in $CDCl_3$

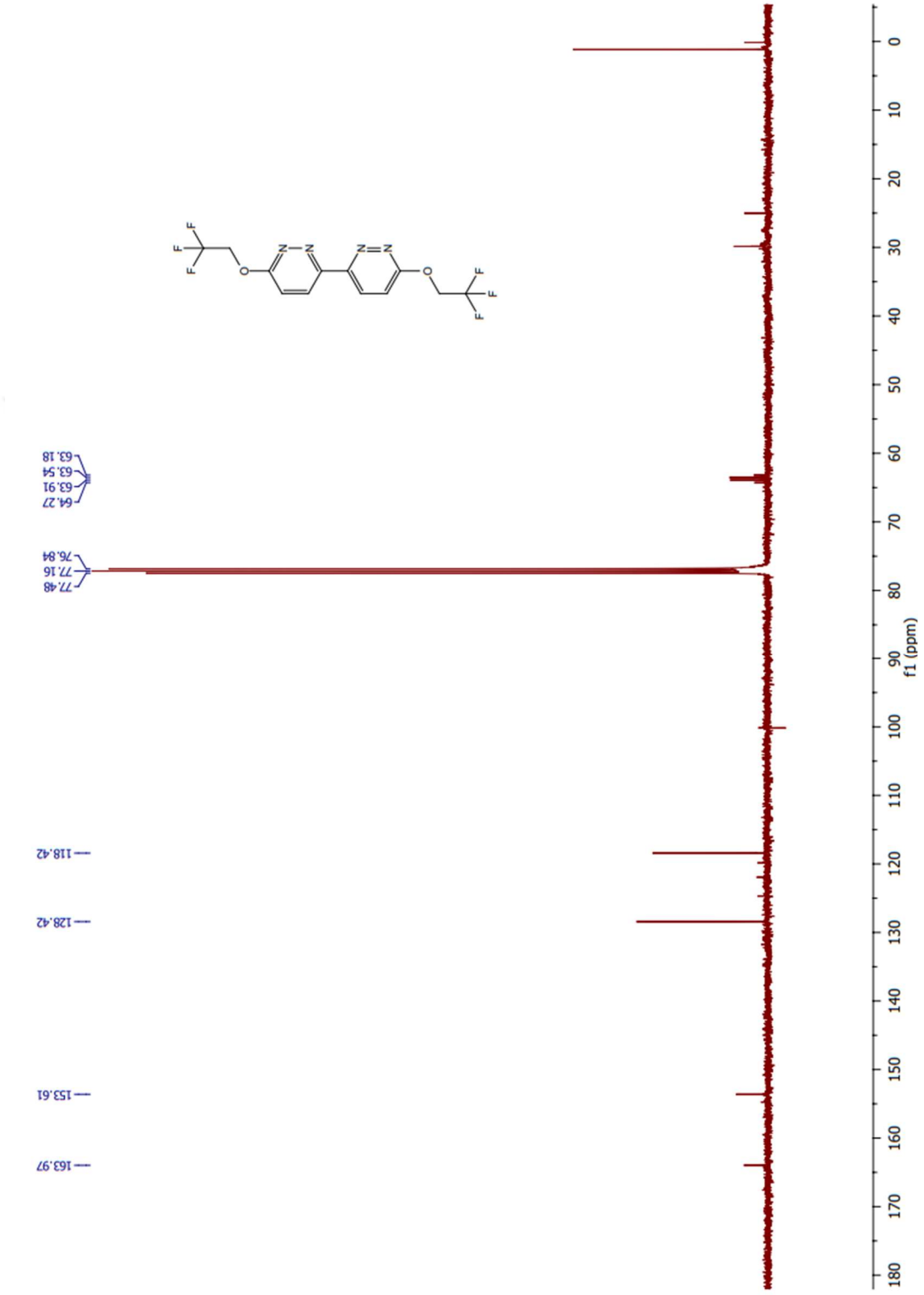

Figure 75. ^{13}C-NMR spectrum of **47** in $CDCl_3$

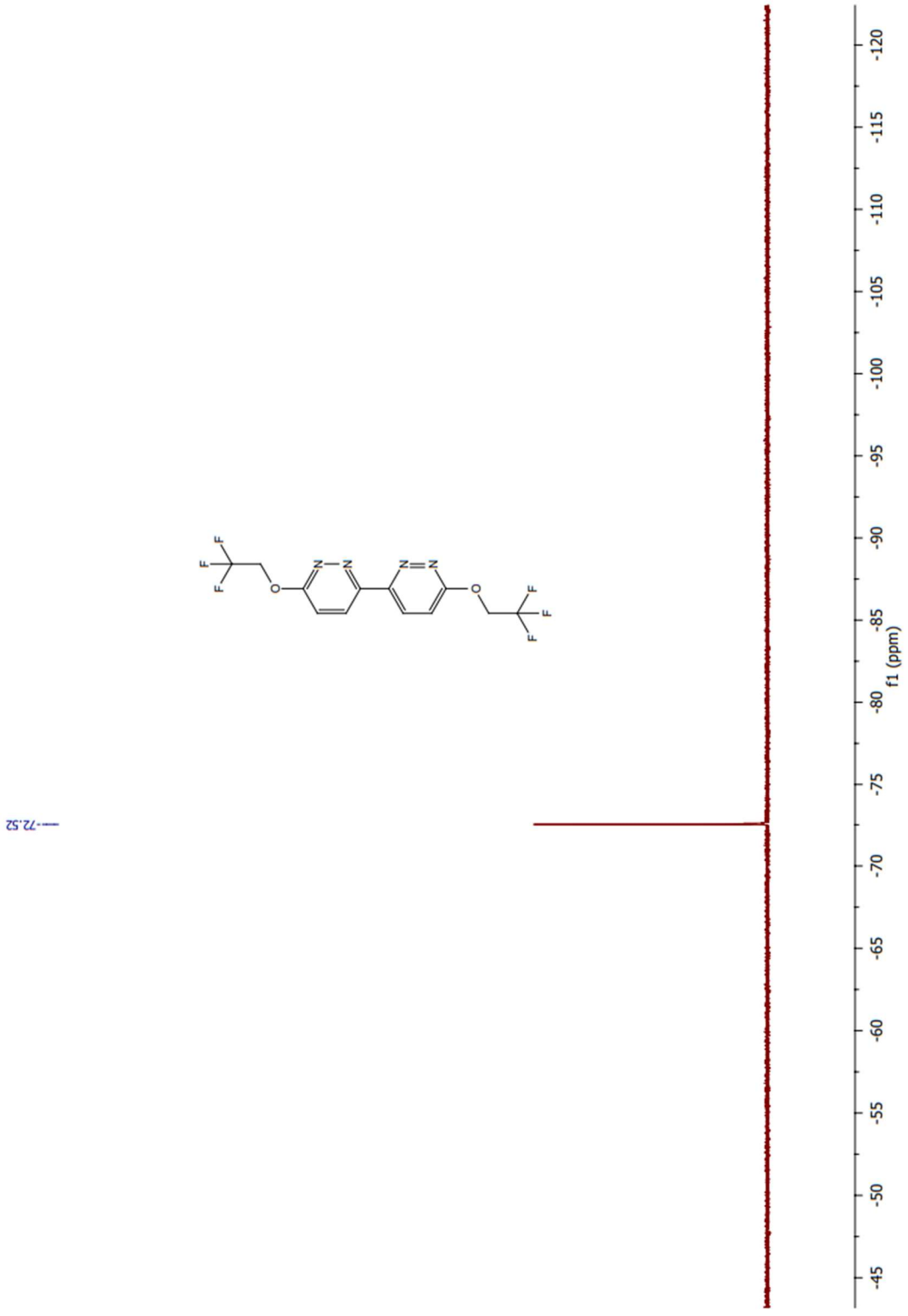

Figure 76. ^{19}F-NMR spectrum of **47** in $CDCl_3$

BIBLIOGRAPHY

[1] Kinney, W. A.; Abou-Gharbia, M.; Garrison, D. T.; Schmid, J.; Kowal, D. M.; Bramlett, D. R.; Miller, T. L.; Tasse, R. P.; Zaleska, M. M.; Moyer, J. A. *J. Med. Chem.*, **1998**, *41*, 236.

[2] Ishikawa, T.; Kudo, K.; Kuroyabu, K.; Uchida, S.; Kudoh, T.; Saito, S. *J. Org. Chem.*, **2008,** *73,* 7498.

[3] Carruthers, W. Cycloaddition Reactions in Organic Synthesis; Pergamon: Exeter, **1990.**

[4] Takahashi, M,; Ichikawa, M.; Aoyagi, S.; Kibayashi, C. *Tetrahedron Letters* **2005,** *46*, 57-59.

[5] Nemoto, H.; Nagai, M.; Moizumi, M.; Kohzuki, K.; Fukomoto, K. *Tetrahedron Letters* **1988,** *29*, 4959-4962.

[6] Danishfesky, S.; Cain, P. *J. Am. Chem. Soc.* **1975,** *97*, 5282-5284.

[7] Shigemori, H.; Bae, M. A.; Yazawa, K.; Sasaki, T.; Kobayashi, J. *J. Org. Chem.* **1992,** *57*, 4317-4320.

[8] Woodward, R. B.; Hoffmann, R. *Angew. Chem. Int. Ed.* **1969**, *8*, 781-932.

[9] Ramamurthy, V.; Siviguru, J.; *Chem. Rev.* **2016,** *116,* 9914-9993.

[10] Schmidt, G. M. *Pure Appl. Chem.* **1971,** *27*, 647-678.

[11] Cohen, M. D.; Schmidt, G. M. *J. Chem. Soc.* **1964,** 2000-2013.

[12] Abdelmoty, I.; Buchholz, V.; Di, L.; Guo, C.; Kowitz, K.; Enkelmann, V.; Wegner, G.; Foxman, B. M. *Cryst. Growth Des.* **2005,** *5*, 2210-2217.

[13] MacGillivary, L.; *CrystEngComm* **2002,** *4,* 37-41.

[14] MacGillivary, L.; Reid, J. L.; Ripmeester, J. A. *J. Am. Chem. Soc.* **2000,** *122,* 7817-7818.

[15] Greiving, H.; Hopf, H.; Jones, P. G.; Bubenitschek, P.; Desvergne, J.P.; Bouas-Laurent, H. *Liebigs Ann.* **1995,** *11,* 1949-1956.

[16] Caronna, T.; Liantonio, R.; Logothetis, T. A.; Metrangolo, P.; Pilati, T.; Resnati, G.; *J. Am. Chem. Soc.* **2004,** *126,* 4500-4501.

[17] Hensens, O. D.; Zink, D.; Williamson, J. M.; Lotti, V. J.; Chang, R. S. L.; Goetz, M. A. *J. Org. Chem.* **1991,** *56,* 3399-3403.

[18] Burke, J. W.; Doskotch, R. W.; Ni, C. Z.; Clardy, J. *J. Am. Chem. Soc.* **1989,** *111*, 5831-5833.

[19] Nicolaou, K. C.; Yang, Z.; Liu, J.J.; Ueno, H.; Nantermet, P. G.; Guy, R. K.; Claiborne, C. F.; Renaud, J.; Couladouros, E. A.; Paulvannan, K.; Sorensen, E. J. *Nature* **1994,** *367,* 630-634.

[20] Mascitti, V.; Corey, E. J. *J. Am. Chem. Soc.* **2004,** *126,* 15664-15665.

[21] Green, B. S.; Lahav, M.; Schmidt, G. M. *J. Chem. Soc. B,* **1971,** 1552-1564.

[22] Gao, X.; Friscic, T.; MacGillivary, L. R. *Angew. Chem. Int. Ed.,* **2004,** *43,* 232-236.

[23] Hopf, H.; Greiving, Helmut.; Beck, C.; Dix, I.; Jones, P. G.; Desvergne, J. P.; Bouas-Laurent, H. *Eur. J. Org. Chem.* **2005,** *3*, 567-581.

[24] Yamada, S.; Azuma, Y.; Aya, K. *Tetrahedron Letters* **2014,** *55*, 2801-2804.

[25] Mir, M. H.; Ong, J. X.; Kole, G. K.; Tan, G. K.; McGlinchey, M. J.; Wu, Y.; Vittal, J. J. *Chem. Commun.,* **2011,** *47,* 11633-11635.

[26] Türkmen, Y. E. *Turk. J. Chem.* **2018,** *42,* 1398-1407.

[27] Mammadova, F.; Hamarat, B.; Ahmadli, D.; Şahin, O.; Bozkaya, U.; Türkmen, Y. E. *ChemistrySelect* **2020,** *5,* 13387-13396.

[28] Yagci, B. B.; Zorlu, Y.; Türkmen, Y. E. *J. Org. Chem.* **2021,** *86,* 13118-13128.

[29] Yagci, B. B.; Munir, B.; Zorlu, Y.; Türkmen, Y. E *Synthesis* **2023,** *55,* 3777-3792.

[30] Li. Z. J.; Cai, L.; Mei, R. F.; Dong J. W.; Li, S. Q.; Yang, X. Q.; Zhou, H.; Yin, T. P.; Ding, Z. T. *Tetrahedron Letters* **2015,** *56,* 7197-7200.

[31] Harada, J.; Ogawa, K. *Chem. Soc. Rev.* **2009,** *38*, 2244-2252.

[32] Sarkar, D.; Bera, N.; Ghosh, . *Eur. J. Org. Chem.* **2020,** 2020, 1310-1326.

[33] Harada, J.; Ogawa, K. *J. Am. Chem. Soc.* **2001,** *123*, 10884-10888.

[34] F. Toda, *Top. Curr. Chem.* **2005,** *154*, 1-40.

[35] Zhang, Y.; Cui, Z.; Li, Z.; Liu, Z. Q. *Org. Lett.* **2012,** *14,* 1838-1841.

[36] Ito, Y.; Hosomi, H.; Ohba, S.; *Tetrahedron Letters* **2000,** *56,* 6833-6844.

[37] Doering, W. E.; Birladeanu, L.; Sarma, K.; Teles, J. H.; Klaerner, F. G.; Gehrke, J. S.; *J. Am. Chem. Soc.* **1994,** *116,* 4289-4297.

[38] Jitoe, A.; Masuda, T.; Nakatani, N.; *Phytochemistry,* **1993,** *32,* 357-363.

[39] Zhang, Y.; Cui, Z.; Li, Z.; Liu, Z. Q. *Org. Lett.* **2012,** *14,* 1838-1841.

[40] Morokuma, K.; Borden, W. T.; Hrovat, D. A. *J. Am. Chem. Soc.* **1988,** *110,* 4475-4476.

[41] Berson, J. A.; Dervan, P. B.; Malherbe, R.; Jenkins, J. A. *J. Am. Chem. Soc.* **1976,** 5937-5968.

[42] Brauers, G.; Ebel, R.; Edrada, R.; Wray, V.; Berg, A.; Grafe, U.; Proksch, P. *J. Nat. Prod.* **2001,** *64,* 651-652.

[43] Raymond L. E.; Howard J. L. *J. Chem. Soc., Perkin Trans. 1*, **1976**, 2149-2155.

[44] Rukachaisirikul, V.; Sommart, U.; Phongpaichit, S.; Towatana, N. H.; Rungjindmai, N.; Sakayaroj, J. *Chem. Pharm. Bull.* **2007,** *55,* 1316-1318.

[45] Li, X. J.; Li, M.; Yao, W.; Lu, H. Y.; Zhao, Y.; Chen, C. F. RSC Adv., **2015**, *5*, 18609–18614.

[46] Goel, A.; Sharma, A.; Katuria, M.; Bhattacharjee, A.; Verma, A.; Mishra, P. R.; Nazir, A.; Mitra, K. *Org. Lett.* **2014,** *16*, 756−759.

[47] Yan, Q.; Zhou, Y.; Ni, B. B.; Ma, Y.; Wang, J.; Pei, J.; Cao, Y. *J. Org. Chem.* **2008**, *73,* 5328–5339.

[48] Kumar, S.; Kumar, D.; Patil, Y.; Patil, S. *J. Mater. Chem. C* **2016**, *4*, 193– 200.

[49] Venkatramaiah, N.; Kumar, S.; Patil, S. Chem. Commun**.**, **2012**,*48***,** 5007-5009.

[50] Allen, C. F.; VanAllan, J. A. *J. Org. Chem.* **1952,** 845-854.

[51] Pascual, S.; Bour, C.; Mendoza, P.; Echavarren, M. *Beilstein J. Org. Chem.* **2011,** *7,* 1520-1525.

[52] Wegner, H. A.; Scott, L. T.; Meijere, A. D. *J. Org. Chem.* **2002,** *68,* 883-887.

[53] Geary, L. M.; Chen, T. Y.; Montgomery, T. P.; Krische, M. J. *J. Am. Chem. Soc.* **2014,** *136,* 16, 5920–5922.

[54] Abe, R.; Nagashima, Y.; Tanaka, J.; Tanaka, K. *ACS Catal.* **2023**, *13*, 3, 1604–1613.

[55] Pal, S.; Metin, Ö.; Türkmen, Y. E. *ACS Omega* **2017**, *2*, 12, 8689–8696.

[56] Ahmadli, D.; Sahin, Y.; Calikyilmaz, E.; Şahin, O.; Türkmen, Y. E. *J. Org. Chem.* **2022**, *87,* 6336−6346.

[57] Fernandes, R. A.; Kumar, P.; Bhowmik, A.; Gorve, D. A.; *Org. Lett.* **2022,** *24, 19,* 3435-3439.

[58] Mavrikaki, V.; Pagonis, A.; Poncin, A.; Mallick, A.; Canaan, S.; Magrioti, V.; Cavalier, J. F. *Bioorg. Chem. Med. Lett.* **2022,** *64,* 128692.

[59] Dakarapu, U. S.; Bokka, A.; Asgari, P.; Hua, Y.; Nguywn, H. H.; Rahman, N.; Jeon, J.; *Org. Lett.* **2015,** *17, 23,* 5792-5795.

[60] Kokotos, G.; Hsu, Y.-H.; Burke, J. E.; Baskakis, C.; Kokotos, C. G.; Magrioti, V.; Dennis, E. A. *J. Med. Chem.* **2010**, *53,* 3602-3610.

[61] Meng, G.; Hu, L.; Chan, H. S. S.; Qiao, J. X.; Yu, J. Q.; *J. Am. Chem. Soc.* **2023,** *145, 24,* 13003-1307.

[62] Wang, Z.; He, Z.; Zhang, L.; Huang, Y.; *J. Am. Chem. Soc.* **2018,** *140, 2,* 735-740.

[63] Chan, A.; Shan, P, Y,; Wu, M.; Lin, P.; Tsai, C.; Hsu, C.; Chiu, T.; Hsu, T.; Yeh, Y.; Lai, Y.; Liu, M.; Tu, L.; *Chem. Commun.* **2023,** *59,* 10660-10663.

[64] Zhang, Y.; Cui, Z.; Li, Z.; Liu, Z. Q.; *Org. Lett.* **2012,** *14, 7,* 1838-1841.